2001

Photogrammetry and remote sensing for visualization of spatial data in a virtual reality environment

Dwipen Bhagawati
Iowa State University

INFORMATION TO USERS

This manuscript has been reproduced from the microfilm master. UMI films the text directly from the original or copy submitted. Thus, some thesis and dissertation copies are in typewriter face, while others may be from any type of computer printer.

The quality of this reproduction is dependent upon the quality of the copy submitted. Broken or indistinct print, colored or poor quality illustrations and photographs, print bleedthrough, substandard margins, and improper alignment can adversely affect reproduction.

In the unlikely event that the author did not send UMI a complete manuscript and there are missing pages, these will be noted. Also, if unauthorized copyright material had to be removed, a note will indicate the deletion.

Oversize materials (e.g., maps, drawings, charts) are reproduced by sectioning the original, beginning at the upper left-hand corner and continuing from left to right in equal sections with small overlaps.

Photographs included in the original manuscript have been reproduced xerographically in this copy. Higher quality 6" x 9" black and white photographic prints are available for any photographs or illustrations appearing in this copy for an additional charge. Contact UMI directly to order.

ProQuest Information and Learning
300 North Zeeb Road, Ann Arbor, MI 48106-1346 USA
800-521-0600

Photogrammetry and remote sensing for visualization of spatial data in a virtual reality environment

by

Dwipen Bhagawati

A dissertation submitted to the graduate faculty

in partial fulfillment of the requirements for the degree of

DOCTOR OF PHILOSOPHY

Major: Civil Engineering (Geometronics)

Program of Study Committee:
Kandiah Jeyapalan, Major Professor
John Pitt
SayKee Ong
Thomas S. Colvin
Udoyara Sunday Tim

Iowa State University

Ames, Iowa

2001

UMI Number: 3048701

ProQuest Information and Learning Company
300 North Zeeb Road
P.O. Box 1346
Ann Arbor, MI 48106-1346

Graduate College
Iowa State University

This is to certify that the Doctoral dissertation of

Dwipen Bhagawati

has met the dissertation requirements of Iowa State University

Signature was redacted for privacy.

Major Professor

Signature was redacted for privacy.

For the Major Program

DEDICATION

I dedicate this work to the memory of my father late Rajendra Nath Bhagawati.

TABLE OF CONTENTS

LIST OF FIGURES xi

LIST OF TABLES xv

CHAPTER 1 INTRODUCTION 1

1.1 VR for Spatial Data 2

1.2 A Review of Current Practices 4

1.2.1 Digital Photogrammetry 4

1.2.2 Geographic Information System 8

1.2.3 VR Systems 10

1.3 The Problem 14

1.4 Roadside Features Data – A Case Study 15

1.4.1 Iowa DOT Video-Log Data Inventory 16

1.4.2 Need for VR 16

1.5 Research Objectives 17

1.6 Thesis Organization 18

CHAPTER 2 VIRTUAL REALITY 20

2.1 Visions of Virtual Reality 20

2.2 What Is Virtual Reality.....22

2.3 Why Virtual Reality Is Different 24

2.3.1 User Oriented Approach.....25

2.3.2 Integrated Environment.....25

2.3.3 Complex System 26

2.4 Anatomy of a Virtual Reality System.....26

2.4.1 User Input 27

2.4.2 Output of the Synthesized Virtual World.....29

2.5 Virtual Reality Systems.....29

2.5.1 Fish Tank 29

2.5.2 Head Mounted Display (HMD).....32

2.5.3 Single Screen Projection.....34

2.5.4 Multiple-Screen Immersive Projection Display System 36

2.6 The CAVE 38

2.6.1 C2.....39

2.6.2 C6.....41

CHAPTER 3 AS BUILT SURVEY.....44

3.1 What Is An As Built Survey.....45

3.2 Review of As Built Survey Methods 47

3.3 IADOT Video-Logging System.....57

3.4 Summary 61

CHAPTER 4 CAMERA CALIBRATION 62

4.1 An Overview of Camera Calibration 63

4.1.1 Lens Distortion 63

4.1.2 Camera Calibration Methods 66

4.1.3 Elements of Exterior Orientation 69

4.1.4 Other Research in Camera Calibration 74

4.1.5 CALIB Software for Camera Calibration 76

4.2 Calibration of Video-Log Camera 76

4.2.1 The Approach and Methods 77

4.2.2 Selection of Site 78

4.2.3 Design of the Target 78

4.2.4 Number and Placement of Targets 79

4.2.5 Camera Positions 80

4.2.6 Determination of Target Locations 82

4.2.7 Data Acquisition at Calibration Site 85

4.2.8 Camera Calibration 91

4.2.9 Validation 91

4.3 Summary 93

CHAPTER 5 PHOTOGRAMMETRIC DATA ACQUISITION 95

5.1 An Overview 96

5.1.1 Analog Approach 96
5.1.2 Analytical Approach 96
5.1.3 Semi-Analytical Approach 101
5.2 A New Methodology 101
5.2.1 The Approach 102
5.2.2 The Procedure 103
5.2.3 Camera Orientation Parameters 104
5.2.4 Number of Images 105
5.2.5 Spacing between Images 106
5.2.6 Initial Estimates of Object Point Coordinates 108
5.2.7 Measurement of Image Coordinates 110
5.2.8 Transformation of Image Coordinates 110
5.2.9 Refining Camera Parameters 113
5.2.10 Determination of Object Point Locations 115
5.2.11 Transformation from Local System to World System 117
5.3 Evaluation 119
5.3.1 EDM Baseline Site (Rural) 120
5.3.2 Lincoln Way-Grand Avenue (City/Residential) 123
5.3.3 Nevada Site (Highway) 125
5.4 Summary 128
CHAPTER 6 REMOTE SENSING 129

6.1 Electro-Magnetic Energy 131
6.1.1 Radiation Sources 134
6.1.2 Interaction in Atmosphere 137
6.2 Remote Sensing Platforms 140
6.2.1 Satellites 142
6.2.2 Aircrafts 143
6.2.3 Ground Based Remote Sensing 143
6.3 Sensing Devices 144
6.3.1 Photographic Camera 145
6.3.2 Non-Photographic Camera 150
6.4 Data Analysis 152
6.5 Digital Image Processing 156
6.5.1 Image Rectification and Restoration 156
6.5.2 Image Enhancements 157
6.5.3 Image Classification 157
6.6 Application of Remote Sensing in VR 159
CHAPTER 7 MODELING VR SCENE 160
7.1 Modeling Approaches 160
7.1.1 Model Based Approach 161
7.1.2 Image Based Approach 161
7.2 VR Model of a Roadway Environment 162

7.2.1 Modeling the Simulated Scene 163

7.2.2 Modeling the Real World Scene 170

7.2.3 Software Tools for Modeling 183

7.3 About VRJuggler 183

CHAPTER 8 RESULTS AND CONCLUSIONS 186

8.1 Camera Calibration 187

8.2 Feature Positioning 188

8.3 Modeling the VR Scene 189

8.4 Recommendations 192

APPENDIX A – VIRTUAL REALITY SYSTEMS 195

Academic Institutions, USA 195

US Government Research Laboratories 196

US Industries 196

International Sites 197

APPENDIX B - IADOT VIDEOLOGGING SYSTEM SPECIFICATIONS .200

APPENDIX C – FEATURE POSITIONING USING SOFTPLOTTER™. ..201

Block Tool 201

Stereo Tool 206

APPENDIX D - LISTING OF VISUAL BASIC PROGRAM CODE 208

APPENDIX E – LISTING OF SIMULATED VR SCENE CODE 213

APPENDIX F - AUTOCAD DRAWING FOR VR MODELING.....223

Elements of the Bridge.....223

The AutoCAD GUI.....224

Organizing the Drawing.....226

Drawing the Bridge Model.....228

Portability.....230

APPENDIX G – MULTIGEN CREATOR™ FOR VR MODELING.....232

Cleaning Up Bridge Model.....233

Modeling Photogrammetric Feature Positioning.....234

Integration of Two Models.....235

REFERENCES.....236

ACKNOWLEDGEMENTS.....249

LIST OF FIGURES

Figure 1.1 Digital elevation model created by digital photogrammetry 6

Figure 2.1 Fish-tank virtual reality system 31

Figure 2.2 Head Mounted Display virtual reality system 33

Figure 2.3 Single projection virtual reality system 35

Figure 2.4 Multiple screen projection virtual reality system 37

Figure 2.5 A view of the C2 40

Figure 2.6 A view of the C6 42

Figure 3.1 Camera mounted on the video logging van 58

Figure 3.2 Computing hardware of the video logging system 59

Figure 3.3 GPS antenna mounted on the video logging van 60

Figure 4.1 The collinearity condition 71

Figure 4.2 Simultaneous bundle adjustment 73

Figure 4.3 Target used for camera calibration 79

Figure 4.4 Positioning of targets for camera calibration 81

Figure 4.5 Layout of camera locations 83

Figure 4.6 Points on the base line for positioning targets 84

Figure 4.7 Traversing 88

Figure 5.1 A local coordinate system for a pair of images 106

Figure 5.2 Illustration of a sample CALIB data input file 107

Figure 5.3 Estimating object point coordinates on image 111

Figure 5.4 Image on viewer for measurement object points 112

Figure 5.5 Image and photo coordinates 113

Figure 5.6 Editing data file and running CALIB 116

Figure 5.7 Spreadsheet for coordinate transformation 117

Figure 5.8 An Interface for coordinate transformation program 118

Figure 5.9 Object points at the EDM baseline site (middle section) 121

Figure 5.10 Object points at the Grand Avenue site 124

Figure 5.11 Object points at the Nevada site 126

Figure 6.1 The electromagnetic spectrum 132

Figure 6.2 Visible part of electromagnetic spectrum and vicinity 133

Figure 6.3 Spectral distribution of blackbody radiation 138

Figure 6.4 Atmospheric absorption at different wavelength 140

Figure 6.5 Remote sensing platforms 141

Figure 6.6 Spectral ranges of sensing devices 145

Figure 6.7 Components of an aerial camera 146

Figure 6.8 Energy interactions with object 153

Figure 6.9 Types of reflectors 154

Figure 6.10 Spectral reflectance curve 155

Figure 7.1 The roadway scene in a simulation window 164

Figure 7.2 Wand interaction menu 166

Figure 7.3 Editing the roadside feature 167

Figure 7.4 Querying the roadside feature 168

Figure 7.5 Measurement of distance inside VR environment 169

Figure 7.6 Measurement of area inside VR environment 170

Figure 7.7 Photogrammetric feature positioning 172

Figure 7.8 AutoCAD drawing of the bridge 174

Figure 7.9 VR scene of the roadway 175

Figure 7.10 Damaged concrete and exposed steel 176

Figure 7.11 Rusting steel elements 177

Figure 7.12 Underside of the bridge 178

Figure 7.13 Crooked texture mapping of tracks 178

Figure 7.14 Rectifying texture images 179

Figure 7.15 Correct texture mapping of the railway track 180

Figure 7.16 Texture mapping for road pavements 181

Figure 7.17 The scene with a view of the pavements 182

Figure 7.18 The scene with a view of the sidewalk 182

Figure 8.1 User in roadway model inside CAVE 190

Figure 8.2 Original image sources for texture 191

Figure F.1 Elements of AutoCAD GUI 225

Figure F.2 Accessing toolbars 226

Figure F.3 Layers in AutoCAD 227

Figure F.4 Solids toolbar 228

Figure F.5 Modify toolbar 229

Figure F.6 Object snap toolbar 230

Figure F.7 Zoom options 230

Figure F.8 Dynamic 3D viewing 231

LIST OF TABLES

Table 1 Ground control coordinates of targets and camera positions 86

Table 2 Accuracy of GPS Locations 90

Table 3 Calibrated values of camera parameters 92

Table 4 Accuracy of position determination 93

Table 5 Accuracy of data reduction for different image spacing 122

Table 6 Accuracy of feature dimension at EDM baseline site 123

Table 7 Accuracy of object positioning at the Grand Avenue site 125

Table 8 Accuracy of object positioning at the Nevada site 127

Table 9 Ground Dimensions at the Nevada site 127

CHAPTER 1 INTRODUCTION

Researchers in many disciplines have started using the tool of Virtual Reality (VR) to gain new insights into problems in their respective disciplines [1]. Recent advances in computer graphics, software and hardware technologies have created many opportunities for VR systems, advanced scientific and engineering applications being among them. In Geometronics, generally photogrammetry and remote sensing are used for management of spatial data inventory. VR technology can be suitably used for management of spatial data inventory. This research demonstrates usefulness of VR technology for inventory management by taking the roadside features as a case study. Management of roadside feature inventory involves positioning and visualization of the features. This research has developed a methodology to demonstrate how photogrammetric principles can be used to position the features using the video-logging images and GPS camera positioning and how image analysis can help produce

appropriate texture for building the VR, which then can be visualized in a Cave Augmented Virtual Environment (CAVE).

The next subsection discusses the more general scenario of relevance of VR technology in the context of management of spatial data, including the current practices of visualization of spatial data in the realms of photogrammetry, Geographic Information Systems (GIS), and existing VR systems. Then a problem is identified and existence of this problem is justified as applied to roadside feature data inventory of the Iowa Department Of Transportation (IADOT), followed by an outline of the research objectives and a description of the organization of this thesis.

1.1 VR for Spatial Data

VR is a computer interface technology that lets the user experience the data directly, that is, in a three-dimensional setting. It can be described as a way for humans to visualize, manipulate and interact with extremely complex data using computers. [2]. The basic concept behind VR is the direct correspondence between the viewing position and viewing direction of images on a display. Immersion is an essential component of a VR environment because it helps to enhance the user's ability to understand, analyze, create and communicate.

Current research interests in such fields as architecture, urban planning, and resource inventory for facility planning and transportation systems include a desire for enhanced visualization of three-dimensional spatial data. The most important aspect of spatial data is that it is related to a feature that exists in the real world and has a location or definite geographic reference. Another important aspect is that each spatial feature of a data entity has attribute information. The best way to utilize geographically referenced data would be to build an environment where the managers may analyze and visualize data so that they can make decisions regarding the management and inventory of spatial data. A VR application for spatial data may provide a means for a comprehensive analysis of such data.

Virtual representation of spatial data requires presentation of both geometric and attribute data. Therefore, information about geometry and attributes of features are to be collected for complete representation in a VR environment. While digital photogrammetry and remote sensing may assist in determining the positional and attribute information, a Geographic Information System helps in understanding the spatial relationships between the feature entities. A VR environment may provide the desired enhancements in visualization of and interaction with these data.

1.2 A Review of Current Practices

Current research includes varieties of systems for visualization and analysis of spatial data. Traditionally, photogrammetrists collected spatial data and represented these spatial data on an elevation model. With the advent of modern techniques, digital photogrammetric methods are used to collect data and extract elevation models from digital images. Other methods include: (1) some kind of virtual environment in a traditional Geographic Information System (GIS), or (2) an independent system that provide functionalities for both spatial and non-spatial analysis of spatial data. In the next three sections, a review of different approaches for visualizing and analyzing spatial data is presented.

1.2.1 Digital Photogrammetry

In visualization, reality is perception in the third dimension. In data visualization, the most important aspect of immersion is stereoscopic vision. Stereoscopic vision is a trusted tool for data collection and visualization in the field of photogrammetry. "Stereoscopy is the science and art of dealing with the use of images to produce a three-dimensional visual model with characteristics analogous to those of actual features viewed using binocular vision" [3].

Stereoscopic vision surrounding the user creates an illusion of immersion in a VR system.

In photogrammetry, stereoscopy has three primary uses: (1) recognize and interpret an object of three-dimensional form, (2) estimate relative heights, and (3) measure height above a known surface. Photogrammetry has evolved from an analog use to analytical and from analytical to digital or soft photogrammetry. Along this way, the techniques of stereovision evolved from simple lens stereoscopes and mirror stereoscopes, stereoscopic microscopes, and mechanical oscillating shutters to the use of stereoscopic glasses synchronized with alternating projection of stereo images. The last of these systems, stereoscopic glasses synchronized with alternate image projection, is used in a present day VR system.

The double-projection direct viewing instruments that use stereoscopic vision are a mainstay in the science of photogrammetry. These instruments include Multiplex, Balplex, and Kelsh, Nistri, and Kern PG-I. These instruments use overlapping images to optically reconstruct and view stereo models for the purpose of map compilation.

New techniques in digital photogrammetry have made it possible to obtain stereovision on the monitor screen of a computer. Basically,

it is the same technique that is used to create the perception of immersion in most VR systems. Figure 1.1 [4] shows a digital elevation model generated from a pair of digital stereo photographs using digital photogrammetric techniques. This model represents the variation of elevations fairly well. However, not much other information is available. It needs to be supplemented with textural information. Also, there is no means to interactively manipulate the model. VR technology can augment such a model with desirable features of visualization and interaction. This, together with the texture from the aerial photographs, can help to build a VR model.

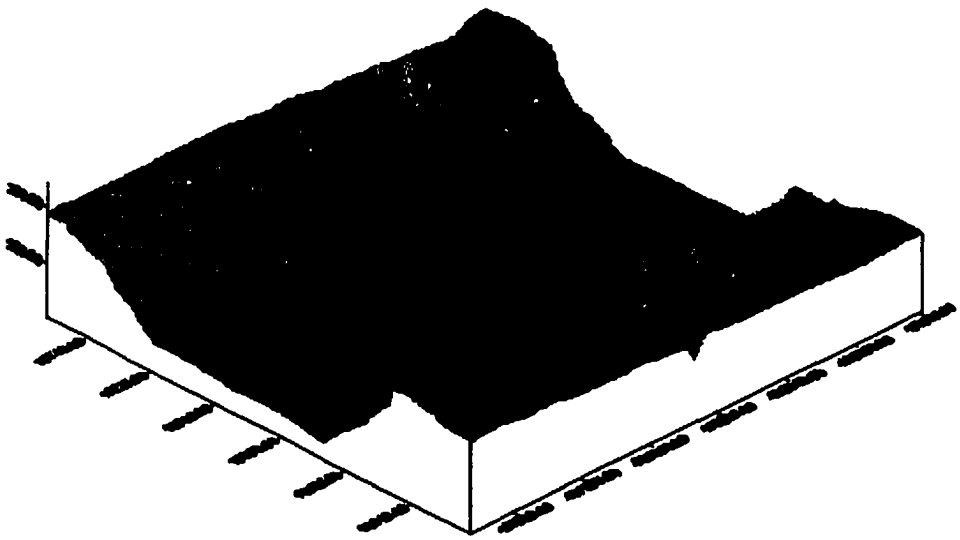

Figure 1.1 Digital elevation model created by digital photogrammetry

1.2.1.1 Remote sensing for attribute collection

"Remote sensing is the science and art of obtaining information about an object, area, or phenomenon through the analysis of data acquired by a device that is not in contact with the object, area, or phenomenon under investigation" [5]. The two basic processes involved are data acquisition and data analysis. In the true sense of this definition, digital imaging is perfect as a method of remote sensing.

Digital photogrammetry uses digital images for the purpose of position determination. The same images may be used for collecting further information through analysis of the image data. Remote sensing techniques extract attribute information about features of interest that appear in the images by interpreting them. We may apply the same principles of remote sensing to terrestrial images acquired from a digital camera mounted on a moving van.

Digital photogrammetry yields quantitative feature information such as size, shape, height, and spacing of features of images. Qualitative information such as the current physical condition of features of interest also can be interpreted by remote sensing.

1.2.2 Geographic Information System

A Geographic Information System (GIS) is a computer system, which deals with geographically referenced data by assembling, storing, manipulating, and displaying them. The real strength of GIS lies in integration of database operations such as querying, statistical analysis, geographic analysis and visualization. GIS is capable of different kinds of visualization including map displays, charts, three-dimensional views, photographic images and multimedia.

1.2.2.1 3D GIS

Until recently, GIS portrayed the world from a 2D perspective. But in the last few years, 3D display and analytical tools have become available. These new 3D GIS tools allow users to generate fly-through of high-resolution scenes for presentations and collaborative work, offering views from virtually any location. Even so, the 3D maps, grids, and visualizations generated by the GIS software would have limited value if they were not connected to databases with extensive underlying information and analytic capability. There are four categories of visualization products that interface directly with GIS [6]: (1) data visualization, (2) landscape visualization, (3) high-realism landscape visualization and, (4) 3-D visualization of solid objects. Instances of 3D

systems, discussed below, incorporate a visualization product that falls into one of these categories.

1.2.2.2 Some 3D GIS Systems

While the input, storage, and 2D output of GIS data have seen remarkable progress, the analysis of GIS data in a 3D setting still requires significant development to yield new insights into the relationship between 3D data [7]. By adding the dimension of height to a footprint of 2D feature data, it is possible to create a 2.5D terrain model. Such a model with relevant attribute data can be used in a similar way to a GIS operating on 2D thematic data. The Environmental Systems and Research Institute (ESRI) developed Arcview 3D Analyst [8] for visualizing 3D data using a Triangulated Irregular Network (TIN). The 2D spatial data is draped over the terrain model, and a perspective view is created based on a number of user-defined parameters. Alternately, 2D primitives are extruded by the value of an attribute parameter of the features. VirtualGIS [9] within the Erdas Imagine makes possible dynamic viewing of the terrain data with fly-through and querying capabilities. In both cases, the basic technique of creating the 3D model is the same. Essentially, existing elevation databases such as a Digital Elevation Model (DEM) or

Triangulated Irregular Network (TIN) are draped over 2D feature themes, enabling dynamic visualization of spatial data in a small-scale environment. The 2D feature themes in such a case may be obtained from an entirely disparate source. If the DEM or the TIN is not available, then it is necessary to build the elevation data using a different tool. This approach does not involve data extraction. Neither does it require an integrated set of plan and elevation data. However, Erdas Imagine has added a new module that includes tools for construction of 3D models by raising 2D footprints of features. The elevation information is computed in real time from an overlapping pair of images. This system provides only a flat screen-based virtual environment without immersion.

1.2.3 VR Systems

This approach involves creating either a model-based or an image-based virtual environment and provides facilities for the analysis of spatial data.

The present trend is to build a truly 3D GIS or a virtual GIS. Current research developments include navigation in a virtual environment and simple querying of the attribute database. As yet, the combination of GIS tools and 3D visualization and interaction remain

insufficiently explored. They tend to complement each other, yet, there is little exchange of information between them. Ervin outlines three characteristics for testing true representations of a GIS in the VR environment: immersion, navigation, and interaction. Only a few of the currently developed virtual GIS systems fulfill these characteristics.

Karma VI [10] is a VR interface on ESRI's Spatial Database Engine (SDE) that supports visualization, manipulation and editing of standard GIS data on the PC platform as well as in a VR environment. The latest version is known as K2VI. The system uses a multi-view (plan view, model view, worldview) mode approach where each view mode has an optional VR display. The plan view displays a traditional 2D representation of the feature data. In the model view, these 2D features are extruded by one of their attribute values, creating 2.5D geometry. In the worldview, the 2D polygons created from the plan view, are used to position 3D Computer Aided Drafting (CAD) objects. The CAD objects are linked to the original GIS shapes using a separate table in SDE. A limited number of runtime interactions are provided. It does not provide run-time editing capabilities. Therefore, it utilizes the already existing GIS database and does not provide an integrated methodology for building the database from existing raw information sources such as video images and GPS positions of camera locations.

At times, applications involving data visualization and analysis are researched for specific purposes. Doug Johnson and Wesley Reetz [11] developed an application involving hydrologic modeling of overland flow. The application accessed and displayed geographic data and displayed a simulation of the flow. The interface was built for the Cave Automated Virtual Environment (CAVE) so that many persons can simultaneously experience the interactions in the immersed environment. As mentioned above, this is an example of a specific application of hydrologic modeling, which is not a generic VR system, to visualize and analyze geographic data.

David Koller et al. [12] created a Virtual GIS at the Georgia Institute of Technology. This system provides interfaces on a PC as well as in a virtual environment. It provides visualization and interaction with spatial data in a VR environment. It can query a GIS database, however, it does not support real-time editing and analysis of data in the virtual environment.

The Digital Mapping Laboratory at Carnegie Mellon University, Pittsburgh, has developed a system for automating a virtual world database for ground based simulations by integrating information from various sources, such as digital map data, aerial and satellite imagery, detailed line drawings, and ground based photography [13]. The

procedure involves two steps: creating a bare-earth terrain representation of an existing or augmented digital elevation model, and overlaying the transportation network model with models of natural and cultural features, such as tree canopies, lakes, agricultural fields, buildings, towers, and telephone lines. Intensification of the spatial database by integrating cultural features extracted from aerial imagery with existing spatial data (possibly at extreme differences in spatial resolution) requires a rigorous geodetic model. Intensification also requires traditional cartographic tasks such as feature generalization, aggregation and replacement. The primary objective of this research was to generate a virtual world database without a real-time user interaction. In the absence of a user interaction, the primary use of such a virtual world would be for visualization and navigation and it has very little data analysis capability.

Hirose et al [14] developed an image based VR system. It included a vehicle mounted image recording system consisting of 8 cameras, a GPS sensor for position data and a 3-angle and 3-axis oscillating gyro angle sensor for orientation data. The time codes of the GPS units and image sensors were logged by an onboard personal computer. The images from 8 cameras pointing to different directions on the horizon were synthesized into a panoramic image after removing

image distortions. When the user looks around, corresponding sections of the panoramic image are displayed, and when the user moves, the appropriate panoramic image set is selected from the image database by using the position data. As the user moves, image morphing between successive acquisitions of images maintains continuity in the view of the VR environment. This was also primarily a visualization tool and has very little correspondence to positioning of individual features and analysis.

1.3 The Problem

The methodologies reviewed so far are not suitable for visualizing and interacting with spatial data. Even though digital photogrammetry also provides means of collecting precise spatial data, it is not a complete system for visualizing and interacting with these data. Existing traditional GIS interfaces are also inadequate. On the other hand, VR systems developed for handling spatial data are either not sufficiently generic to handle every kind of data source, or they are not able to interact and manipulate the spatial data. Therefore, a new methodology needs to be developed to create a VR environment that will provide immersion, navigation and interaction.

Many systems have preferred the CAVE environment. CAVE is a fully immersed, multiple screen projective display system that offers stereoscopic surround projections to several users simultaneously. It satisfies the ideal requirements of a VR environment, which are immersion, navigation and user-interaction. Therefore the CAVE may be considered the most ideal VR system for interacting with spatial data currently available.

1.4 Roadside Features Data – A Case Study

Management of an inventory of roadside feature data involves the collection of huge amounts of data by disparate methods. With the onset of automated data acquisition techniques for the collection of roadside feature information, there is a need for methods to visualize these data. An investigation into automated data acquisition of roadside features [15] reviewed the state of the art data acquisition and visualization technologies including, but not limited to, Geographic Information Systems (GIS), Global Positioning Systems (GPS), high-resolution digital cameras, and Inertial Navigation Systems (INS). However, the method of interactive display of the collected data was found to be unsatisfactory. A visualization environment needs to be developed that retains the GIS capabilities of editing and analyzing

spatial data and provides the user with enhanced capabilities to visualize, interact and manipulate features.

1.4.1 Iowa DOT Video-Log Data Inventory

Iowa Department of Transformation has been building a huge inventory of digital images of roadside features. These images are taken from a mobile van. The positions of the images are obtained from a Real Time Kinematics (RTK) GPS system. This is an ongoing process of an As Built Survey, where already existing features are surveyed. It is important that data so collected are put to the maximum possible usage.

1.4.2 Need for VR

The previous discussion shows that current practices of interactive visualization of roadside feature data in the form of 2D maps, CAD drawings, digital images and tabular data, and streaming image sequences can be improved. A virtual roadway environment can be developed, which contains GIS capabilities of editing and analyzing of spatial data and provide users with enhanced capabilities such as visualization, interaction and manipulation of feature objects in the immersed 3D environment.

1.5 Research Objectives

A VR application with integrated GIS functions would include such aspects as a geometric model of feature objects in a scene, attribute database of feature objects, interactive editing of the scene, and analysis of the geographic data and navigation. Digital photogrammetry can provide positional and geometric information while remote sensing techniques help in collecting attribute information to build a VR application for spatial data.

The objective of this research is to develop a methodology for efficient visualization and analysis of spatial data using the case of the existing roadside feature inventory database of the Iowa DOT. The methodology includes several components, which are described below.

1. Develop an inexpensive and efficient procedure for calibrating the digital camera used for data collection,
2. Develop a cost-effective procedure for extracting location and geometry information of feature data from digital images using soft-photogrammetric techniques.
3. Compare and validate feature position information extracted from the previous step to ground truth data with a Total Station survey.

4. Integrate information of feature position and geometry with existing data from engineering drawings of highway structures such as bridges.
5. Create a VR application for visualizing roadside feature data in the immersed environment of the CAVE.
6. Provide user-interaction to edit the roadside features and to navigate through the scene in the virtual environment.

1.6 Thesis Organization

The fields of research relevant to this study include VR, GIS, As Built Surveys for data collection, calibration of digital cameras, 3D reconstruction of virtual worlds, and soft-photogrammetry. Chapter 2 includes a general review of the current technology of VR. An As Built Survey is an essential component of data collection for building a VR system for real world content that includes spatial feature objects. Chapter 3 contains reviews of various methods of an As Built Survey for roadside feature data collection that are relevant to the subject matter of this study. An inalienable part of photogrammetric data collection is camera calibration procedures. Theories of calibration of digital cameras as well as current research and development efforts in the area of camera calibration are included in chapter 4. This chapter

also outlines a detailed methodology adopted in this research for calibrating the digital camera used in the video-logging van. Building a virtual world for spatial data makes it necessary to extract positional and attribute information about the scene. A procedure for soft-photogrammetric feature extraction used in this research is described in chapter 5. Remote sensing techniques of digital image processing for data collection and information extraction are discussed in chapter 6. Chapter 7 discusses the current research techniques and the steps adopted in this research in the area of modeling spatial data for the VR environment. Results and conclusions are included in chapter 8.

CHAPTER 2 VIRTUAL REALITY

The term virtual reality describes different artificial environments depending upon the context of its application. Primarily, it is about interaction between humans and computers. It has potential for novel interactions that are not technologically possible today. In this chapter, different virtual reality systems are presented, described and discussed with special reference to the multi-projection immersive environments C2 and C6.

2.1 Visions of Virtual Reality

The term virtual reality espouses different visions in the minds of scientists and researchers, some of which are realities today. In the future, virtual reality systems are expected to further enhance and simplify the ways humans interact with computers. For example, in the field of automobile design, virtual reality environments are being used to test the interior design of cars. The designers look around in the virtual interior of a car and decide on possible improvements or

changes. Virtual reality may make it possible to test a mechanical design of the car without physically producing a prototype, to perform every kind of interaction possible in a real car including performance testing and evaluations of the vehicle.

Virtual reality may make it possible to create a scene of distant places for users to experience without visiting the actual location. A virtual trip to the moon, for example, or to the Seven Wonders of the World may be possible with the comfort of staying at home. Such environments may also serve as educational tools.

In a virtual setting, virtual reality brings several people together who are geographically separated by long distance. This can enhance the way people conduct business. Instead of traveling to attend business meetings, people can enter a virtual setting to see and interact with the virtual embodiment of others as they would in real life. Over time, this way of meeting and interacting among people may become the norm in communication.

Virtual reality may also change how scientists and researchers view and analyze spatial data to make decisions for managing natural and manmade resources. It may be possible for people to interact with spatial features and change spatial relationships among a group of objects in a virtual setting by modeling different scenarios.

Virtual reality has opened the horizons for many such exciting possibilities. However, there are technological challenges that researchers and scientists must overcome to make these visions a reality. The research presented in this thesis deals with application of virtual reality technology in the analysis of spatial feature data.

2.2 What Is Virtual Reality

"A virtual reality system is a single or multi-user system, capable of producing an interactive, immersive, multi-sensory, and 3D synthetic environment that uses position-tracking and real-time update of visual, auditory and other displays (e.g., tactile) in response to the user's motions to give the user a sense of being "in" the environment" [16]. Here, the term "Virtual Environment" is used instead of "virtual reality", because of the common misconception of the term "virtual reality". This definition encompasses a few definite features that contribute to a virtual reality environment.

Virtual reality systems must be **interactive,** which allow the user to input changes with immediate modifications. Therefore the user can interactively guide the application putting the user in control. Because the user's action modifies the virtual environment, the user

gets a sense of connection to the application that makes it seem natural.

Virtual reality must be **immersive**, an immersion so convincing that the user is willing to accept the virtual environment for the real one, and participates in it. Even though the term "immersion" sounds all encompassing, there can be three separate aspects involved with immersion: perceptual immersion, a sense of presence, and a sense of engagement.

Perceptual immersion refers to the user actually having a perception of the computer generated virtual environment conveyed by the system through sensory cues. Therefore, the virtual reality environment should be capable of providing appropriate sensory input to the user.

When the user senses the virtual world in the user position inside the environment as the reference, it provides the sense of **presence**. The user seems to be a part of the environment.

The last element of immersion is **engagement**. Engagement is the extent of involvement that the user feels in the virtual reality environment.

Virtual reality can provide cues to multiple human sensory organs and is therefore, multi-sensory. The user may get input from

the environment to simulate the following senses: visual, auditory, haptic, smell, and taste. The more sensory inputs the greater the level of immersion. Involvement of more senses in the process of experiencing the environment enhances the completeness of the virtual representation of the world. Therefore, the multi-sensory nature of the virtual environment provides a higher degree of engagement and greater sense of presence.

The computer must synthesize the virtual reality environment at the run time of the application. The displayed world is not static and pre-constructed but modified by user input. This is why virtual reality is **synthetic**.

A virtual reality system uses several methods of inputs simultaneously, thus making it capable of multi-modal interaction. Multi-modal application makes the interaction more natural than in a non-virtual reality application.

2.3 Why Virtual Reality Is Different

Unique characteristics set apart virtual reality applications from other conventional interactive applications. These characteristics form the basis of special requirements for the virtual reality applications discussed below.

2.3.1 User Oriented Approach

In a virtual reality application, user perception of the environment is the utmost concern. The user must perceive the application in the correct way. This is the single most important aspect of virtual reality applications. If the user perceives the environment in an improper way, any other issue, including efficiency of the algorithm, robustness of the application, or ease of use etc., is of no value, and the application is faulty.

Another aspect of the user-centered approach to virtual reality applications is that stringent degrees of performance during the regular response time of the application must be maintained. Otherwise, the user may suffer from undesirable physical effects such as dizziness. Such a requirement is normally not necessary in a traditional interactive application because, in such a case, the user will be annoyed at most without any physical harm.

2.3.2 Integrated Environment

A virtual reality application usually uses different devices and system components that behave differently. Among them, each component needs different degrees of system interaction. Each component also differs in performance, robustness, interfaces, and

ease of use. Virtual reality systems need a working integration of such disparate components.

2.3.3 Complex System

The virtual reality system consists of a wide range of hardware components integrated with many advanced software tools and algorithms. The task of getting all these disparate components and systems to work as one single unit makes the virtual reality system an extremely complex one to develop and perform without fault.

2.4 Anatomy of a Virtual Reality System

A virtual reality application uses a combination of hardware and software components to present a virtual environment to the users. The software components manage the hardware components of the systems to create the virtual world. The hardware components basically perform two jobs: obtain user input through user-controlled input devices, and output a multi-sensory illusion of the virtual world in response to the user input.

2.4.1 User Input

The user input to the system is primarily of two types: user position information, and user interaction information. User position computes and synthesizes the virtual world based on the current user position. The user interaction information, in the form of user orientation and custom inputs, allows the system to modify the synthetic world accordingly. While user position information is captured through a tracking system, the user interaction information is received from gloves, wands, and such other devices.

2.4.1.1 Tracking system

The tracking system generally consists of a device called the tracker that moves in space depending on user activity with a base unit that remains stationary. The tracker is usually attached to the user. The tracker system computes the position of the tracker or trackers with reference to the position of the stationary base unit, and accordingly the virtual world is synthesized so that the tracker is part of the environment.

2.4.1.2 User interaction

The input of the user depends upon the type of user action such as touch, voice, movement etc. Even though the primary interaction devices involve input from the hand, other devices that involve such methods as speech recognition, bio-signals and locomotive inputs are also evolving.

The hand is a natural method that humans use to interact with their environment. While the hand position may be used to perform collision detection, "gestures" may be used to convey other input information. The glove simulates the user inputs through the hand gestures. Gesture recognition software recognizes the user action from a set of predetermined gestures used to interact with the system. This information is passed on to the system so that the virtual world may be re-synthesized as desired by the user.

Another user interaction device is the wand, which can capture user interaction in the form of analog or digital values. It may also capture the user orientation so that appropriate view of the virtual world may be synthesized and presented to the user.

As more inputs become available, the virtual reality systems will be capable of handling different types of input devices simultaneously.

2.4.2 Output of the Synthesized Virtual World

Depending on the user position and user interaction information, the virtual reality system synthesizes the virtual world and outputs a multi-sensory illusion of the virtual world to the user. The output may be one or a combination of visual, auditory tactile, haptic, or other sensory formats. The visual display is the most common format of output, sometimes combined with localized sounds. Visual display devices include projection-based systems, such as Head Mounted Displays, and Cathode Ray Tubes. Some of the most common types of visual display systems are described in the next section.

2.5 Virtual Reality Systems

Different classes of virtual reality systems are used today and briefly described below.

2.5.1 Fish Tank

A fish tank virtual reality is the most basic type of virtual reality system (See Figure 2.1). It is essentially an extension of the traditional desktop computer system and is, therefore, known as the desktop virtual reality system. The system usually includes a graphics

workstation and the virtual world is displayed on the desktop monitor. A head-tracking device tracks the head position of a single user. The virtual world is synthesized based on the input information from the tracker device. The display may be either monoscopic or stereoscopic. There are certain advantages and disadvantages of having a fish tank virtual reality system.

2.5.1.1 Advantages

The hardware is part of a traditional computer system; therefore, it is relatively **inexpensive**.

Only a few more devices are to be added to make the traditional computer system the virtual reality system. Because the average user is usually familiar with the procedure for setting up a desktop computer system, it is comparatively **easy to set up and run** the system.

Higher display resolution of desktop monitors allows applications to display finer graphic details such as small texts with **greater clarity**.

Even though the system responds to interactions from only one user, it accommodates **multiple users** to view the virtual world.

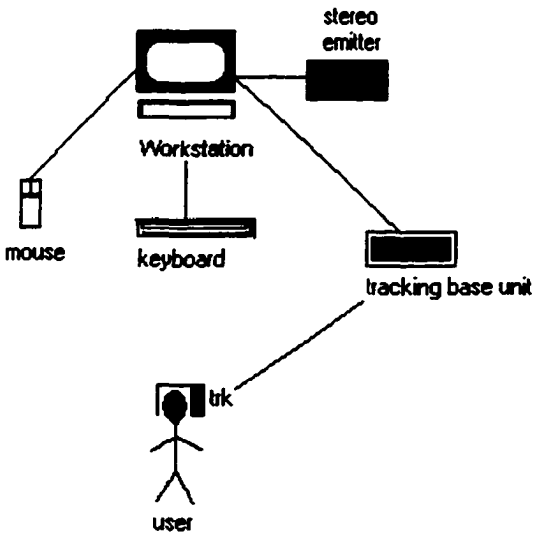

Figure 2.1 Fish-tank virtual reality system

2.5.1.2 Disadvantages

The small monitor size restricts the user's field of vision. The smaller field of view results in a **limited sensory illusion of immersion.**

The system tends to provide imperfect stereoscopic viewing at the edges because of one eye missing the view, which is known as **stereoscopic frame violation**.

2.5.2 Head Mounted Display (HMD)

A head mounted display system is housed inside a helmet to be worn by the user. The helmet effectively shields the user's view from the outside world, which helps to create the sense of total immersion. The system displays the virtual world onto two screens that are placed directly in front of the user's eyes inside the helmet. Figure 2.2 shows the layout of a HMD system.

Additional requirements of a head mounted display system include a high frame rate and synchronized stereo frame display. A lower frame rate and non-synchronized stereo display in a head mounted display system may promote cyber sickness in the user due to the fully covered field of view.

2.5.2.1 Advantages

By effectively isolating the outside world from the user's field of vision and placing the screens directly in front of the user's eyes, the head mounted display virtual reality systems creates a **complete visual immersion**.

This system **eliminates stereoscopic frame violation** by avoiding any projection surface.

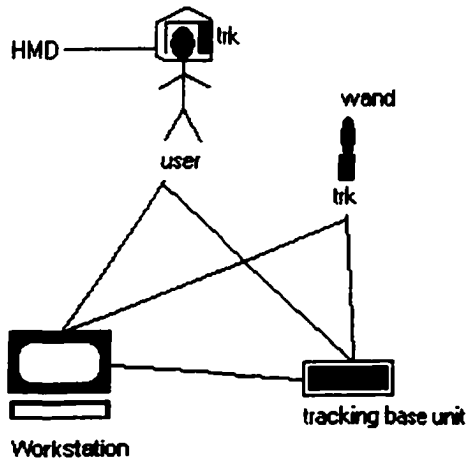

Figure 2.2 Head Mounted Display virtual reality system

Since the helmet houses most of the complex hardware, there are very few other devices to set up. Therefore, the head mounted display system is **easy to set up and maintain** compared to other more complex virtual reality systems.

2.5.2.2 Disadvantages

The weight of the helmet may cause physical discomfort and strain after prolonged use. The system creates an **imposition** on natural movements of the user.

The system acts as a total **barrier** between the user and the outside world.

Only a **single user** can use the system at a time. Therefore, it is not suitable for applications that need a group of people to interact inside a single environment.

2.5.3 Single Screen Projection

A single screen projection system (See Figure 2.3) displays the virtual world on a screen or tabletop. While sometimes the screen display is named a power wall, the tabletop display is called a virtual workbench [17]. The user is tracked and the view is synthesized accordingly. The user can interact with the system with such input devices as the wand and glove. It has a much larger field of view. A low frame rate is capable of making the user dizzy during interactions with the virtual environment. It is usually more difficult to generate stereoscopic frames on a single screen projection system than in a fish tank system.

2.5.3.1 Advantages

The projection onto a large screen creates a **large field of view**, which creates a greater sense of immersion in the virtual environment.

Because of the larger space to interact with the virtual environment, the scene may be rendered at the **true scale**. This provides better understanding of sizes of the virtual objects.

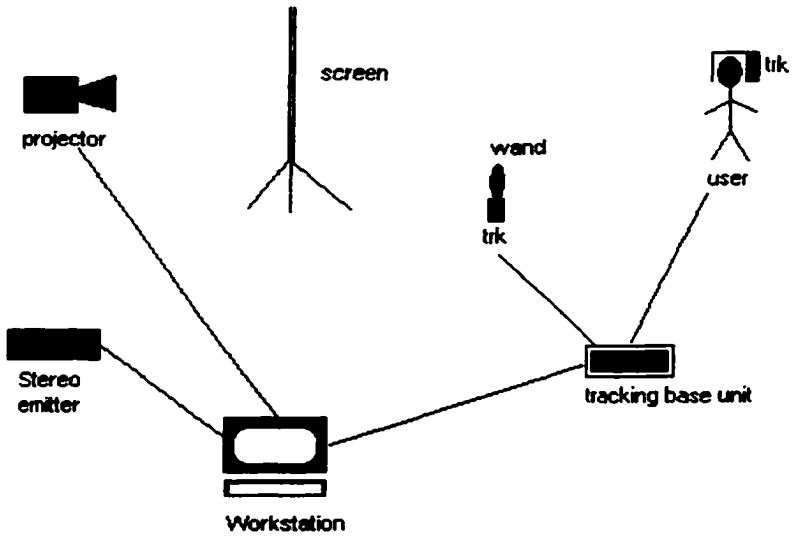

Figure 2.3 Single projection virtual reality system

Unlike in the head mounted display system, there are no devices that impose physical discomfort to the user. Therefore, this system is **non-invasive** on the user.

Also, **multiple users** can simultaneously view a scene in a single screen projection system.

2.5.3.2 Disadvantages

Stereoscopic frame violations occur at two sites: near the edges of the projection surface and when the hand of the user hides a sight from one of the eyes. This violation creates incorrect depth

perception of objects in the area where the violation occurs.So the **user's movement is restricted** to a small area in front of the projection surface.

2.5.4 Multiple-Screen Immersive Projection Display System

A multiple screen projection system involves projection of images onto multiple adjoining screens or walls (See Figure 2.4).

Most systems provide stereo display of images. One or more users may be tracked to generate synthesis and the appropriate display of the virtual world. The system involves a much greater degree of complexities because of the need to synchronize images projected onto different walls. The job may be much more difficult depending upon whether the images for the different walls come from a single graphics engine on a single machine or from multiple graphics engines on a single machine or from multiple graphics engines on multiple machines. The synchronization among the images is necessary to correctly display and update each display simultaneously.

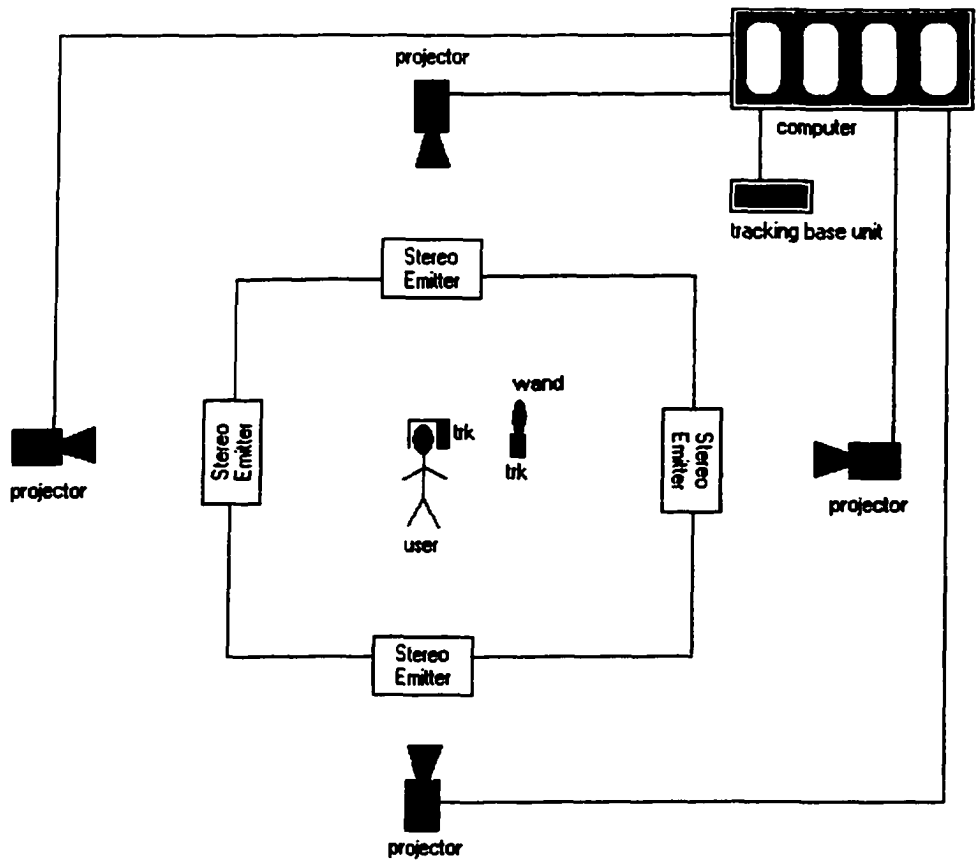

Figure 2.4 Multiple screen projection virtual reality system

2.5.4.1 Advantages

The multiple screen projection system has a much **larger field of view** covering the entire range of visual field, possibly in all directions.

Similar to the single screen projection system, the hardware devices are **non-invasive** with no user discomfort, which is very helpful for extended use of the system.

Multiple users can share the environment simultaneously, while a large space accommodates a larger group of people. That is why it is very suitable for applications that need a group of people to be in the virtual environment to fully utilize the potentials of a specific application.

2.5.4.2 Disadvantages

This kind of environment **requires a larger space** to set up the operation of the system.

Stereoscopic frame violations occur when a part of the scene is obstructed from the view of an eye. Such occlusions create incorrect perception of depth in the environment.

Since the multiple screens projection system involves integration of several hardware components including the walls and projectors, each of these components need to be precisely calibrated and adjusted for the correct update and display of the virtual scene.

2.6 The CAVE

The CAVE is a projection based virtual reality system. It was first developed at the Electronic Visualization Lab (EVL) at the University of Illinois, Chicago. Carolina Cruz-Neira, Dan Sandin, and

Tom DeFanti and other students and staff of EVL created it. [18]. The CAVE was first demonstrated at the SIGGRAPH '92 conference. Since then, many caves have been constructed at various sites. The existing caves are listed in Appendix [To be numbered]. In a CAVE, it is possible for many people to view a virtual world simultaneously and share the VR experience. While one user is the pilot, the other users are passive viewers.

Iowa State University has two CAVEs, C2 and C6, which were constructed based on research done by Dr. Carolina Cruz-Neira [19]. The following sections give a brief description of the C2 and C6 virtual reality systems.

2.6.1 C2

C2 is The CAVE that uses a projection based virtual reality system. It provides immersive synthetic environments for many users to use the system simultaneously, and navigate and interact in virtual worlds. Figure 2.5 shows a scene of the C2 [20].

The system has a 12 by 12 foot stereoscopic floor area surrounded on three sides by stereoscopic projection walls and a three dimensional sound system. Four projectors project stereographic displays on the three walls and the floor. The images on the three

walls are projected from behind while those on the floor are projected from the top. A series of mirrors are used to optimize usage of floor area by reflecting the projection light beams.

Figure 2.5 A view of the C2

A view of the projected stereographic display through lightweight Crystal Eyes shutter glasses creates the perception of three-dimensional immersion. Infrared transmitters synchronize the glasses with the projectors. The glasses and projectors are designed to alternate at a rate of 60 Hz.

Three-dimensional sound provided at C2 enhances the user's perception of immersiveness. Directional sounds are produced through four speakers mounted at each of the four top corners of the area.

2.6.2 C6

Like the C2, C6 is also a CAVE that uses a projection based virtual reality system. It provides immersive synthetic environments for the user to navigate and interact in virtual worlds. However, unlike C2, C6 has a 10 by 10 by 10 feet arena surrounded by stereoscopic projection surfaces on all six sides. Six projectors are mounted to project onto all six projection surfaces of the C6 at a frequency of 96 Hz. Therefore C6 provides a 360-degree immersion to display virtual environments. Figure 2.6 shows a sketch of the C6 [21].

The C6 has powerful computational abilities carried out using an SGI Onyx2 computer with six InfiniteReality2 graphic display generators. This machine has 24 units of 400MHz R12K processors with 12 Gigabytes each for system memory. Antialiasing and volume rendered graphic applications are supported by the IR2s, each of which has four 64Mbyte raster manager cards installed. High bandwidth

gigabit networking is also supported by connection to the Internet2/VBNS. A file server supports large file access.

Unlike the C2, the C6 uses a wireless tracking system. The sensors attached to the glasses and the wand track the user's position, orientation and interactions. The viewing system is similar to that in C2, except the users wear wireless glasses. These glasses are active LCD shuttering glasses of two kinds: 60GX glasses from Nuvision and CrystalEyes glasses from StereoGraphics.

Figure 2.6 A view of the C6

The C6 supports spatial 3D surround sound through 8 speakers located at each outside corner of the C6. All users can hear the 3D ambient sound produced by these speakers. In addition, each user

may be tracked through wireless headphones to hear 3D sound for individual users position in the C6.

In this research, C6 is used to demonstrate the VR application for an As Built Survey of roadside features and management of roadside feature inventory.

CHAPTER 3 AS BUILT SURVEY

Usually, construction of virtual worlds has been confined to environments with synthetically generated contents. However, recent advances in computer graphics hardware encompass three-dimensional modeling and rendering software and three dimensional display capabilities. Because of these developments, there has been an increasing interest in creating virtual worlds based on real world objects and scenes. New research is being done on various aspects of such virtual worlds.

Important aspects in the construction of a virtual world based on real world content include accuracy of geometry and sense of realism in display. Digital photogrammetric techniques have been studied to create a model-based approach for generating virtual worlds. Jeyapalan et.al. [22] showed that digital photogrammetry is useful for data collection in a highway setting. This chapter reviews As Built Survey methods for collecting existing spatial data, discusses the role of digital photogrammetry in these methods, and describes a specific data

collection system, namely, the Video-logging system of the Iowa Department of Transportation. A brief discussion concludes the chapter.

3.1 What Is An As Built Survey

The term As Built Survey is generally used to mean the type of topographic surveys showing post-construction environments of engineering projects. An As Built Survey has been a very useful tool for monitoring inventories of resources and for obtaining data of existing real world features for building the virtual model. This research looks at the visualization of roadside feature data. Even though the database of video-logging images with GPS positional information is available, it is necessary to find out if this is an efficient and cost effective method for the As Built Survey.

Recent advances in GPS, Total Station and soft photogrammetry enable surveyors and photogrammetrists to undertake As Built Surveys of roadside features at a cost that is affordable within the maintenance budget of state, city and county agencies. Typically, a preliminary survey for road development and construction costs about $15,000 to $20,000 per mile. An As Built Survey is attractive if the cost is less than $ 1,000/mile. Jeyapalan et al discuss the use of Total

Station, video logging and soft photogrammetry for an As Built Survey [23] of roadside features in rural, urban and metropolitan settings. A Total Station survey was found to be optimal for collecting data to create 2D GIS models showing roadside features at a scale of 1" = 25' or smaller. On the other hand, Real Time Kinematics Differential Global Positioning System (RTK-DGPS) was found suitable for mapping at a scale 1" = 50' or smaller. Both systems are time consuming in the field. Soft photogrammetry with digital video logging imagery can be used to map roadside features at 1" =25' or smaller. It saves field data collection time; however, it requires calibration and stereo data collection time in the office. A mapping accuracy of 1" = 100' is sufficient in a rural area whereas a mapping accuracy of 1" = 50' and 1" = 25' may be required in urban and metropolitan areas, respectively.

Real world data for creating the 3D model may be collected using either a single sensor or a host of sensors. Even though it would have been ideal to obtain the required data with a single sensor type such as Charged Coupled Device (CCD) cameras, thereby obliterating the need for integration of data from disparate sources, the use of data from multiple sensors are investigated.

A survey of automated data acquisition techniques for mapping roadside features revealed that a host of technologies are being

currently used to achieve automation in collection of roadside feature data (15). These technologies combine different and sometimes disparate techniques to achieve the desired results. In most cases, use of a Global Positioning System (GPS) in one mode or the other is indispensable. Other sensors used for supplementing the GPS positioning include digital CCD cameras, video cameras, Inertial Navigation System (INS), laser technology, odometers etc. All these data can be suitably incorporated in building a virtual world. A discussion of the salient features of each of the technologies and their capabilities as reported in published articles are presented below.

3.2 Review of As Built Survey Methods

GRAFTEK Italia of Villanterio, Italy designed a mobile mapping system named the DAVIDE [24]. This van was developed for applications such as road-sign surveys or in preliminary work for laying down fiber-optic cable. It can perform data acquisition and image processing on the road. It can acquire images from the surrounding landscape and road network, compress and store them on a digital tape complete with position reference and time stamp. Four fixed CCD cameras pointing to the Left, Right, Front and Rear, two fixed digital cameras and one movable CCD camera are mounted on

the van. The cameras acquire data continuously on voice command. The van's differential Global Positioning System receiver, inertial platform and dual odometers give it a position accuracy of 1 m. Three computers are used and they are interconnected by Ethernet network. One of them is Pentium based containing a voice interface, a Man Machine Interface (MMI) and maps. The MMI was developed using LabVIEW graphical programming software of National Instruments, Austin TX. The other two computers are Macintosh Quadra 950s. One is used for JPEG image compression and the other for image processing.

The Vanguard Mobile Survey System is being used by the Georgia Department of Transportation [25]. The vanguard system allows the user to conduct a no contact laser survey from a van parked on the shoulder of the road. This eliminated the need for lane closure. The system was used for rehabilitating 330 miles of highway, including 60 miles of high-occupancy-vehicle- lanes of Interstates 75 and 85. The PaveMoss software read data directly from the Vanguard, thus accelerating the process of using the acquired data.

A road-sign inventory project [26] in a suburb of Melbourne was discussed at the 18th Annual AM/FM International Conference, held in Baltimore, Maryland, in March 1995. Phillip J. Lack of rapid Map

Australia Pty Ltd. described the technique of combining laser gun mapping systems with pen based computing to increase data collection efficiency during the inventory project. By pointing and shooting a laser gun, operators were able to map in dangerous traffic regions, record the measurements directly into digital form, and process the inventory using Rapid Map's Rapid Sign software. Then they go back to the field with a pen-based computer and conduct a more detailed survey. The pen computer detailed 26 specific attributes, including a digital photo, if required. On an average, less than one minute is required to collect each sign. Several operators may work simultaneously on the system. The cost of acquisition is stated to be $5-10 per feature.

The John E. Chance and Associates Company developed the TruckMAP System [27]. This system is an integration of three components: the Positioning System, the Imaging and Ranging System, and the Processing System. The positioning system uses either OMNI-STAR Differential GPS (DGPS) or 'On-The-Fly' Kinematics GPS (OTF KGPS). It establishes the positions of the objects in real world coordinates, using a reflector-less laser rangefinder and a high accuracy azimuth engine. Total Station positioning is used in case of sky blockage and non-availability of GPS. The system uses two rover receivers in the vehicle. The JECA C-band satellite receiver, OMNI-

STAR, is used for receiving standard RTCM-104 differential corrections. It uses a network of differential reference stations and operates independent of base stations. To provide sub-decimeter horizontal and vertical accuracy, the OTF-KGPS system utilizes local base stations. The Imaging and Ranging System consists of a reflector-less laser rangefinder with a video camera mounted on top. The laser is aimed at specific objects up to 200 meters away, the camera is aligned and an image is shot. A digitized position and time reference is recorded on each frame of video. The processing system is capable of processing in real time all the data recorded in digital format and output into any file format required. Custom software transforms the GPS World Geodetic System 84 datum coordinates to any local coordinate system.

The University of Calgary and Geofit Inc, a high-tech company in Laval, Quebec jointly developed a mobile highway mapping system [28]. The system named VISAT stands for Video-Inertial-SATellite and integrates inertial and GPS technology with video cameras. The total system consists of the data acquisition system VISAT and a data processing system called GEOSTATION [29]. The Navigation component of the VISAT prototype system consists of two ASHTECH Z12 GPS receivers and an LTN 90-100 strap down INS. The GPS, when operated in the differential mode, is capable of providing accurate position and

velocity information when the carrier phase is used. The accuracy degradation of GPS due to poor satellite geometry, cycle slips, satellite outages, and dynamic lag during maneuvers is overcome with integration of GPS with INS. For short time intervals, INS yields accurate velocity, position and attitude; but to achieve improvement in long-term accuracy at all frequencies, the INS data that tend to drift at low frequencies, are updated periodically with GPS velocities and positions. The imaging component of the VISAT prototype consists of three COHU 4912 CCD cameras with 512 X 480 resolutions to record features along the highway within a corridor of about 50 m. The cameras send three simultaneous images per second to the Matrox IMAGE-CLD frame grabber at the rate of 0.75 MB/sec. The imaging component is capable of grabbing and storing three images to a SCSI hard disk in 0.5 sec. Each of the images relate to a unique position of the van. The integrated GPS/INS/CCD cameras makes it possible to determine the 3-D coordinate of any object in the field of view of at least two CCD cameras without the need of external control. The pilot project results indicated that highway velocities of 60 km/hr could be maintained with adequate data transfer and target positioning in a post-processing mode at a workstation. Run-to-run and day-to-day

repeatability achieved in the pilot project is about 25 cm (RMS) in horizontal and about 5 cm (RMS) in height.

The Center for Mapping of the Ohio State University developed another mobile mapping system [30]. The prototype for a highway mapping system, GPSVan is a mobile system for creating digital road maps and highway inventories while being driven at regular highway speed. The GPSVan integrates a global positioning system receiver, a gyro-based inertial system, a wheel counter, a digital stereovision system, and color video cameras in a van. The GPS and the inertial systems achieve absolute positioning. Post processing yields continuous road alignments as well as the orientation of the van even in areas of satellite signal blockage by trees, buildings, tunnels or bridges. The digital stereovision system allows positioning of every feature in the field of view of the camera pair in three dimensions relative to the van. The position and attitude of the GPSVan is used to transform all features into a global system. The roadside features such as traffic signs, intersections, and bridges can be collected and stored as attributes related to the current position of the van by the operator hitting a button on the touch screen when the van passes the desired feature, or, feature may be identified in color video logs. Further research is under way to develop advanced feature extraction functions

to automatically detect road edges and centerlines, and to read text on traffic signs [31]. The absolute positioning of the road alignment is 1 to 3 meters. Stereoscopic positioning with the vision system yields positions of up to 50 cm in front of the van. No object control is needed as the GPS and gyros measure all orientation parameters.

Williamson County, a rural county located in the south-central part of Illinois, has developed a countywide Geographic Information system (GIS) using mobile mapping technology for use by emergency service agencies, and the county assessor's office [32]. The county used the mobile mapping system developed by the Center for Mapping at The Ohio State University. The choice to implement the mobile mapping system, among other reasons, was due to the modest cost of the technology, and the ability of the system to collect a wealth of information on road features that are mapped.

A new GPSVan™ was constructed for General Railway Signal (Rochester, NY), a licensee of the mobile mapping technology of the Ohio State University [33]. The system includes several modules: a GPS and dead reckoning system, a stereovision system (SVS), and a video system. The digital SVS employs two fully digital, full-frame, non-interlaced CCD cameras. The host computer controls both the exposure time and shutter speed. A signal processing subsystem reads

the image data from the cameras and stores them on an 8-mm tape. The post processing, including the photogrammetric processing (typically 3D-feature extraction) is done offline by the TransMap software.

The Iowa Department of Transportation (IADOT) in 1990 explored possibilities of using video technology as a resource for states to manage highway facilities [34] replacing the traditional 16 and 35 mm film format used in photo logging. The Federal Highway Administration sponsored the project. One of the major objectives of this study was to examine whether the state of art video technology could capture and store usable roadway images while operating in a mobile environment. Elimination of film conversion in the case of film format photo logging had the potential of lowering the cost by $4 to $5 per logging mile. In addition, the image would be available immediately without delays caused by film developing and transferring data from the image.

The Synectics Corporation developed a Photogrammetric Laser System (PLS) under a National Science Information grant [35]. PLS is supposed to significantly reduce the cost of rapidly measuring three-dimensional surfaces. It may be applied as either a stationary observation unit or as a mobile unit. The laser illuminates a small area

on the surface being measured to create a target. The position of the target is automatically determined by the modified stereo cameras and recorded simultaneously with a digital image of the scene. The PLS produces data that are directly compatible with most three-dimensional data processing systems such as Computer Aided Design (CAD), Geographic Information System (GIS), and others. This system greatly increases the speed of and accuracy of surface data acquisition, reduces costs through automatic measurements, and doesn't deviate from conventional photogrammetric process.

Applied Analytic Corporation developed a Position and Orientation system for Land Vehicle (POS/LV) [36]. POS is a Kalman filter-based integrated navigation system. It is designed for land, marine and airborne survey applications. POS computes real-time position (latitude, longitude, altitude) and orientation (roll, pitch, heading) solution combining a Kalman filter with inertial navigation algorithms. The inertial sensor component comprises a self-contained inertial measurement unit (IMU) in which are mounted three gyros and three accelerometers in orthogonal triads. The primary aiding sensor for most applications is GPS or differential GPS. Other vehicle specific aiding sensors, such as the odometer for land vehicles, can be included in the blended solution to enhance the POS performance. POS/LV was

developed to measure vehicle motion dynamics for the purpose of computing road inspection parameters such as the transverse slope of the road and the longitudinal profile of the road. The POS/LV was installed in the Automatic Road Analyzer (ARANTM) road inspection vans developed by Roadware Corporation of Paris, Ontario. The cross fall and longitudinal profile of the road as computed by ARANTM using POS/LV were compared to results of an independent survey and the accuracy was found to be better than 1.1 cm RMS.

GPSVision™ System is a mobile mapping system that can be used to collect stereo digital images along highways, state roads and residential streets, while traveling at the posted speed limits [37]. By integrating GPS, INS and stereo digital images, the data can be processed into usable computer files. These files can be accessed by feature extraction software to locate positions of visible physical facilities such as manholes, curb lines, traffic signs, pedestals and building locations. The positions and attributes of these visible features (latitude, longitude and elevation) are stored in ASCII format and are easily transportable to standard GIS systems wherein the data may be displayed and manipulated.

El-Hakim et al. [38] presented an approach based on 3D range sensor data, a multiple CCD camera and a color high-resolution digital

still camera. The multiple CCD cameras provide images for photogrammetric bundle adjustments to register the 3D images from the range sensor in one coordinate system. The images from the high-resolution still camera provide the texture for the final model.

Digital Mapping Laboratory is developing a system for automating the construction of virtual world database for ground based simulation by integrating information from various sources, including digital map data, aerial and satellite imagery, detailed line drawings, and ground based photography [13].

It is clear from this review that As Built Survey methods generally employ multiple sensors and integrate the data in a suitable way. At the Iowa Department of Transportation (IADOT), a new system that employs multiple sensors replaces the old video-logging system. This research uses data from the new system to demonstrate the ability to use such systems for As Built Survey and create virtual models. This system is discussed in more detail in the next section.

3.3 IADOT Video-Logging System

At present the IADOT uses a new video logging system mounted on a Van. The system consists of an image subsystem, a computing

subsystem and a positioning subsystem. All these three subsystems are integrated to function as a single unit.

The imaging system is a Mandli RDVX2000 that includes a Mandli RDVX2020 camera with Mandli RDVX2030 Camera lens. Figure 3.1 shows the digital camera mounted on the interior of the van.

The computing subsystem consists of a Dell Precision 410 as the central processing unit and includes an image processor, an I/O channel processor, and a peripheral processing unit, in addition to Norton Utilities Virus Scan software. Figure 3.2 shows the computing hardware and peripherals

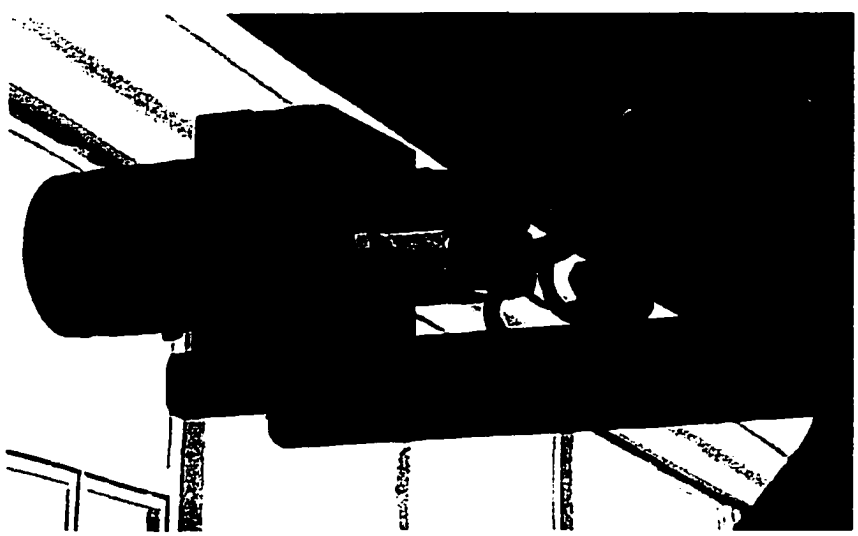

Figure 3.1 Camera mounted on the video logging van

Figure 3.2 Computing hardware of the video logging system

The positioning system consists of a GPS and an Inertial Navigation System (INS). The GPS is a Mandli RDVX5000 that can collect Real Time Kinematics GPS data and includes a GPS receiver NovaTel 3151R. The INS components consist of fiber optic gyros, two pendulums and distance measuring devices. Figure 3.3 shows the video logging van with the GPS antenna mounted at the top. The antenna is offset to the rear of the van at a distance of 2.2 meters from the camera exposure point.

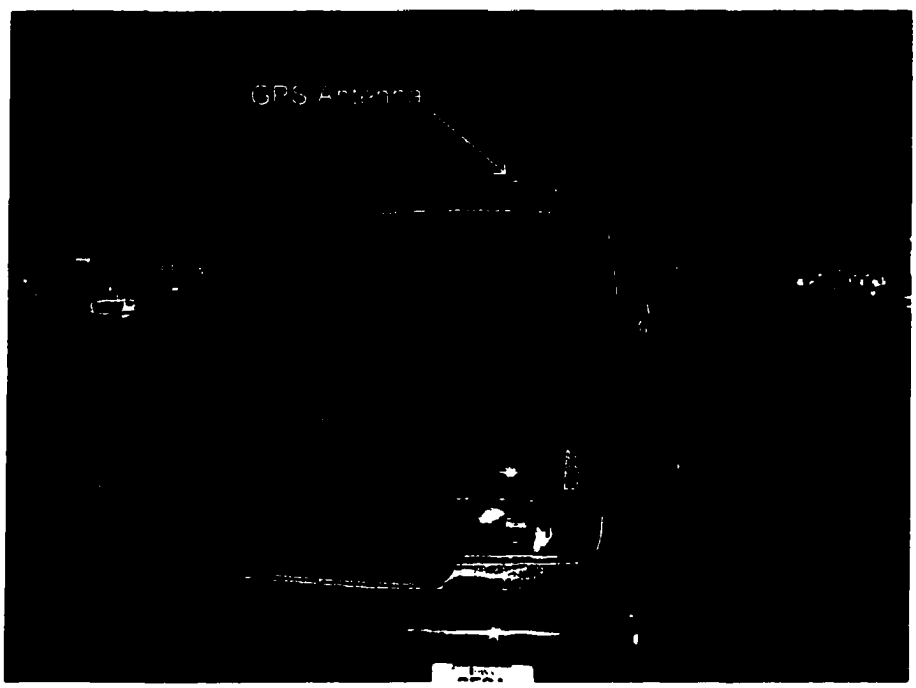

Figure 3.3 GPS antenna mounted on the video logging van

Other accessories include an NEC LCD1500M monitor, Wacom PL 300 data display board, power inverter and backup batteries. A complete listing of the specifications of the various components of the video logging system is given in Appendix A.

3.4 Summary

In most cases, data acquisition through multiple sensors is required for creation of virtual worlds with real world contents. Usually, data is in a digital image format. Digital photogrammetry is an additional and important link in most virtual world construction procedures. The potential of digital photogrammetry for a constructing virtual world has been demonstrated by their use in many studies. The IADOT video logging system is good for an As Built Survey that provides image data with corresponding RTK-GPS positioning. These data processed by digital photogrammetry to collect the required geometric information and build a virtual world out of the existing roadside scene was used in this research.

CHAPTER 4 CAMERA CALIBRATION

The first step in creating a VR world with real world data involves data acquisition. Generally, an As Built Survey collects data for the real world content of the VR application. The review of current methods of As Built Survey methods in Chapter 2 shows that most of the data acquisition systems use a digital camera with other sensors such as GPS and INS. Photogrammetric processing of the digital images require the camera to be calibrated. Using a digital camera mounted on the video-logging system for data collection requires special arrangements. As outlined in the introductory chapter, one method developed in this study involves calibration of the digital video-logging camera. This method sets up a calibration range, acquires data for calibration and does the necessary computation. This chapter describes the various methods of camera calibration used in current research, and describes the special arrangements and procedure adopted in this study.

4.1 An Overview of Camera Calibration

Calibration of the camera is defined as the process whereby the geometric characteristics of the mapping camera are determined [39]. Camera calibration is performed so that the images obtained by the camera may be used for precise positioning of features by photogrammetric computations. The geometric characteristics are usually expressed in terms of some constants, which are usually called the elements of interior orientation.

The elements of interior orientation of a camera may include: (1) equivalent focal length, (2) calibrated focal length, (3) average radial lens distortion, (4) tangential lens distortion, (5) principal point location, (6) distances between opposite fiducial marks, (7) angle of intersection of fiducial lines, and (8) flatness of focal plane. In addition, resolution is also determined in camera calibration.

4.1.1 Lens Distortion

The lens distortion parameters provide the means to correct any image position to the corresponding value from a perfectly distortion-free lens. Usually, the lens distortion is modeled by two sets of mathematical formulae: one for "Radial Distortion", and the other for

"Decentering Distortion". These two distortions are briefly described in the next subsections.

4.1.1.1 Radial distortion

An image is radially distorted if it is formed either radially closer or farther away from the principal point location that a perfect lens would produce [40]. The radial distortion δ_r can be represented by a polynomial series of odd powered terms:

$$\delta_r = K_1 r + K_2 r^3 + K_3 r^5 + \ldots \qquad [4.1]$$

where the *K*s are the coefficients of radial distortion corresponding to infinity focus, δ_r is in micrometers and

$$r^2 = (x - x_p)^2 + (y - y_p)^2 \qquad [4.2]$$

where r, x, x_p, y, and y_p, are in millimeters.

Radial distortions in most of the cameras lenses are adequately modeled by the three parameters K_1, K_2, and K_3. Special lenses such as "fish-eye", may require additional parameters of up to five in number.

Radial distortion in non-metric cameras with small formats is adequately modeled by K_1 alone [2].

4.1.1.2 Decentering distortion

A camera lens system consists of several pieces of spherical surfaces. Ideally, these pieces are mounted collinear to the optical axis. A misalignment of the lenses produces what is known as the decentering distortion. The decentering distortion is represented by a polynomial function [2] truncated to:

$$\Delta x_s = \left(1 - \frac{c}{s}\right)\left[P_1\left(r^2 + 2(x - x_p)^2\right) + 2P_2(x - x_p)(y - y_p)\right] \qquad [4.3]$$

$$\Delta y_s = \left(1 - \frac{c}{s}\right)\left[P_2\left(r^2 + 2(y - y_p)^2\right) + 2P_1(x - x_p)(y - y_p)\right] \qquad [4.4]$$

where the parameters P_1, P_2 are the values at infinity focus of the decentering distortions,

Δx_s, Δy_s are the components of decentering distortion at an image point x, y,

r is the radial distance to the image point, and

c is the principal distance for a lens focused on an object plane at a distance s from the camera.

Usually, the decentering error is relatively small. The magnitude of the error may be about 30 μm at the edge of the format. However, for large-scale photography and extensive depth of field, as in case of close-range applications, the decentering distortion may not be neglected.

4.1.2 Camera Calibration Methods

In general, there are three categories of calibration methods for determining interior orientation in a camera [41]: (1) laboratory methods, (2) field methods, and (3) stellar methods. The laboratory methods involve a multicollimeter or a goniometer. The field method and the stellar method involve photographing an array of target points whose relative positions are accurately known. These methods of camera calibration for aerial cameras have been standardized over the years. Even though no standard procedure exists for calibration of a non-metric camera, a number of procedures have emerged. The methods of calibrating a non-metric camera may be categorized into three broad approaches: (1) laboratory calibration, (2) on-the-job calibration, and (3) self-calibration. The digital camera belongs to the

group of non-metric cameras. These approaches are briefly discussed below.

4.1.2.1 Laboratory calibration

The same laboratory methods as used for the metric camera involving a multicollimeter or a goniometer can be applied to the non-metric cameras. But, there are other methods such as Test Range calibration. This method uses targets set-up in a three-dimensional test range. Targets are usually placed on several planes of building facades or stairs. A facility inside a room would typically place some targets on a wall and others in front of the wall using steel rods for a three-dimensional layout. The target locations (X, Y, Z coordinates) are determined through three-dimensional intersections. Sometimes, a metric camera of higher precision is used to determine target locations for calibration of cameras of lower precision.

For one camera position, there are a total of fourteen unknowns, namely, six exterior orientation parameters that include the spatial camera location X_0, Y_0, Z_0, the three angles of orientation ω, φ, κ, eight parameters of interior orientation: x_0, y_0, c, K_1, K_2, K_3, P_1, and P_2.Therefore, a minimum of seven object points are required. Higher

number of targets helps in getting more precise results through least square solutions.

The calibration test range may be set up to use multiple camera positions. Such a configuration may provide a stronger solution. The Simultaneous Multi-Frame Analytical Calibration (SMAC) method was developed to use a multiple camera format for calibration [40].

4.1.2.2 On-the-job calibration

On the job calibration is suitable for non-metric cameras because it determines the elements of interior orientation in the same solution as the object points and exterior orientation elements. The usual procedure is to place objects of known dimensions in the field to be photographed. At least one full control point (i.e., X_0, Y_0, Z_0) is to be provided for each of the two parameters to be determined.

4.1.2.3 Self-calibration

Like the on-the-job method, the self-calibration technique for camera calibration also includes object-space-control and unknown object points in the same solution. The mathematical formulation combines the collinearity equation with the radial and decentering lens distortion equations. However, this approach does not require object space control coordinates for the solution.

$$x_{ij} - x_p + \frac{(x_{ij} - x_p)}{r}\delta r + \Delta x = -c_x\left[\frac{m_{11}(X_j - X_{Li}) + m_{12}(Y_j - Y_{Li}) + m_{13}(Z_j - Z_{Li})}{m_{31}(X_j - X_{Li}) + m_{32}(Y_j - Y_{Li}) + m_{33}(Z_j - Z_{Li})}\right] \quad [4.5]$$

$$y_{ij} - y_p + \frac{(y_{ij} - y_p)}{r}\delta r + \Delta y = -c_y\left[\frac{m_{21}(X_j - X_{Li}) + m_{22}(Y_j - Y_{Li}) + m_{23}(Z_j - Z_{Li})}{m_{31}(X_j - X_{Li}) + m_{32}(Y_j - Y_{Li}) + m_{33}(Z_j - Z_{Li})}\right] \quad [4.6]$$

where the subscripts indicate:

L: the perspective center

i: the i-th photograph

j: the j-th object point

c_x, c_y: principal distances derived from the use of observed image x_{ij} and y_{ij} coordinates, respectively. Usually, these two terms are simplified to a single value c.

4.1.3 Elements of Exterior Orientation

The elements of exterior orientation of the camera include six independent parameters that describe the space position and the angular orientation [42]. The space position is normally given by the three-dimensional coordinate X_L, Y_L, Z_L of the camera exposure station

with reference to the ground coordinate system. The angular orientation is the amount and direction of the tilt of the camera axis, which may be expressed either in the omega-phi-kappa (ω-ϕ-κ) system or the tilt-swing-azimuth (t-s-α) system.

There are many different graphical and numerical methods available for determination of the elements of exterior orientation. In general, these methods require photographic images of at least three control points whose X, Y and Z ground coordinates are known. In addition, it is necessary to know the calibrated focal length of the camera. Some of these methods are the *Anderson scale point method, Church method, and Space resection by collinearity.*

4.1.3.1 Space Resection by Collinearity

Collinearity is the condition that the exposure station, any object point and its image point all lie along a straight line. In the figure 4.1 points *L, a and A* are collinear. The basic equations for the x photo-coordinate and y photo-coordinate are given by

$$x = -c\left[\frac{m_{11}(X - X_L) + m_{12}(Y - Y_L) + m_{13}(Z - Z_L)}{m_{31}(X - X_L) + m_{32}(Y - Y_L) + m_{33}(Z - Z_L)}\right] \qquad [4.7a]$$

$$y = -c\left[\frac{m_{21}(X - X_L) + m_{22}(Y - Y_L) + m_{23}(Z - Z_L)}{m_{31}(X - X_L) + m_{32}(Y - Y_L) + m_{33}(Z - Z_L)}\right] \qquad [4.7b]$$

where c is the camera principal distance,

x and y are photo-coordinates of an image point,

X_L, Y_L, Z_L are the camera location parameters, and

$m_{11}, m_{12}, \ldots\ldots m_{33}$, are the elements of the camera rotation matrix.

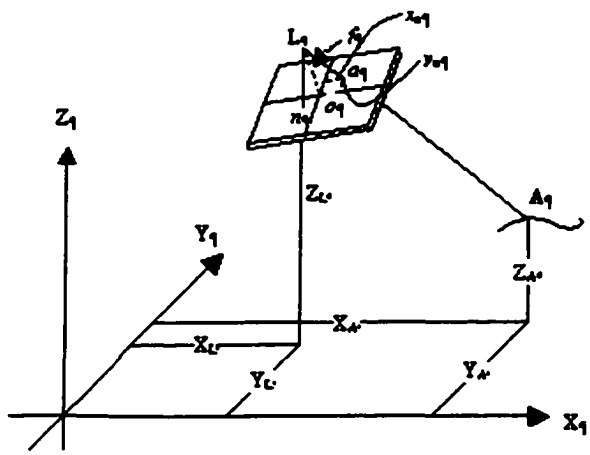

Figure 4.1 The collinearity condition

Since the collinearity equations are non-linear, they are linearized using Taylor's theorem and can be written as given below.

$$v_x = b_{11}(d\omega) + b_{12}(d\phi) + b_{13}(d\kappa) - b_{14}(dX_L) - b_{15}(dY_L) - b_{16}(dZ_L) + b_{17}(dX) + b_{18}(dY) + b_{19}(dZ) + J$$

$$v_y = b_{21}(d\omega) + b_{22}(d\phi) + b_{23}(d\kappa) - b_{24}(dX_L) - b_{25}(dY_L) - b_{26}(dZ_L) + b_{27}(dX) + b_{28}(dY) + b_{29}(dZ) + K$$

Where,

v_x , v_y are residual errors in measured x and y image coordinates,

$d\omega$, $d\phi$, $d\kappa$ are corrections to the initial approximations of the orientation angles of the photo,

dX_L, dY_L, dZ_L are corrections to the initial approximations for the exposure station coordinates

dX, dY, dZ are corrections to the initial approximations for the object space coordinates of the point, and

b_{11}, b_{12}, ... , b_{25}, b_{26} are the coefficients of Taylor series expansion.

Linearization by Taylor's series expansion ignores non-linear terms of higher order derivatives. Therefore, what we get are approximations that must be solved iteratively until the magnitude of the corrections become negligibly small. The unknown corrections are

solved using the method of least squares with a number of control points.

4.1.3.2 Simultaneous Bundle Adjustment

Simultaneous Bundle Adjustment is an extension of photogrammetric principles to adjust all photogrammetric measurements to ground control values in a single solution. It also allows simultaneous calibration of the recording system, which is the photogrammetric camera in this case. Basically, it is an analytical triangulation technique that may be suitably manipulated for simultaneous camera calibration. The basic arrangement for triangulation by simultaneous bundle adjustment is shown in the Figure 4.2.

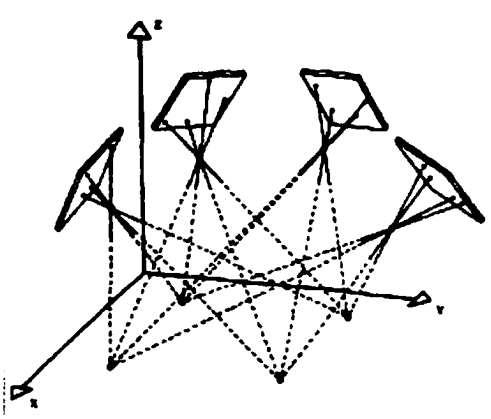

Figure 4.2 Simultaneous bundle adjustment

The calibration may be done separately for single photographs, combined with a series of photographs, or jointly with all photographs in a block. If the distortion parameters of the optical system are considered known, then only the position of the perspective center in the image space has to be determined. The calibration may be carried out using spatial ground control points. Without any ground control points, camera calibration may still be achieved by considering lines, distances, and directions in the object space. Wester-Ebbinghaus [43] describes various schemes for simultaneous camera calibration in the context of non-topographic photogrammetry.

4.1.4 Other Research in Camera Calibration

Camera calibration is an important stage in the 3D reconstruction of images. There have been disparate approaches in this regard. A review of innovations in methods of camera calibration is presented below.

Wei et al. proposed a new *implicit* method of camera calibration in which the physical parameters are not explicitly computed [44]. This was used for both 3D measurements and generation of image coordinates. This method is based on projective mapping between the image plane and two calibration planes.

Huttori et al. developed a method for calculating the approximations of exterior orientation parameters and coordinates of object points associated with an object space coordinate system [45]. This method uses a process of decomposition of the rotation matrix into angular elements and can be used for semi-automatic bundle adjustment and camera calibration.

Obercampf et al. suggested a technique for computing camera position and orientation with regard to a known object using four or more coplanar feature points [46]. It consists of iteratively perfecting one or two pose estimates and producing a related quality measurement for each pose using the scaled orthographic projection estimation.

Bani Hashemi used a Fourier technique to determine the orientation of a camera with respect to a calibration object [47]. This technique is limited to orthographic projection. In this method, the camera orientation is entirely decoupled from translation.

Wei et al. proposed a method for self-calibration of robotic hand cameras by means of active motion [48]. Through tracking a set of world points of unknown coordinates during robotic motion, the internal parameters of the camera (including distortions) and the mounting parameters as well as coordinates of the world points are

estimated. Initial estimates for the unknown parameters are not necessary. The calibration procedure uses a planar wall facility.

4.1.5 CALIB Software for Camera Calibration

For this research, calibration software CALIB developed by Dr. K. Jeyapalan performs the camera calibration. CALIB uses the principles of photogrammetric bundle adjustment. It models the distortion using six parameters, namely, K_1, K_2, K_3, P_1, P_2, and P_3. This software is versatile in the sense that it may be used for various situations involving different approaches such as test-range calibration, on-the-job calibration and also self-calibration. The software provides a special data input format that allows the user to choose appropriately the weights for various parameters such as the ground point coordinates, interior orientation parameters and the exterior orientation parameters. Accordingly, the same software may be used for camera calibration as well as for ground point determination.

4.2 Calibration of Video-Log Camera

The case study for this research uses the video-logging van, which is owned by Iowa Department of Transportation (IADOT). This van uses a digital camera to collect digital images. A Real Time

Kinematics Global Positioning System (RTK-GPS) logs the image locations using photogrammetric principles. However, the camera needs to be calibrated first before the images can be used for data extraction. This section describes various aspects of the method and procedures adopted for calibration of the digital camera. The various components include the test site, the targets, lay out of camera positions and the calibration computations. These aspects are described in more details under the respective headings

4.2.1 The Approach and Methods

To design a scheme for camera calibration, it is necessary to examine the data collection system at hand, which includes the digital camera mounted in the video-logging van at all times. The van also carries an RTK-GPS system for collecting the camera positions with the GPS antenna exposed to the open sky.

Under these circumstances, it was decided that an outdoor test range would be needed. A camera calibration range usually consists of a facility for mounting targets in such a way that the camera may capture their images. Since the camera in this case is mounted on a van, it is necessary to set up a range so that the van can drive into it.

4.2.2 Selection of Site

The requirement of the test site includes easy and repeated accessibility by the van over a period of about six months. In addition to a vertical planar configuration of targets, it is desirable to offset the targets in the horizontal direction so that a high degree of correlation among the calibration parameters is avoided. With the above requirements in mind, a suitable site was located at the Town Engineering Hall on the Iowa State University campus. The site includes the west wall of the building and an adjacent docking platform and yard. While the wall accommodates the vertical planar configuration of the targets, the platform wall provides the offset in the vertical direction. The docking yard provides ample accessibility for positioning the video logging van for repeatedly acquiring video data.

4.2.3 Design of the Target

The targets for any photogrammetric calibration need to be designed appropriately by accommodating the characteristics of the imaging system, the image quality and the required depth of image for the current situation. The present situation involves image acquisition from a distance varying from 8 to 20 meters. Image resolution of the video logging system is 1300 X 1030 pixels. To determine the Field Of

View (FOV) of the imaging system, a simple mensuration site was set up, and video logging images were acquired. The FOV for the required situation was thus determined to be approximately 44 degrees. Given the above information, it was decided that a traditional surveying target, as shown in Figure 4.3, would suffice for the task at hand. The vertical as well as horizontal split of the target area into alternate red and white quadrants provides good clarity and resolution.

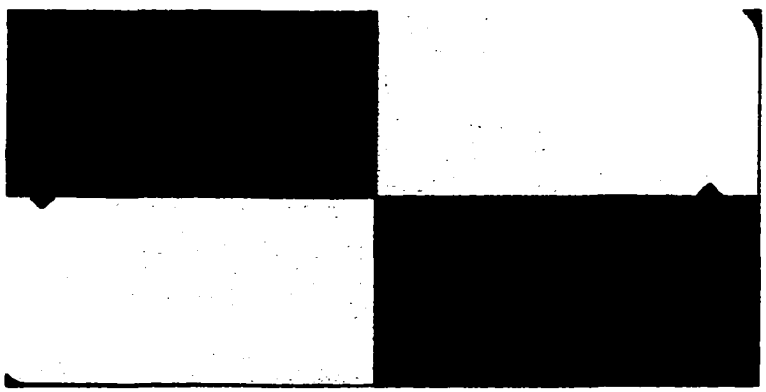

Figure 4.3 Target used for camera calibration

4.2.4 Number and Placement of Targets

The targets need to be placed in such a way that they would be well distributed over the field of view in order that the photogrammetric characteristics of the imaging system are satisfactorily determined. The

target positions are designed to cover the area of interest at varying radial distances from the center.

With due consideration given to the varying camera distance, at least eight targets need to be visible from the closest camera position to satisfy the modeling routine requirements. Since the FOV is constant, the area of interest gets larger as the camera moves farther from the targets. Therefore, more targets will need to be placed to cover the image format adequately. It was decided to use a total of thirty-six targets arranged in such a fashion as to satisfy the above considerations. Figure 4.4 shows the target placements.

4.2.5 Camera Positions

The video-logging system produces overlapping images whose positions are separated in the direction of the camera axis. Therefore, a similar situation is simulated at the calibration range by acquiring images from different positions approximately along the direction of the camera axis.

Four such positions, at distances of 25', 38', 50' and 60', were selected. However, to simulate stereo viewing of the scene, images with lateral overlaps are required.

Figure 4.4 Positioning of targets for camera calibration

Therefore, additional positions, offset to both sides at 5' from the center at the 25' and 38' positions of the centerline, were fixed. The outline of the camera positions is shown in figure 4.5. After designing all the necessary parameters as outlined above, the targets are fixed to the walls and the docking platform

4.2.6 Determination of Target Locations

Precise determination of the target locations is necessary for the calibration procedure to yield appropriate results. A triangulation scheme is designed to determine the target location. A local Cartesian coordinate system is adopted for a baseline 25' long which is oriented approximately due North-South and parallel to the target locations. With the baseline as the x-axis, and the vertically upward direction as the z, the y-axis is fixed by the right-handed coordinate system.

The length of the baseline is measured accurately with a fiberglass tape to an accuracy of ±0.025'. A geodimeter total station with angular accuracy of 1" was used to measure angles to the target locations with respect to the baseline direction. Measurements were made at four positions, viz. 0', 5', 20' and 25' respectively (See figure 4.6). Two additional positions are adopted to provide a check.

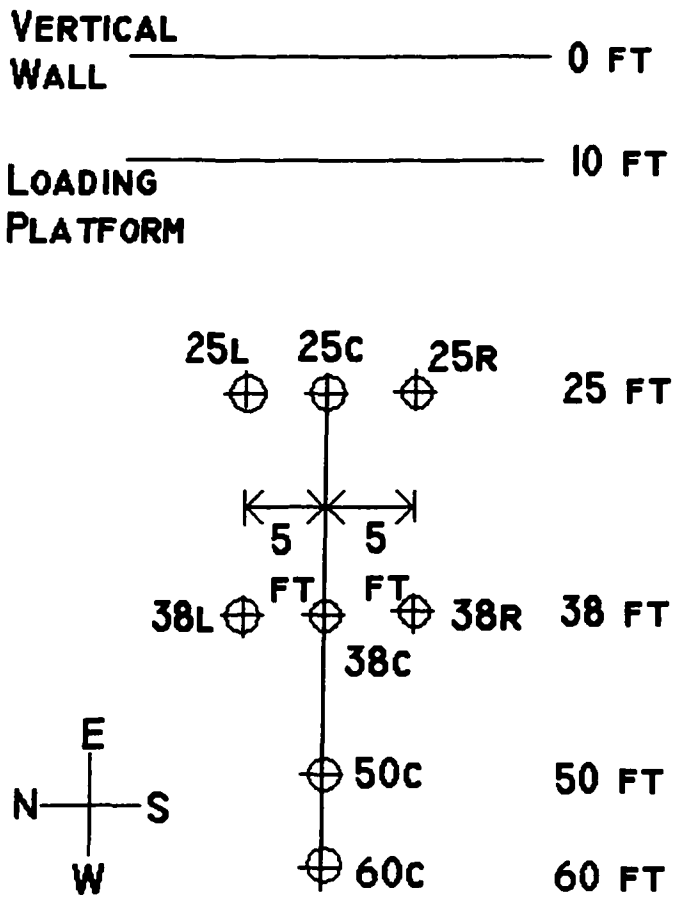

Figure 4.5 Layout of camera locations

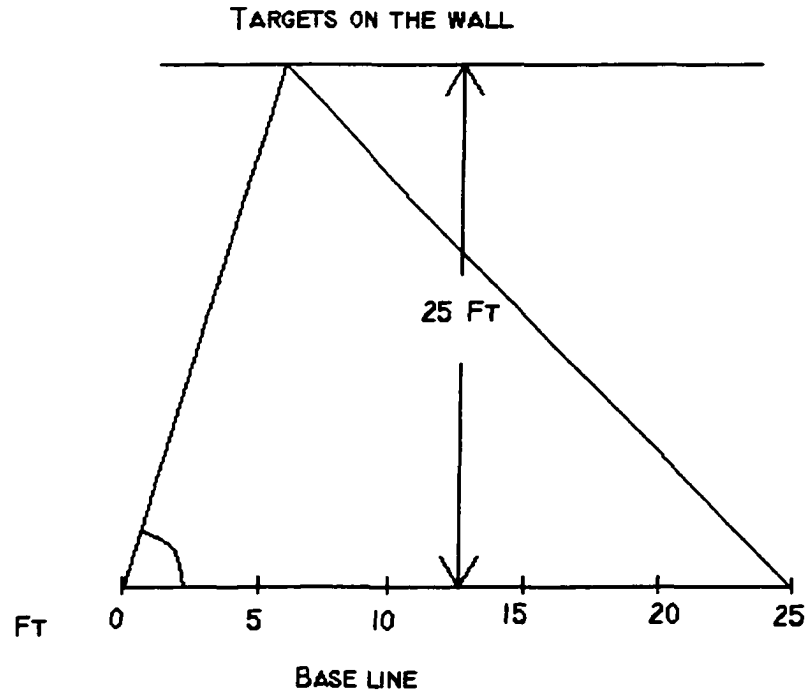

Figure 4.6 Points on the base line for positioning targets

4.2.6.1 Accuracy of Target Locations

The target locations were computed using the baseline of length 25' between positions 0' and 25'. Blunders were detected by comparing the computed values from the measurements for 15' long baseline at positions 5' and 20'. Then, the standard errors of the locations were computed using errors propagated by angle and baseline

measurements. The values of standard errors for the respective target locations were found to be 1.4 mm, 1.5 mm and 0.5 mm for X, Y and Z. The computed coordinates of targets are presented in table 1.

4.2.6.2 Conversion to State Plane Coordinate System

A Total Station traverse was done using the Geodimeter Total Station between the baseline at the calibration range and control points Sarath and RO1 as shown in figure 4.7.

These two control points are located to the north of the Town Engineering Building. The traverse computation yielded a connection between the local coordinate system of the calibration range and the State Plane Coordinate System (SPCS) using the known values of the control point coordinates. The coordinates of the stations 0 and 25 on the baseline were transformed into the SPCS. Further computation of coordinate transformation yielded coordinates of all relevant points in the calibration range in the SPCS.

4.2.7 Data Acquisition at Calibration Site

The IADOT van equipped with the Mandli video-log system was used for acquisition of video images of the control point targets at the calibration site. Figures 3.1 through Figure 3.3 show the video-logging van and different components of the system.

Table 1 Ground control coordinates of targets and camera positions

POINT	Description	Local Coordinates		State Plane Coordinates	
		X(m)	Y(m)	NORTHING	EASTING
11	Control Point	1.823	7.634	1058828.198	1487317.537
12	Control Point	3.713	7.636	1058826.322	1487317.524
13	Control Point	6.136	7.640	1058823.916	1487317.506
14	Control Point	8.518	7.646	1058821.552	1487317.487
15	Control Point	10.699	7.650	1058819.386	1487317.469
21	Control Point	3.008	7.639	1058827.022	1487317.526
22	Control Point	4.380	7.641	1058825.659	1487317.516
23	Control Point	6.118	7.647	1058823.934	1487317.500
24	Control Point	7.846	7.650	1058822.219	1487317.486
25	Control Point	9.233	7.654	1058820.842	1487317.474
31	Control Point	1.784	7.639	1058828.237	1487317.532
32	Control Point	3.001	7.639	1058827.029	1487317.525
33	Control Point	4.393	7.644	1058825.647	1487317.512
34	Control Point	6.141	7.645	1058823.912	1487317.501
35	Control Point	7.848	7.649	1058822.216	1487317.487
36	Control Point	9.214	7.653	1058820.861	1487317.475
37	Control Point	10.700	7.659	1058819.385	1487317.461
41	Control Point	1.792	7.642	1058828.229	1487317.530
42	Control Point	3.008	7.644	1058827.022	1487317.521
43	Control Point	4.388	7.646	1058825.652	1487317.510
44	Control Point	6.116	7.650	1058823.936	1487317.497
45	Control Point	7.849	7.652	1058822.216	1487317.484

Table 1 (Continued)

POINT	Description	Local Coordinates		State Plane Coordinates	
		X(m)	Y(m)	NORTHING	EASTING
46	Control Point	9.207	7.655	1058820.868	1487317.473
47	Control Point	10.683	7.660	1058819.402	1487317.460
51	Control Point	3.004	7.748	1058827.026	1487317.417
52	Control Point	4.378	7.753	1058825.663	1487317.404
53	Control Point	6.112	7.659	1058823.940	1487317.487
54	Control Point	7.847	7.759	1058822.218	1487317.378
55	Control Point	9.212	7.765	1058820.863	1487317.364
61	Control Point	2.398	4.598	1058827.609	1487320.548
62	Control Point	3.460	4.604	1058826.555	1487320.536
63	Control Point	4.609	4.603	1058825.415	1487320.530
64	Control Point	5.924	4.607	1058824.109	1487320.519
65	Control Point	7.168	4.607	1058822.874	1487320.511
66	Control Point	8.507	4.611	1058821.545	1487320.500
67	Control Point	9.774	4.495	1058820.286	1487320.607
60C	Camera Position	5.234	-10.816	1058824.703	1487335.835
50C	Camera Position	5.166	-7.733	1058824.789	1487332.775
38C	Camera Position	5.038	-3.834	1058824.939	1487328.904
25C	Camera Position	4.933	-0.042	1058825.066	1487325.140
38L	Camera Position	3.569	-3.699	1058826.398	1487328.779
25L	Camera Position	3.462	-0.157	1058826.526	1487325.262
38R	Camera Position	6.630	-3.731	1058823.359	1487328.792
25R	Camera Position	6.534	0.022	1058823.477	1487325.067

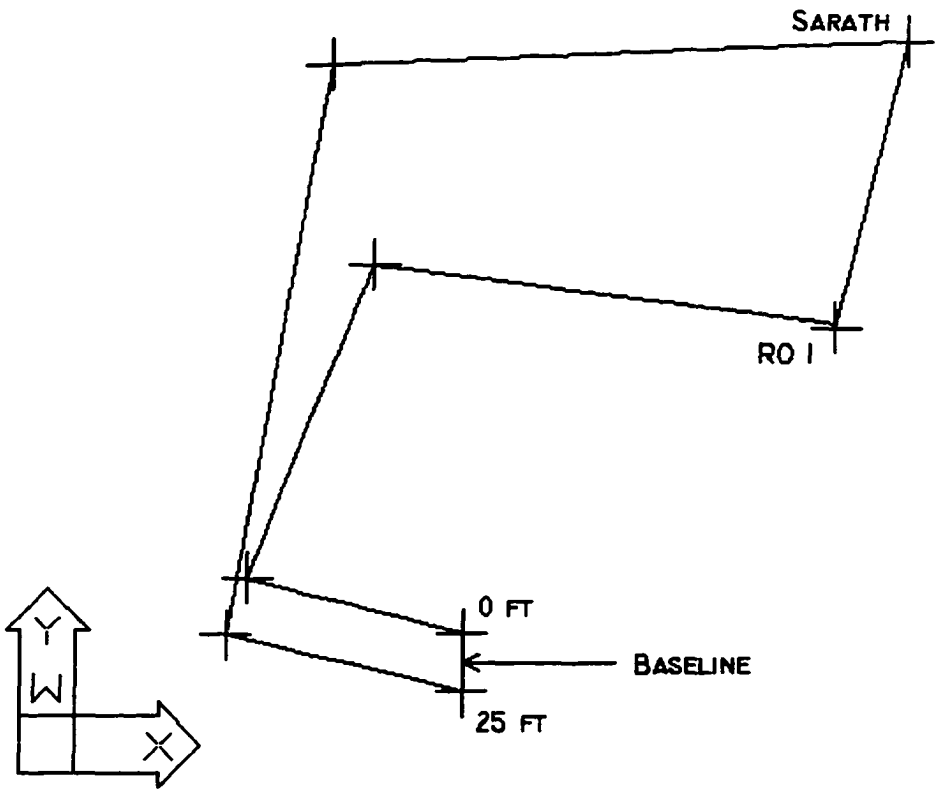

Figure 4.7 Traversing

4.2.7.1 Acquisition of Video Images

At each of the designed camera locations, the van would stand for a short duration of time collecting video images. A total of ten images were collected at each position of the camera for capturing the targets. A total of eight such positions would yield sufficient images for studying camera calibration with images overlapping in the direction of

the line of sight as well as in the transverse direction to provide overlapping stereo pairs.

4.2.7.2 Camera Locations By Triangulation

While the van is collecting digital video images and GPS signals at each location, the camera location is also determined by using a triangulation system. Two Total Station equipments are setup at the two extremities of a secondary base line. Directions to the camera locations were measured with from the direction of this secondary baseline. The secondary baseline was used to have convenient and unencumbered instrument stations while working simultaneously with the video-logging system. This baseline location was previously determined with reference to the primary baseline at the calibration range. The directions measured from the two instrument positions and the baseline length was used to determine the camera locations in a local coordinate system, which were transformed to the State Plane Coordinate system.

4.2.7.3 Camera Locations by GPS

The Mandli System in the van also collects GPS signals to determine the current location of the van. The collected data is post processed using nearby base station data to determine the locations of

the van. While evaluating the GPS positions, it is necessary to account for the offset of the GPS antenna from the video camera location.

4.2.7.4 Comparison of GPS locations with ground survey locations

The post processing of the GPS data yielded camera positions in geographical coordinate systems. These values were transformed into State Plane coordinates for comparison with the camera locations determined through ground survey methods as outlined above (See table 2).

Table 2 Accuracy of GPS Locations

Serial Number	Position Code	Differences	
		Northing (m)	Easting (m)
6	60C	0.825	26.354
22	38C	0.354	13.111
33	25C	-2.198	4.217

The difference in the easting appears high enough to warrant a conclusion about multi-path errors in the GPS data collection due to the presence of building walls on three sides of the calibration range. However, the GPS data at the test range are not of much consequence

as the calibration procedure involves determining camera locations using the Total Station triangulation survey.

4.2.8 Camera Calibration

Processing of the data collected at the calibration range has two steps: (1) calibration of the interior orientation parameters of the digital video camera, and (2) using these parameters to determine positions. A camera calibration software CALIB is used for the purpose of camera calibration and validation of target location. The software needs the measured image coordinates of the targets, control coordinates of the targets, and camera location as input. The output contains the camera interior orientation parameters of the camera and angles of the exterior orientation parameters. This was done using three images placed longitudinally. Calibration was also done using a total of sixteen images where eight were acquired before video logging of the test sites and another eight afterwards. Table 3 shows the calibration results.

4.2.9 Validation

The calibrated parameters were used to determine target locations using CALIB and another digital photogrammetric software SoftPlotter™. This software lets the user view in stereo.

Table 3 Calibrated values of camera parameters

Parameter	Calibrated Value
x_o (pixels)	4.2487e-02
y_o (pixels)	8.1226e-03
c (pixels)	-1.8200e+03
K_1	1.2790e-09
K_2	-2.2770e-15
K_3	-1.1000e-23
P_1	-1.8948e-08
P_2	0.0000e+00
P_3	0.0000e+00
ω (radians)	-0.010378
φ (radians)	-0.039845
κ (radians)	-0.089582

In addition to the three images at 60, 38 and 25 feet points, a separate computation was carried out for a pair of images offset to either side at the 38 feet point (Refer to Figure 4.3) for position computations. An outline of the procedure for position determination using SoftPlotter™ is presented in Appendix (To be numbered). The

accuracies achieved in positioning the targets using the calibrated parameters are presented in Table 4.

Table 4 Accuracy of position determination

Method	Accuracies (m)		
	X	Y	Z
CALIB with three images	0.027	0.024	0.105
SoftPlotter with longitudinal pair	0.067	0.063	0.245
SoftPlotter with stereo pair	0.029	0.037	0.130

4.3 Summary

Digital image cameras used for video-logging purposes can be calibrated so that the images may be used for extracting feature locations. The calibration range for this project was designed, set up and evaluated to accommodate the video-logging van at a drive up location. This provides means for repeated acquisition of calibration data every time before field data collection. A geodimeter total station obtained the necessary accuracy to establish the control targets. Three images, separated in direction of the camera axis, were used to calibrate the camera. Calibrated parameters yielded an accuracy of 2.7

cm, 2.4 cm, and 10.5 cm for X, Y and Z respectively, for the positions of controls. The validation using the second digital photogrammetric software SoftPlotter™ yielded comparable accuracy. The GPS survey was not accurate, because of multi-path errors. In addition to the interior orientation parameters, the calibration procedure also yielded the camera rotation angles, which can be used for reduction of field data. The procedure for data reduction is described in details in the chapter 5.

CHAPTER 5 PHOTOGRAMMETRIC DATA ACQUISITION

A review of current practices of As Built Survey methods in chapter 3 showed that many systems used digital cameras for data acquisition. Processing of such data usually uses close photogrammetric methods and GPS [49]. The term close range photogrammetry is usually applied when the object distances are within about 300m [50]. The digital camera used frequently for the As Built Survey is a non-metric camera. This chapter describes the different methods of data reduction in close range photogrammetry and the special methodology developed for processing the data collected by the video-log system of the Iowa DOT. However, this methodology applies to any mobile mapping system that acquires digital images and corresponding image positions using GPS.

5.1 An Overview

Depending upon the camera and final output, there are three traditional approaches for data reduction: (1) analog, (2) analytical, and (3) semi-analytical [50]. These same approaches can be applied for data reduction in close range photogrammetry [51].

5.1.1 Analog Approach

The analog approach uses using an analog plotter, which is based on the principles of central perspective. These machines are mostly designed for near-vertical aerial photography and accommodate a small range in principal distance and rotations. On the other hand, non-metric imagery usually contains large and sometimes irregular distortions. Also, close range photogrammetry usually involves large rotation angles and high base to depth ratio. Therefore, the analog machines are generally unsuitable for close range applications. However, when the required accuracy of the end product is not very high, this approach may be useful.

5.1.2 Analytical Approach

In the analytical approach, the basic unit of computation is the bundle of rays in the image and object space passing through the

exposure stations. The computation involves simultaneous least square adjustment of bundles from all exposure stations and the determination of the exterior orientation parameters of the cameras and adjustment of the object positions. Another analytical method that has gained popularity is the Direct Linear Transformation (DLT) method. These two mathematical models of data reduction in analytical photogrammetry are described below.

5.1.2.1 Bundle Adjustment

The mathematical formulation of the bundle is known as the collinearity equation, which basically states that the image point (x, y), the object point (X, Y, Z) and the exposure station of the camera (X_L, Y_L, Z_L) are on a straight line.

$$\left.\begin{aligned} F_x &= x - x_0 + c\frac{m_{11}(X-X_L)+m_{12}(Y-Y_L)+m_{13}(Z-Z_L)}{m_{31}(X-X_L)+m_{32}(Y-Y_L)+m_{33}(Z-Z_L)} = 0 \\ F_y &= y - y_0 + c\frac{m_{21}(X-X_L)+m_{22}(Y-Y_L)+m_{23}(Z-Z_L)}{m_{31}(X-X_L)+m_{32}(Y-Y_L)+m_{33}(Z-Z_L)} = 0 \end{aligned}\right\} \quad [5.1]$$

Considering the camera interior orientation parameters x_0, y_0 and c to be known, this equation contains six unknowns: X_L, Y_L, Z_L and the

three rotation parameters (ω, φ, κ). Therefore, minimums of three object-space control points are required. The camera locations and rotation parameters are then used to compute the unknown object space coordinates of other measured image points.

Since these equations are non-linear, they need to be linearized using Taylor's series, and thus requires initial approximations, and an iterative solution.

In a non-metric camera, image displacements are usually unknown. The effects of such deviations are compensated by modifying the mathematical model and introducing additional parameters into the collinearity equations as shown below [51]:

$$\left.\begin{aligned} x - x_0 + \Delta x_p &= -c\frac{m_{11}(X-X_L)+m_{12}(Y-Y_L)+m_{13}(Z-Z_L)}{m_{31}(X-X_L)+m_{32}(Y-Y_L)+m_{33}(Z-Z_L)} = 0 \\ y - y_0 + \Delta y_p &= -c\frac{m_{21}(X-X_L)+m_{22}(Y-Y_L)+m_{23}(Z-Z_L)}{m_{31}(X-X_L)+m_{32}(Y-Y_L)+m_{33}(Z-Z_L)} = 0 \end{aligned}\right\} \quad [5.2]$$

where Δx_p, and Δy_p are functions of several unknown parameters and are adjusted simultaneously with the other unknowns in the equations.

5.1.2.2 DLT

A digital camera is a type of non-metric camera that does not contain any fiducial marks. The DLT approach is a special technique that is suitable for any non-metric camera [52, 53,54] that does not explicitly contain the interior orientation elements involving the fiducial information. The solution is obtained by directly transforming comparator coordinates in case of diapositives and pixel coordinates in case of digital images into object-based coordinates. By doing so, the step of converting comparator/pixel coordinates to photo-coordinates is eliminated. The DLT method was originally developed to use eleven parameters (L_1, L_2, ... L_{11}) and five lens distortion co-efficients (K_1, K_2, K_3, P_1 and P_2) based on the following pair of equations:

$$\left.\begin{aligned} & x + (x - x_0)(K_1 r^2 + K_2 r^4 + K_3 r^6 + \ldots) \\ & \quad + \left(r^2 + 2[x - x_0]^2\right)P_1 + 2(y - y_0)(x - x_0)P_2 \\ & \quad = \frac{L_1 X + L_2 Y + L_3 Z + L_4}{L_9 X + L_{10} Y + L_{11} Z + 1} \end{aligned}\right\} \qquad [5.3a]$$

$$\left.\begin{aligned} & y+(y-y_0)(K_1r^2+K_2r^4+K_3r^6+\ldots) \\ & \quad +2(x-x_0)(y-y_0)P_1+(r^2+2[y-y_0]^2)P_2 \\ & \quad =\frac{L_5X+L_6Y+L_7Z+L_8}{L_9X+L_{10}Y+L_{11}Z+1} \end{aligned}\right\} \qquad [5.3b]$$

where x and y are measured comparator or pixel coordinate of an image point;

x_0, and y_0 define the position of the principal point in the comparator or pixel coordinate system,

$r^2 = (x^2 + y^2)$ is the radial distance of image point from the principal point, and

X, Y, Z are the object space coordinate of the point imaged.

Later studies showed that no significant improvements were achieved by incorporating the lens distortion co-efficients, K_2, K_3, P_1 and P_2 and were therefore eliminated. Substituting x' for $(x - x_0)$ and y' for $(y - y_0)$, the above equations were reduced to the following form.

$$x + x'K\,r^2 = \frac{L_1X+L_2Y+L_3Z+L_4}{L_9X+L_{10}Y+L_{11}Z+1} \qquad [5.4a]$$

$$y + y'K r^2 = \frac{L_5X + L_6Y + L_7Z + L_8}{L_9X + L_{10}Y + L_{11}Z + 1} \qquad [5.4b]$$

This method has been successfully used to obtain object space coordinates from digitized image coordinates of video-graphically acquired images [55].

5.1.3 Semi-Analytical Approach

The semi-analytical approach involves an analog stereo plotter for basic measurements of image points, which are processed using numerical routines. In general, relative orientation is performed on the stereo plotter while absolute orientation (scaling and leveling) is done analytically. However, with the advent of powerful computer hardware and evolution of digital photogrammetric software, the semi-analytical approach that partially uses an analog stereo plotter is likely to fade away.

5.2 A New Methodology

This study involves the digital images acquired by the Iowa DOT using the video logging van. The images are obtained from a digital camera at an interval of approximately 25 feet as the van moves on the

road. The camera is pointed slightly towards the right so that the roadside features on the right side of the road are imaged properly. To collect the features on the other side of the road, the van must drive in the opposite direction.

5.2.1 The Approach

The images are in digital form. Analog and semi-analytical approach that use analog stereo plotter are automatically eliminated from consideration. A method based on the analytical approach needs to be used.

In the DLT technique, the elements of interior and exterior camera orientation parameters are implicit in the DLT parameters. The elements of interior and exterior camera orientation parameters are implicit in the eleven DLT parameters. Therefore, for each frame, the parameters need to be determined. As such, it would not be feasible to use any of the calibrated DLT parameters obtained at the calibration range for object point determination. On the other hand, the analytical photogrammetric software CALIB uses the bundle adjustment procedure. This software is suitable for both calibration and object point determination. In this case, the various camera parameters can

be explicitly specified and weighted. Therefore, CALIB was selected for data reduction in this study.

5.2.2 The Procedure

Determination of object point location needs imaging the same object on at least two images. In the present case, there is only one camera that moves almost in the direction of the camera axis. Given this special method of data imaging the object points, a number of aspects need careful consideration:

1. obtaining the camera orientation elements,
2. choosing an appropriate number of images,
3. choosing an appropriate longitudinal between spacing overlapping images,
4. setting up a local coordinate system,
5. estimating approximations for object points,
6. measurement of image coordinates,
7. transformation from image coordinates to photo coordinates,
8. determination of feature location and dimensions,
9. transformation of computed object point position from the local coordinate system to the world coordinate system, and
10. validation of the results.

These are described in the following subsections.

5.2.3 Camera Orientation Parameters

The calibration procedure using the analytical software CALIB yields the interior orientation parameters of principal point coordinates (x_0, y_0), the focal length c, and six distortion parameters K_1, K_2, K_3, P_1, P_2, and P_3. The calibration procedure also provides the relative rotation angles at the test site. For a pair of overlapping images and one object point, the unknowns are twelve exterior orientation elements and X, Y, Z. Of these, six elements of the camera locations for two camera positions are available from the RTK-GPS system. A local coordinate system as defined by the two camera positions uses the rotation angles yielded by the calibration procedure. This leaves four equations generated for one object point on two images and the three object point coordinates X, Y, Z as the unknown parameters.

The uncertainty about the rotation angles can be tackled appropriately by taking advantage of versatility of the analytical software CALIB. A unique feature of the CALIB software is that the user may treat any of the parameters as known or unknown by suitable assignments of weights for each of the orientation parameters. Similarly, object point coordinates may be treated as either control

point or an unknown point by using suitable weights to the estimated or known values of these parameters.

The local coordinates system as defined by the camera locations are shown below in figure 5.1. The line through the two camera positions in the forward direction defines the negative Z-axis. Perpendicular to the Z-axis and to the right side of the driving direction is the X-axis while a right-handed coordinates system defines the Y-axis in an approximately vertical direction. The κ-angle about the Z-axis is unlikely to change except in a sharp curve with high super-elevation. Similarly, the ω-angle about the X-axis will not change on a flat section of the road. Finally, the φ-angle about the Y-axis is also constant on a straight road segment. Therefore, based on the particular field situation, as evident from the images, suitable weights may be applied to the rotation angles to arrive at a viable solution. An illustration of the weighing schemes for camera orientation and distortion parameters in a sample CALIB data file is presented in Figure 5.2.

5.2.4 Number of Images

A minimum of two overlapping images is required for position determination by photogrammetric resection. More images increase the

degree of redundancy in computing an adjusted position. More redundancy may be suitable for extensive statistical sampling.

However, more images also mean more measurement of image coordinates. In case of a collection of mass points, where time is an important factor, more than two images may be a costly affair. Therefore, it was decided to use just one pair of images for position determination of the features.

5.2.5 Spacing between Images

As the video logging van travels, it samples images and corresponding GPS locations at an interval of about 25 feet.

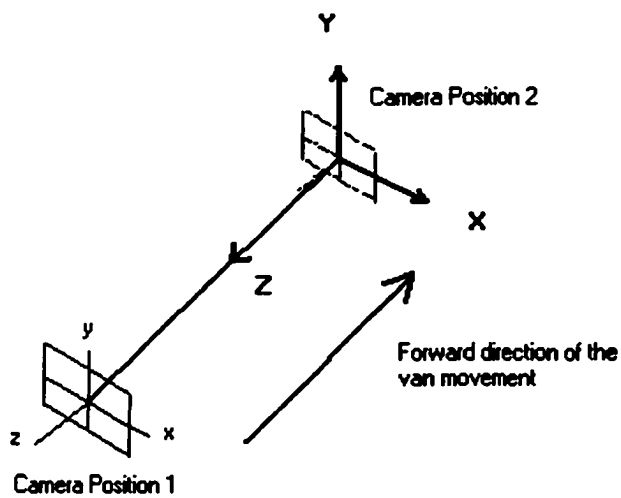

Figure 5.1 A local coordinate system for a pair of images

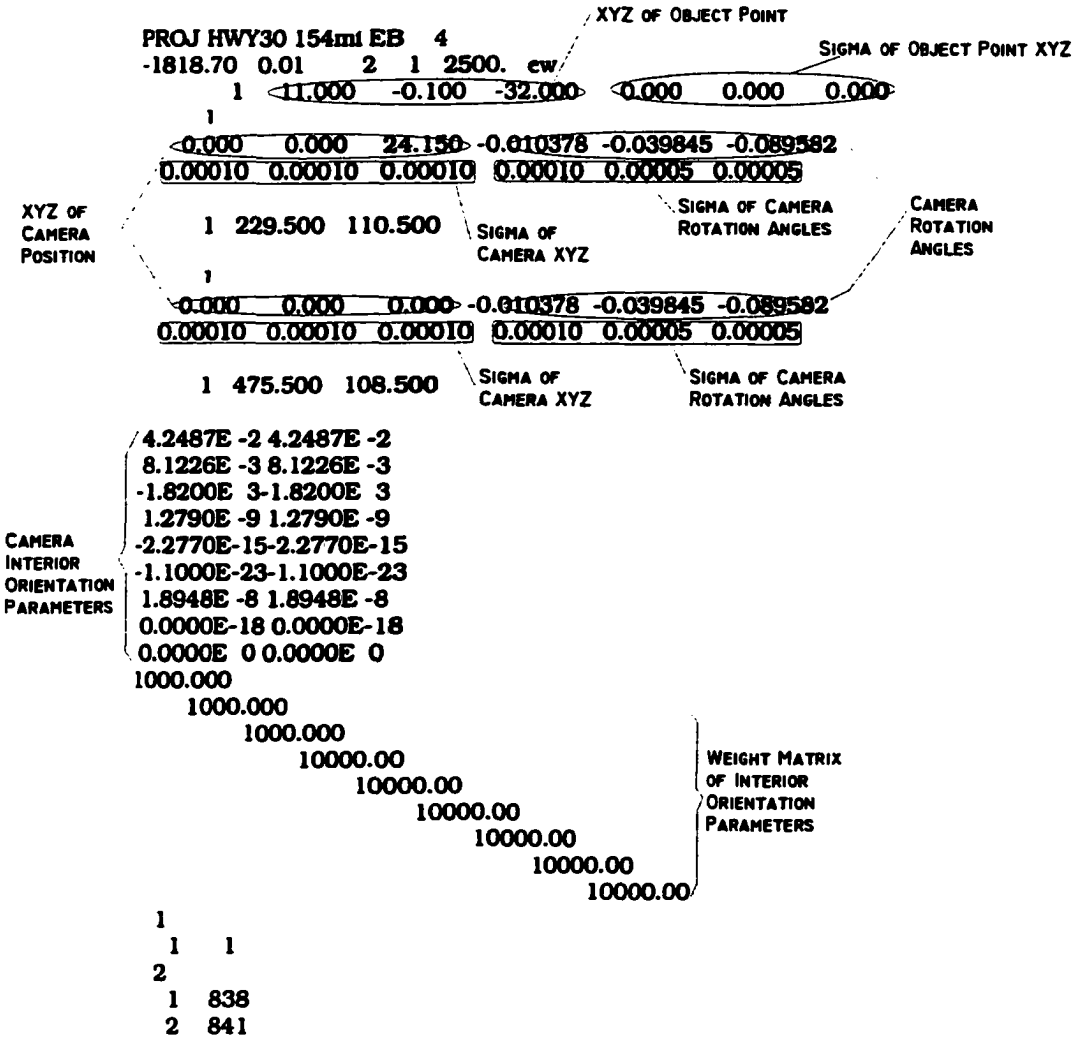

Figure 5.2 Illustration of a sample CALIB data input file

The camera points slightly to the right side of the road. A good measure of overlap is observed among a large number of images captured sequentially. Therefore, a pair of images may be chosen in such a way that the two images are overlapping and are separated by either 25 feet, or 50 feet or 75 feet and so on. The separation between the camera locations influences the angles of resection of a point of interest between the two images, which in turn, has a bearing on the accuracy of the solution achieved by the mathematical computations involved.

One of the two images is selected so that it is closest to the feature of interest, and the other image is to be spaced at an optimum distance. The optimum spacing between the overlapping images happens to be between 75 to 100 feet.

5.2.6 Initial Estimates of Object Point Coordinates

The estimate of a feature's location involves values along the x-, y- and z-axis. Estimating the x- and y-values is relatively more straight forward that estimating the z-value. This is due to the perspective view of the area as provided by the images and the scheme of the local coordinates system. The X-axis is the offset of the feature from the line-of-sight of the pair of images and can be estimated by looking at the

images, without many extra clues. The Y-axis is in the vertical direction. The knowledge that the camera is mounted at 1.92 meters above the ground provides a basis for estimating the y-location of the feature point. The Z-axis extends in the direction opposite to the direction of travel. Therefore, estimating the z-value is the most challenging of the three. With images captured sequentially at an interval of about 25 feet, a better relative location of a roadside feature, with respect to one of the images of the pair, can be chosen for the photogrammetric computation. The idea is to examine the last image on which the feature of interest appears. For example, if photo number 271 is being used as the reference for the local coordinate system, as one moves forward, a feature does not appear on an image after the image number 274, which is the third from image number 271. It means that the feature points away from the reference camera position by slightly more than $3 \times 25 = 75$ feet. See figure 5.3 for an illustration.

Further, the reference image may be examined to select a linear feature, such as the road edge. On this linear feature, it is possible to identify points that indicate the start of the field of view of each image. Looking at the images from the calibration range that the nearest point that appears on an image is about 25 feet away from the camera position. This knowledge, coupled with the points identified in the

previous step, yields a fairly good estimate for the z-value, which is suitable input to CALIB.

5.2.7 Measurement of Image Coordinates

CALIB implements the principle of collinearity. Therefore, measured photo coordinates of object points are the input to the program. These coordinates are to be measured on the digital images collected by the video-logging van. Displaying the image in an image viewer on the computer screen can accomplish this task. In this study, the XV [56] software is used for this purpose. Figure 5.4 shows a digital image displayed in an image viewer for measurement of coordinates.

5.2.8 Transformation of Image Coordinates

The image coordinates measured in above step yields the location in an image coordinate system consisting of number of columns as one axis and the number of rows as the other axis with the origin at the upper left corner of the image. However, these values need to be transformed into a photo coordinate system with the origin at the center of the image. Figure 5.5 shows the image and photo coordinate systems.

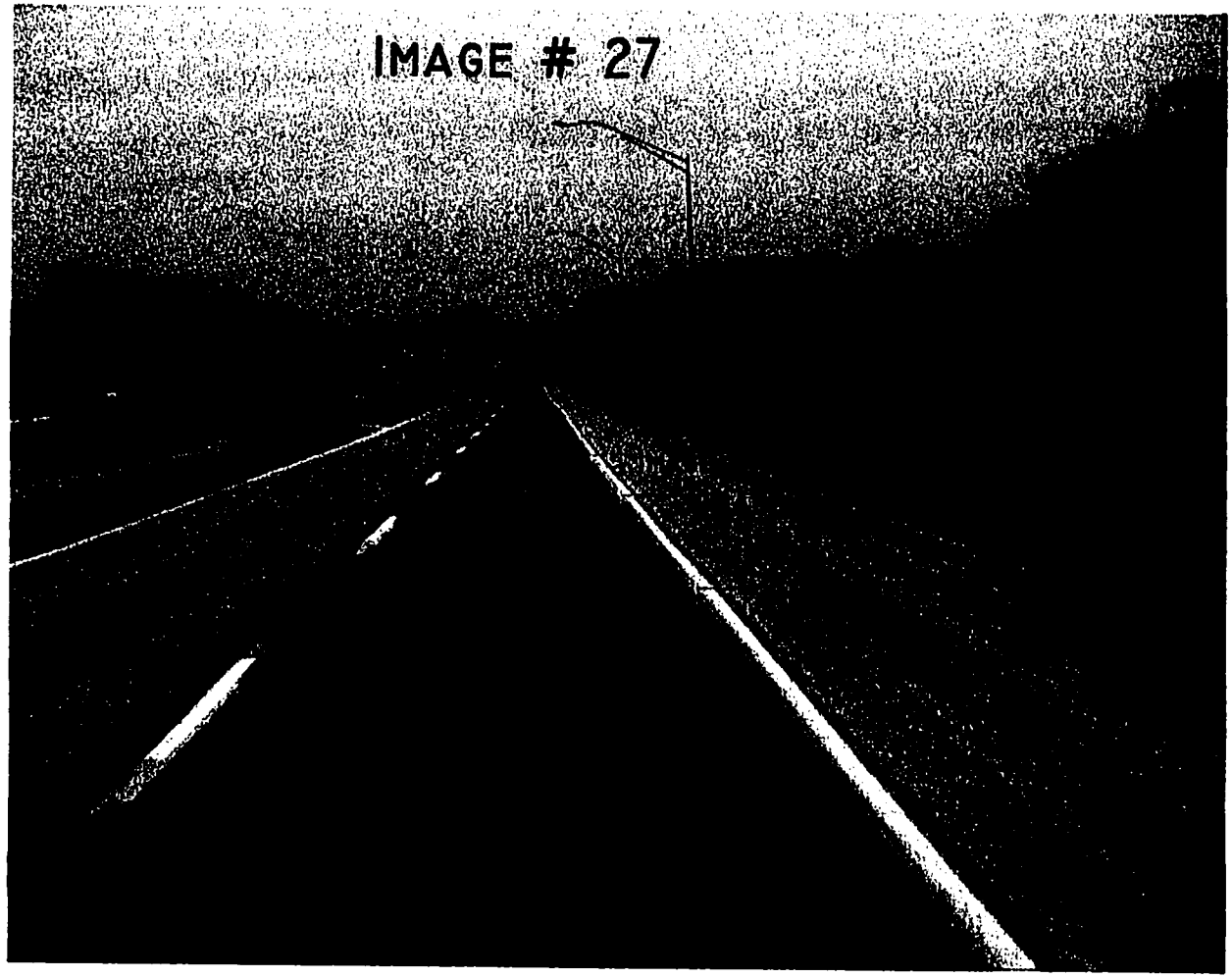

Figure 5.3 Estimating object point coordinates on image

Figure 5.4 Image on viewer for measurement object points

The following formula is used to do this transformation.

$$\left.\begin{aligned} x_p &= c_i - C_i + 0.5 \\ y_p &= R_i - r_i + 0.5 \end{aligned}\right\} \quad [5.5]$$

where,

$x_p \rightarrow$ x value in the photo coordinate system

$y_p \rightarrow$ y value in the photo coordinate system

$c_i \rightarrow$ column number in the image coordinate system

$r_i \rightarrow$ row number in the image coordinate system

$C_i \rightarrow$ total number of columns in the image

$R_i \rightarrow$ total number of rows in the image

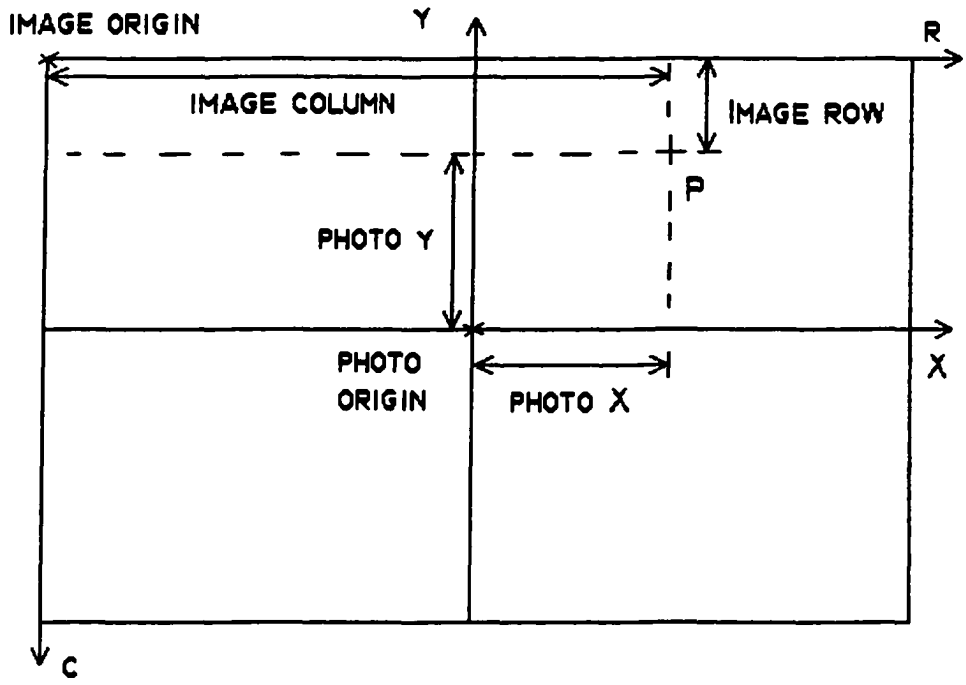

Figure 5.5 Image and photo coordinates

5.2.9 Refining Camera Parameters

There are nine elements of Interior Orientation (IO) and six elements of Exterior Orientation (EO) that are calibrated during the camera calibration procedure. Out of these, the IO elements, including the focal length, are assumed to be constant throughout the calibration

and the data collection phases. Therefore, the values of the elements of IO are obtained from the calibration phase and treated as constant by assigning relatively higher weights. The EO elements consist of two types: the xyz positions and the rotation angles ω, φ, and κ. The xyz positions are obtained fairly accurately from the GPS log of the image after transforming them into the local coordinate system. These values are also treated as constants by assigning relatively larger weights to them. However, the direction elements (i.e., ω, φ, and κ) have a potential to change depending upon the instantaneous positioning of the van. Therefore, the ω, φ, and κ obtained from the calibration set up are somewhat tentative in the beginning. A fairly well defined feature location tests these direction elements. If the preliminary run of the CALIB shows high residuals on the computed values, then the weights of the angles are relaxed so that the computed values may change to yield lower residuals. The angle for which the weight needs to be changed is identified by observing the computed values of the parameters as well as the computed residuals. Finally, while determining other feature locations, the optimum computed value of the angle is obtained and assigned higher weights.

5.2.10 Determination of Object Point Locations

When the final camera parameters to be used for a specific site are known, other feature points of unknown locations can be determined. There are two ways to do it. Either, compute all the points at once, or compute them individually. The first method, seemingly straightforward, has the possibility of being marred by one or two bad points. These points may turn out to be bad due to poor initial approximation or poor resection geometry depending upon where they appear in the photo format of the pair of images. If they do, the software computations may diverge. It is usually a difficult task to identify the bad points. On the other hand, the second method is easier to handle and normally yields some results that can be analyzed to locate the source of the problem.

A simple and systematic procedure can be outlined to determine feature locations one by one. The user needs to have three windows open at the same time for fast processing of the data: (1) An image viewer for determining image coordinates of the point of interest as shown in figure 5.4, (2) a second window for modifying the data file and running the CALIB software with new data as shown in figure 5.6, and (3) an interface with a spreadsheet as shown in figure 5.7.

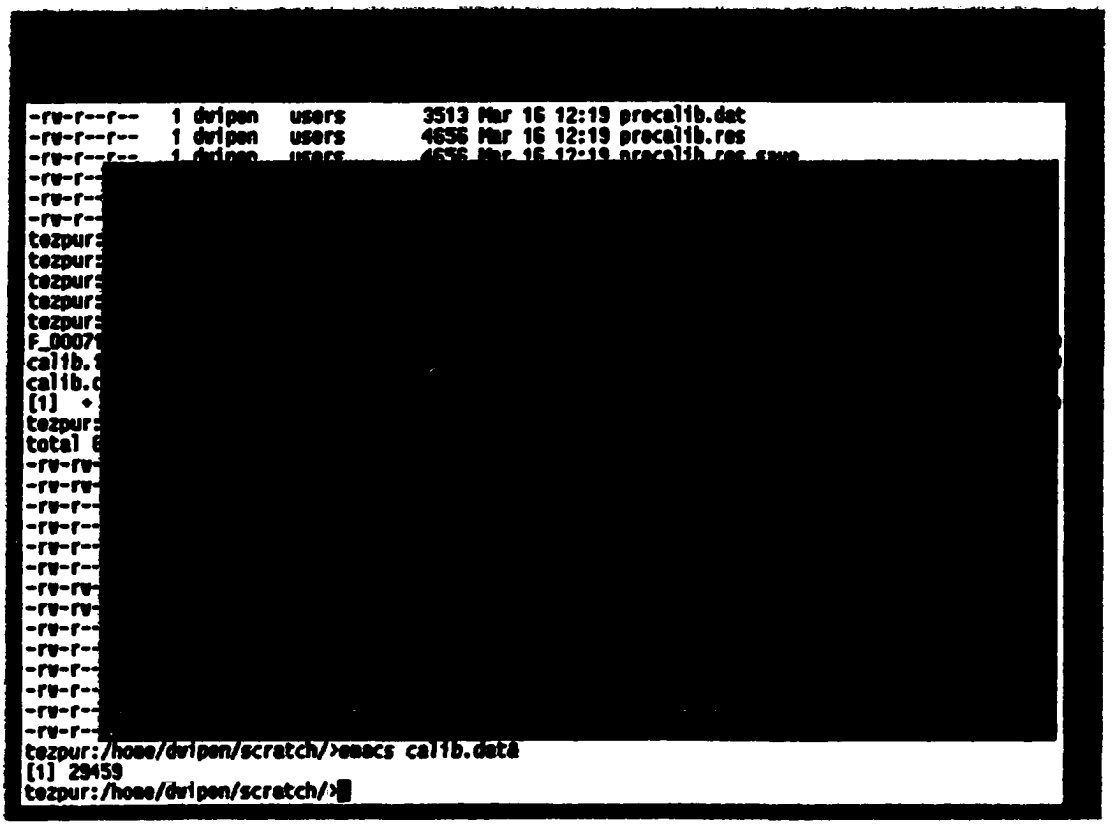

Figure 5.6 Editing data file and running CALIB

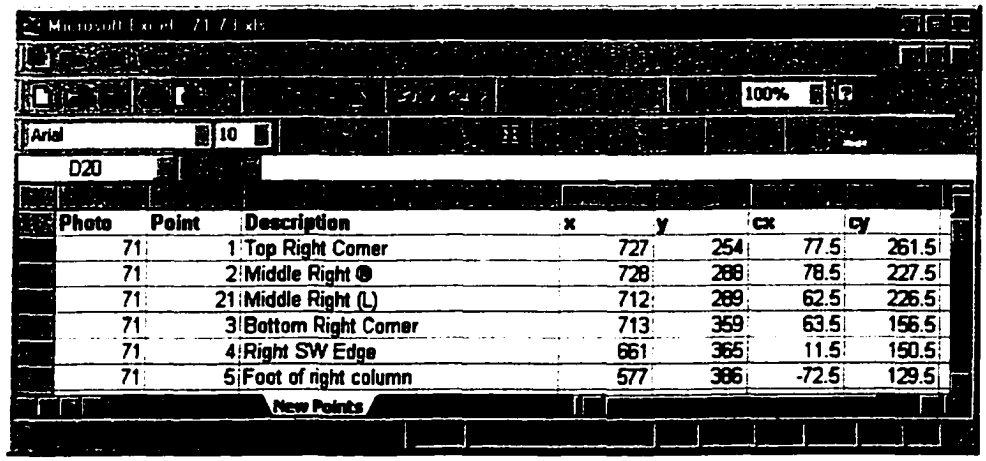

Photo	Point	Description	x	y	cx	cy
71	1	Top Right Corner	727	254	77.5	261.5
71	2	Middle Right ®	728	288	78.5	227.5
71	21	Middle Right (L)	712	289	62.5	226.5
71	3	Bottom Right Corner	713	359	63.5	156.5
71	4	Right SW Edge	661	365	11.5	150.5
71	5	Foot of right column	577	386	-72.5	129.5

Figure 5.7 Spreadsheet for coordinate transformation

The interface is used for two purposes: [1] to quickly transform image coordinates to photo coordinates for use as input to CALIB and, [2] to enter the computed position of feature data obtained from the CALIB output data file. This method is easy and much quicker.

5.2.11 Transformation from Local System to World System

The computation in CALIB yields the object point locations with reference to the local coordinate system. For any meaningful comparison, these numbers need to be transformed to a world coordinate system. By knowing the world coordinates of the two

camera positions, the local coordinates of the object point can be transformed to the world system.

A simple interface was developed using Visual Basic to accomplish this task. The interface is shown in Figure 8. The user inputs the world coordinates (Northing and Easting) of the two camera positions into the specified text boxes. Also, the X and Z values of the object point are computed by CALIB with reference to the local coordinate system. The Transform button triggers the computation. The Clear button permits the user to clear all fields, while the exit button exits the program. The algorithm check against non-numerical values entered into the text box and prompts the user for a correction in case of an incorrect data entry.

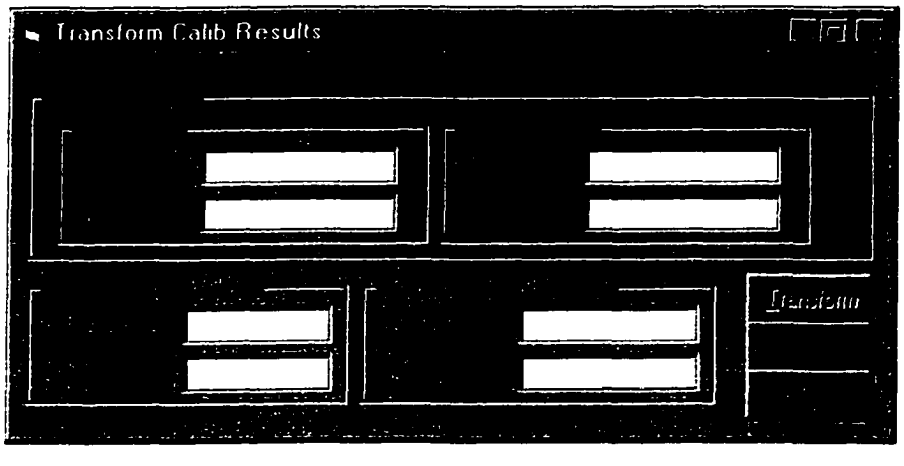

Figure 5.8 An Interface for coordinate transformation program

The Transform button becomes active when all the input fields are filled with numerical data. When the user hits the transform button, the transformed coordinates of the object points are displayed in the labeled text boxes. A listing of the program is included in Appendix D.

5.3 Evaluation

A comparison of the computed positions with ground truth data validates the results. The above procedure was tested at three different test sites. These sites are representative of three different environments and road conditions, namely, (1) rural area, (2) residential and metropolitan area and (3) freeway. Feature data collection was done at three sites: 1) DEM Calibration Baseline site to the southwest of Ames, 2) Railroad bridge on the Grand Avenue, Ames, and 3) US Highway 30 to the south of Nevada. The data acquisition of each of the three sites was completed in less than 30 minutes.

The ground data was obtained by using a Total Station Survey and RTK GPS survey. The computed positions are compared in terms of absolute distances and feature dimensions. For example, the height of electric poles is measured using a total station and compared to the

computed height as obtained from the data collection procedure, outlined above.

5.3.1 EDM Baseline Site (Rural)

This baseline was set up in a ditch by the side of a rural road in South-West Ames, Iowa for the calibration of surveying instruments. It contains several control points lying in a straight line in the east-west direction over a distance of about one mile. This stretch of the road is representative of a rural road where minimal roadside features are found that need to be mapped. Both, the Total Station Survey and RTK system collected the control data for the roadside features.

Three stretches of this road were chosen for verification of accuracy for feature collection: one at the east end, another in the middle and the third one at the west end. General roadside features include power poles, fence posts and traffic signposts. The image in figure 5.9 shows the kind of features that can be seen on this road. The measured feature points are marked and numbered on the images.

5.3.1.1 Optimum Image Separation

Feature locations were determined using two images at a time with separation ranging from 25 feet to 150 feet. Positional accuracy of features with different separation distances is shown in table 5. It can

be seen from the result that the best degree of accuracy was achieved with images spaced at 75 feet to 100 feet. This can be explained by the better geometric strength resulting from the spacing between the images.

Figure 5.9 Object points at the EDM baseline site (middle section)

5.3.1.2 Accuracy of Data reduction

Table 5 also shows that an accuracy of better than one meter can be achieved by using the data reduction procedure for video-log data developed in this study. In addition to measurement of locations, feature dimension has also been performed.

Table 5 Accuracy of data reduction for different image spacing

Image Spacing (ft)	Accuracy in		
	Northing (meters)	Easting (meters)	Elevation (meters)
25	0.225	1.831	-0.236
50	0.073	1.330	-0.304
75	-0.185	0.554	-0.428
100	-0.039	1.347	-0.422
125	-0.116	1.030	-0.450
150	-0.023	1.631	-0.460
25	0.943	0.967	0.173
50	0.167	-1.644	-0.082
75	0.291	-0.914	-0.098
100	0.634	0.345	0.004
125	-0.050	-2.031	-0.237
150	-0.203	-2.578	-0.286
25	4.690	1.984	0.881
50	-0.055	1.329	-0.390
75	-0.039	1.646	-0.319
100	-0.306	0.548	-0.343
125	0.461	3.534	-0.188
150	1.894	9.559	0.147

Heights of electric poles were determined at the east, middle and west segments of the baseline site. Table 6 shows the comparison of heights of the electric poles at the three segments with the Total Station Survey results. The results show accuracy of 10 cm or less at the middle and west segments. The higher difference at the east end may be attributed to incorrect intersection of the ground point from grass cover.

Table 6 Accuracy of feature dimension at EDM baseline site

Location	**Difference (meters)**
East	-1.22
Middle	-0.10
West	-0.07

5.3.2 Lincoln Way-Grand Avenue (City/Residential)

This site is in the heart of the city of Ames covering parts of Lincoln Way, Grand Avenue and some of the surrounding areas. It is a representative sample of both residential and city metropolitan areas.The site consists of several road site features including a railroad bridge, light poles, manholes, sidewalks, and paved roadway. The railroad bridge has an underpass with a much-involved degree of terrain variation (See Figure 5.10). Therefore, a large number of points

must be determined if the geometry is to be reconstructed for facilitating an accurate viewing of the data. This is why the special method developed in this study has been employed to collect a large number of feature points. A few points, which are well defined on the ground and on the images, were first selected.

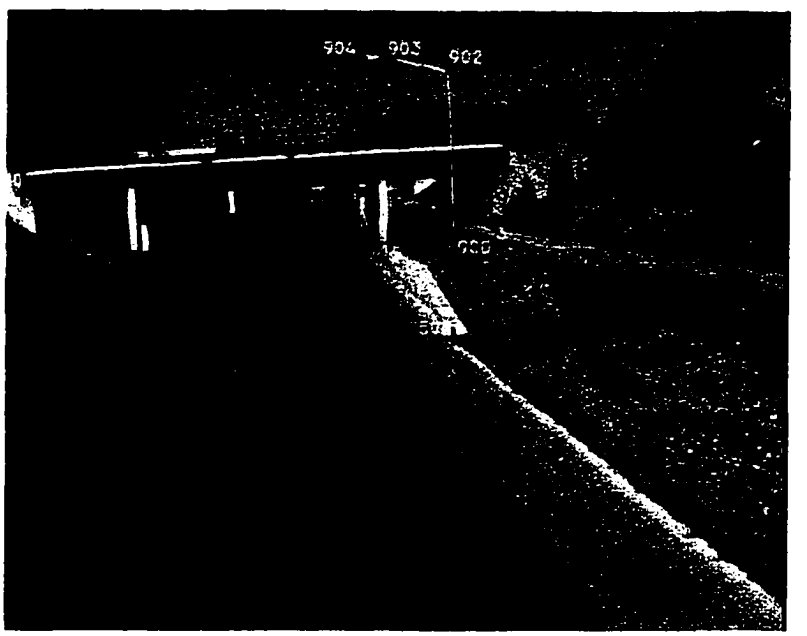

Figure 5.10 Object points at the Grand Avenue site

With a good estimate of the camera positions and relative feature positions, a strong photogrammetric solution has been achieved. Using the camera parameters for this optimum solution, more feature point locations were determined quickly, one by one.

The ground truth data at this site were derived from the Total Station survey using a local coordinate system. The video locations were transformed to the local coordinate system for the purpose of comparison. The data accuracy was tested on two features: (1) the edge of the road pavement, and (2) an electrical utility pole. The difference in the actual position as measured on the arbitrary coordinate system is presented in Table 7. It can be seen that an accuracy of better than 10 centimeters was achieved on the two features.

Table 7 Accuracy of object positioning at the Grand Avenue site

Point Description	**Accuracy in Northing (meters)**	**Accuracy in Easting (meters)**
Electric Pole	-0.086	-0.035
Road Edge	-0.073	0.073

5.3.3 Nevada Site (Highway)

The Nevada site consists of a section of the US Highway 30 to the south of Nevada. This site is representative of a freeway road environment. The site includes such features as a divided highway, traffic intersection, electrical utility poles and traffic signposts. Object positions were computed for figure 5.11, showing an image of this site.

Object points that were used for computation are also shown numbered in the figure.

As in case of the Grand Avenue site, the ground truth data were obtained using a Total Station survey. In this case, the ground truth data were transformed to the State Plane Coordinate system. Similarly, the video location data too was transformed to the State Plane Coordinate system.

Figure 5.11 Object points at the Nevada site

Spatial locations of the two electrical utility poles were available from the ground truth data measured by the Total Station survey. Therefore, these poles were selected for evaluation of positional

accuracy of the data reduction procedure at this site. Table 8 shows a comparison of the computed object positions with reference to ground truth data. It can be seen that sub-meter accuracy has been achieved in location the features. In addition to electrical utility poles, positions of a few other points as shown in figure 5.11 were also computed. These additional points provided means for computing a couple of ground dimensions which were then compared with the ground truth data from the Total Station survey. The results are shown in Table 9. An accuracy of about 10 centimeters is achieved in these measurements.

Table 8 Accuracy of object positioning at the Nevada site

Description	Accuracy in Northing (meters)	Accuracy in Easting (meters)
First Pole	-0.090	0.071
Second Pole	-0.166	0.362

Table 9 Ground Dimensions at the Nevada site

Dimension	**Ground dimension (meters)**	**Calib dimension (meters)**
Pole to other edge of road	12.860	13.005
First pole to second pole	54.912	54.836

5.4 Summary

Evaluation of the data reduction procedure developed in this study for using digital images and RTK-GPS shows acceptable results with accuracies suitable for an As Build survey of roadside features. Digital images and corresponding camera positions as obtained from video-logging system were used to precisely position roadside features. Feature dimensions were also determined using the same principles, the achieved accuracies are presented. The overlapping digital images obtained from the video-log van system are separated in the direction of the camera axis. It is found that a separation of about 75 to 100 feet between the images was optimal for the photogrammetric data reduction procedure. The a priori feature locations can be very closely estimated by using the procedure developed for the purpose. Features were located at less than one meter from the actual position. Feature dimensions were also determined with similar accuracy.

CHAPTER 6 REMOTE SENSING

Lillesand and Keifer defines [5] Remote Sensing as "the science and art of obtaining information about an object, area, or phenomenon through the analysis of data acquired by a device that is not in contact with the object, area, or phenomenon under investigation". Therefore, when one looks at an object and recognizes it through its appearance, then it is a form of remote sensing. This can be very useful in As Built Survey. Remote sensing can extract texture information from the same digital images, which are usually processed in digital photogrammetry to extract geometric information. Remote sensing can also digitally enhance and classify the images to highlight certain area of interest. For example, some parts on a concrete bridge may contain structurally damaged areas that may not be detected. However, digital image processing can enhance such images to make them more prominent.

Creation of VR applications need both geometric and textural information. The geometry provides the shapes and texture provides the realistic appearance. Texture can be extracted from simple images

of objects; it can also be extracted from images that are classified and enhanced using remote sensing. Thus it enhances information on the VR models, and improves the usefulness of the VR application. This chapter describes various aspects of remote sensing for data acquisition and analysis.

Air-photo interpretation was a precursor to development of remote sensing. It was initially developed as a military reconnaissance tool during World War I. Subsequently, many civilian applications including timber surveys, agricultural soil conservation, geological studies, mineral exploration and flood plain management were developed. In terms of scientific principles, equipment and methods of data collection and analysis, remote sensing is much broader than air-photo interpretation. Today air-photo interpretation is regarded as only one of several aspects of remote sensing [57,58].

Remote sensing consists of two basic processes, namely, (1) data acquisition, and (2) data analysis. The process of data acquisition involves a sensor, mounted on a platform, sensing electromagnetic radiation coming in from the remote object that is being studied, and recording it on a specific format such as photographic paper or a magnetic or digital tape. Development of the sensors and their operation depended much on the characteristics of the electro-

magnetic radiation and their interactions with the atmosphere and the remote objects. Data analysis involves interpretation of the recorded energy information to gain knowledge of properties of the remote object. Depending on the format of data acquisition, specific procedures can be adopted for extracting the desired information from the remotely sensed data. Important components in these two processes include principles of electromagnetic energy, sensor platform, different sensors and principles of data analysis. With the advent of powerful computer technology, methods of digital image processing are used for data analysis. All these aspects of remote sensing are described in the following sections. While doing so, lecture notes by Dr. K Jeyapalan on course CE-519 Remote Sensing in of spring of 1997 were referred to.

6.1 Electro-Magnetic Energy

Visible light, sound, heat, and radio waves are some forms of electromagnetic energy that radiate from a source and interact with the medium passed through, and also with the objects they strike. The radiation of electro-magnetic energy obeys the basic wave theory, which is described by the equation

$$c = \nu\lambda \qquad [6.1]$$

Where c is the velocity of light, which is a constant (3×10^8 m/sec), ν is the frequency in Hertz, and λ is the wavelength of the electromagnetic radiation. The frequency and wavelength of any wave are related inversely, and either of the two can be used to characterize a wave. The wavelength is generally used to characterize a particular wave and the most common unit used is the micrometer (μm), which is equal to 1×10^{-6} meters. The entire range of electro-magnetic wavelengths is termed as the electromagnetic spectrum and may be represented on a logarithmic scale as shown in figure 6.1. Figure 6.2 shows a more detailed representation of the electromagnetic spectrum in the vicinity of that part which is visible to the human eye.

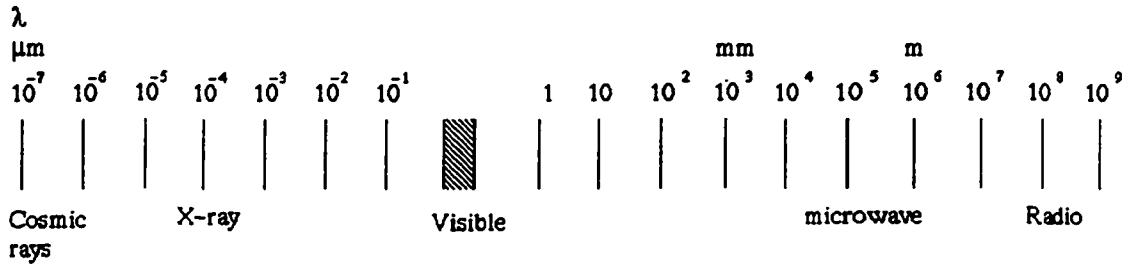

Figure 6.1 The electromagnetic spectrum

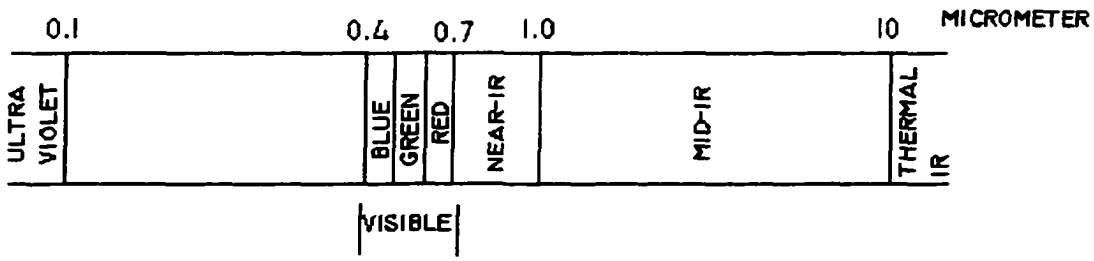

Figure 6.2 Visible part of electromagnetic spectrum and vicinity

The particle theory describes electromagnetic radiation in terms of discrete units of energy called photons or quanta. This theory associates the energy content of a radiation to its frequency as in the equation

$$Q = h\nu \qquad [6.2]$$

Where

Q = energy of a quantum, Jules (J)

h = Plank's constant, 6.626×10^{-34} J sec

ν = frequency

The quantum of energy can be related to the wavelength by substituting the expression of ν in from equation 6.1 into equation 6.2

$$Q = \frac{hc}{\lambda} \qquad [6.3]$$

Radiation with higher frequency or shorter wavelength, such as ultra-violet ray, is associated with higher energy content, and can be sensed by the sensors relatively easily. On the other hand, radiation with low frequency or longer wavelength, such as thermal infra-red or microwave, is associated with a low energy content, is difficult to sense, and is used to sense large objects only. A sensor usually senses only a part of the whole spectrum. Many factors including the characteristics of energy sources, energy interaction with the atmosphere and the remote object influence the design aspects of a sensor. These factors are discussed in the following subsections.

6.1.1 Radiation Sources

Remote sensing systems are categorized into active or passive depending upon the source of the radiation energy. An active remote sensing system is one that generates and sends the radiation to be

reflected by the object to be sensed. There are many active remote-sensing systems that use different segments of the electromagnetic spectrum. A camera with a flashgun is an example of an active remote-sensing system. The flashgun is the source of radiation in this case. The laser scanning system is another example. On the other hand, a passive remote sensing system does not generate energy. Such systems sense the energy reflected or emitted by the remote object. Common sources of energy for passive systems are the sun and the earth. The passive systems are usually used for remote sensing and active systems are used in special circumstances.

Any object with absolute temperature above 0° K can be treated as a source of radiation because it continuously emits electromagnetic energy. The radiation from the sun and various terrestrial features on the earth surface has widely varied magnitude and spectral composition. The amount of energy radiated by an object is a function of the temperature of the object and is expressed by the Stephan-Boltzmann law, which states that

$$M = \sigma T^4 \qquad [6.4]$$

Where

M = total radiant exitance from the surface of the object, Watts (W) m^{-2}

σ = Stepha-Boltzmann constant, 5.6697×10^{-8} W m^{-2} $^oK^{-4}$

T = absolute temperature (^oK) of the emitting material

This is also the formulation of the principle of ideal black body radiation. It is evident that the emitted energy varies proportional to the fourth power of the temperature. Therefore, the sun with a surface temperature of 6000^{o}K emits much more energy than the earth with an average surface temperature of 300^{o}K. Radiated energy is not uniform across the spectrum. For each energy source, the highest amount of energy is radiated at a particular wavelength that dominates the spectrum. The Wein's Displacement Law given below gives this dominating wavelength.

$$\lambda_m = \frac{A}{T} \qquad [6.5]$$

where,

λ_m = wavelength of maximum spectral radiance, μm

A = 2898 μm ^{o}K

T = temperature ^{o}K

The Figure 6.3 illustrates the spectrum of black body radiation depending upon the surface temperature of the emitting body. It also shows that the higher temperature produces greater emitted energy and the shifts the dominant wavelength to the shorter wavelength zone. It can be seen that the sun with a surface temperature of 6000 ^{o}K has a spectral composition that ranges from 0.1 μm to 100 μm and peaks at the visible band. On the other hand, the earth with an average temperature of 300 ^{o}K has a much smaller spectral range of about 46 μm ranging from about 4 μm to 50, μm peaking at 10 μm, which is the thermal infrared zone of the electromagnetic spectrum.

6.1.2 Interaction in Atmosphere

Before a sensor senses the radiant energy coming from a source, the energy has to pass through the intervening media, the atmosphere. The atmosphere affects the radiation in two ways: (1) by scattering and (2) by absorption. The particles present in the atmosphere affects scattering of the radiation passing through the atmosphere. On the other hand, absorption results in loss of energy during transmission.

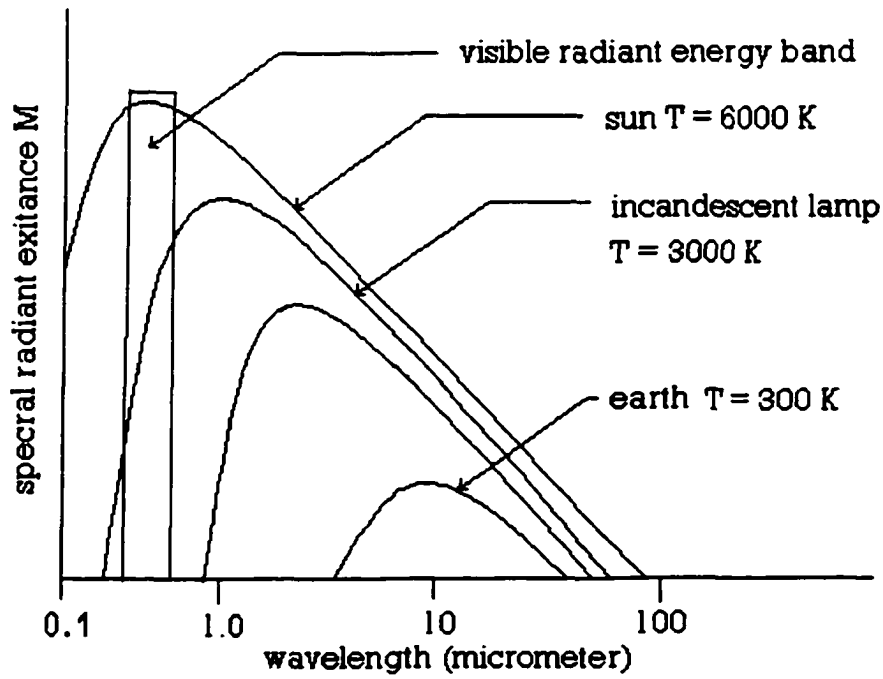

Figure 6.3 Spectral distribution of blackbody radiation

6.1.2.1 Scattering

Scattering depends on the particle size relative to the wavelength of the radiation. Scattering affected by particles much smaller than the wavelength of the energy is called Rayleigh's scatter. Since it is inversely proportional to the wavelength the shorter wavelengths are more affected. The blue sky is the result of high frequency blue lights in a clear sky containing minute gas molecules. Rayleigh's scatter

creates a haze in satellite imagery and reduces contrast. It is controlled by using a filter.

When the particle size is comparable to the wavelength of the radiation, Mie scatter results. This type of scatter is more predominant in the longer wavelength region of the electromagnetic spectrum. Mie scatter is affected by presence of water vapor and dust particles. It results in an overcast sky.

Non-Selective scatter results when the size of the particles is much larger than the wavelength. A water droplet is an example of such a particle. This type of scatter is independent of the wavelength of the radiation. Presence of non-selective scatter makes it difficult to distinguish between fog and clouds, both of which appear white.

6.1.2.2 Absorption

Carbon dioxide, water vapor and ozone present in the atmosphere act like absorbing agents. However, the absorption takes place only in a selective manner depending upon the wavelength. The radiant energy at certain wavelength is either partially or completely absorbed, while at other wavelengths there is no absorption at all. Figure 6.4 illustrates the absorption phenomenon at various wavelengths. Water vapor, carbon dioxide, and ozone molecules affect

various absorption bands. In these bands, radiant energy is not available for sensors. Therefore, the sensors must be designed to use the wave bands when the radiant energy is transmitted with no or little absorption. These special bands are known as atmospheric windows. The atmospheric window that exists at the visible band and in its vicinity on the electromagnetic spectrum is used in many of the contemporary sensing devices. Sensors designed for special applications that use thermal infrared and microwave sensing use the other windows.

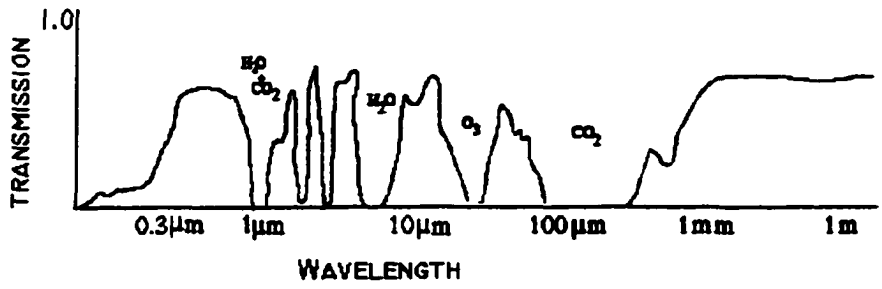

Figure 6.4 Atmospheric absorption at different wavelength

6.2 Remote Sensing Platforms

Remote sensing systems differ according to the various kinds of platform housing the sensing device. The choice of a particular platform type and associated sensing device usually depends upon

factors such as desired spatial resolution, geometric accuracy, and repeatability of data acquisition, scale, and type of application. The distance from the remote object to the sensor directly affects many of these factors. Figure 6.5 shows the various systems used for remote sensing. A brief discussion of these platforms and the sensors the are given in the following subsections.

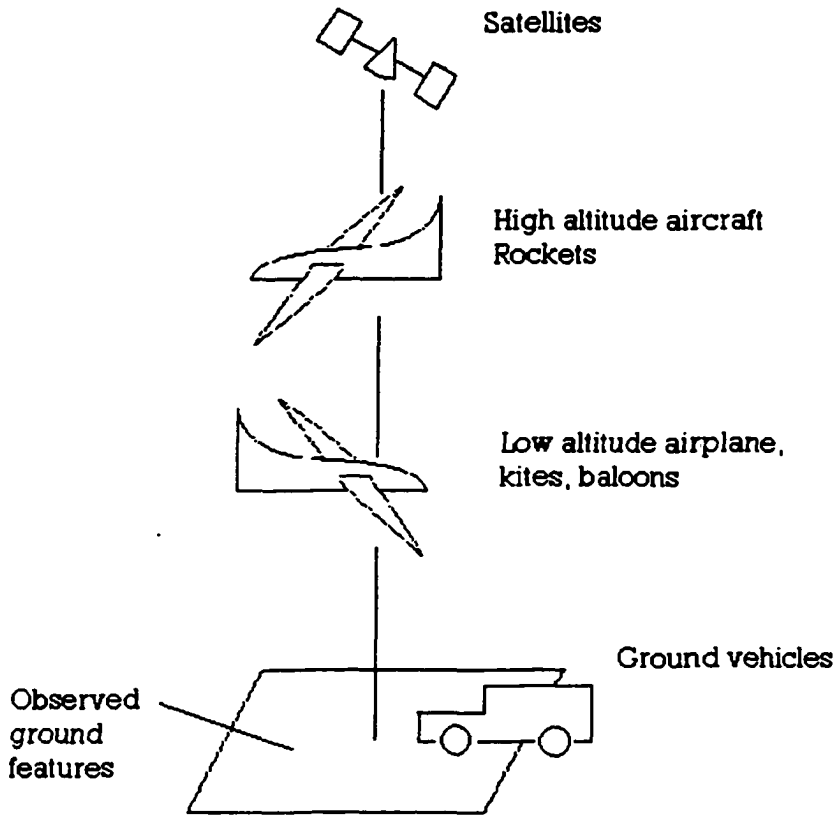

Figure 6.5 Remote sensing platforms

6.2.1 Satellites

Satellite vehicles are suitable for acquisition of earth resource data in a repetitive manner. A very large area is covered by satellite imageries. Therefore, these are used for applications involving earth resources. They are also used for change detection and updating topographic maps

The earth resource satellites are of two types: sun-synchronous and Geostationary. Sun synchronous satellites are placed in an orbit at an altitude of about 900 KM. These satellites cross over the equator at the same local time every day. They are suitable for obtaining repetitive coverage of any location on earth's surface over a period of about eighteen days. Data from the sun-synchronous satellites are useful for applications involving natural resource inventory, agricultural monitoring and flood plain management. Examples of sun-synchronous satellites include the Landsat series, *Systeme Pour l'Observation de la Terre* (SPOT) series, Japanese Remote Sensing Satellites (JRS) and Indian Remote Sensing satellites (IRS), Defense Meteorological Satellite Program (DMSP) satellites

Geostationary satellites orbit the earth at an altitude of about 35,000 KM maintaining the same relative position with respect to the earth surface. These satellites are useful for obtaining continuous data

of the same location of the earth's surface. These satellites are mainly used for meteorological applications. Examples of geo-synchronous satellites are Geostationary Operational Environmental Satellites (GOES).

6.2.2 Aircrafts

High altitude and low altitude aircraft are primarily used for aerial photography where an aerial camera is the sensor. The aerial photographs are of high resolution and are suitable for accurate cartographic applications. The aerial camera is always mounted to have its axis in a near vertical position.. Taking this special situation into consideration, mathematical formulations for aerial photographs were developed.

6.2.3 Ground Based Remote Sensing

In recent times, ground based remote sensing systems are gaining popularity. These systems usually consist of a digital camera for imaging, associated sensors of Global Positioning System (GPS) and Inertial Navigation Systems (INS) that help accurate positioning of objects that appear in the imageries. Contrary to nearly vertical camera axis in an aerial photograph, the ground-based systems have the

camera axis in a near horizontal direction. Therefore, the camera axis may be tilted at large angles to the reference coordinate system. These systems usually use digital photogrammtric system for data extraction.

6.3 Sensing Devices

Remote sensing devices are developed to use various segments of the electromagnetic spectrum as illustrated in Figure 6.6. In the early stages in the development of remote sensing, aerial cameras were the sensors used in the visible band of the electromagnetic spectrum. In addition to the visible range consisting of the red, green and blue bands, the photographic systems can sense near infrared band of the spectrum. The satellite systems use such sensing devices as Multi-Spectral Scanner (MSS), Thematic Mapper (TM), Return Beam Videocon (RBV) camera, High Resolution Visible Imaging System (HRV), Linear Imaging Self Scanning Sensor (LISS), and Wide Field Sensors (WiFS). These are designed to cover specific parts of the electromagnetic system. On the other hand, active remote sensing devices such as Side Looking Airborne Radar (SLAR), and Light Detection And Ranging (LIDAR) senses energy in the microwave region of the spectrum and are mounted on aircrafts. These systems have

their own advantages and limitations and are useful for particular applications

6.3.1 Photographic Camera

A photographic camera detects quantum of energy and records it on a photographic plate. It consists of, among others, a photographic lens, a film, and a case for housing these two elements.

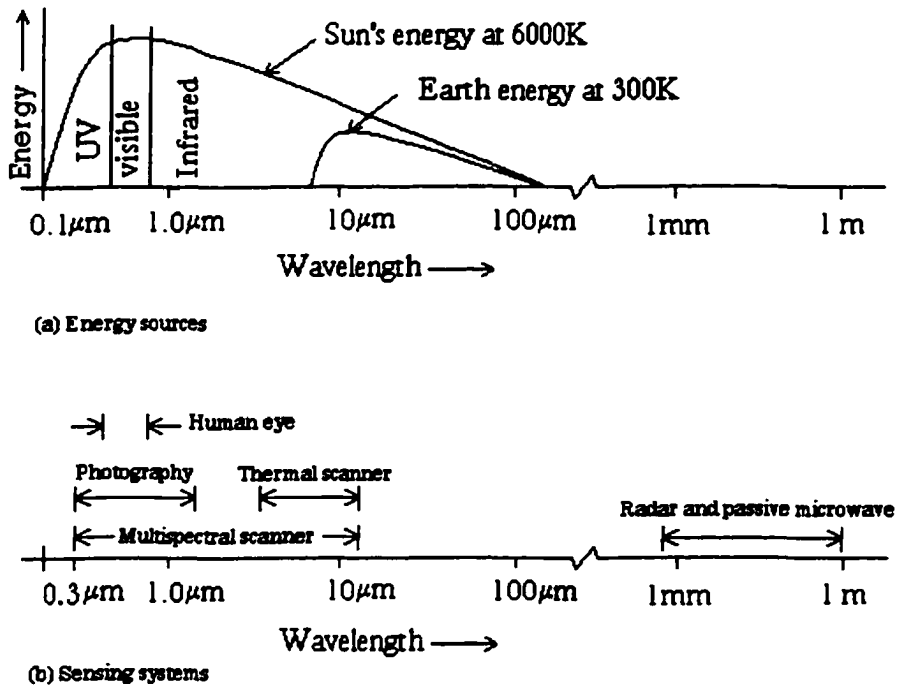

Figure 6.6 Spectral ranges of sensing devices

Figure 6.7 shows the various components of an aerial photographic camera. The lens should be free from aberrations and geometric distortions because the aberrations degrade the image sharpness and the distortions degrade the geometric quality of the photograph.

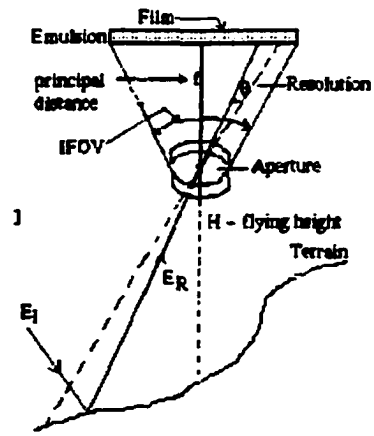

Figure 6.7 Components of an aerial camera

The angular separation θ is a measure of the resolution of the lens and is given by the equation

$$\theta = \frac{1.22\lambda}{A} \qquad [6.6]$$

where

λ = wavelength of the incident energy

A = aperture of the lens

The lens focuses the photons in the incoming radiation onto the film, which is covered by photosensitive emulsion. As a result of the reaction, dark silver (Ag) particles are precipitated with density proportional to the intensity of the radiant flux. The quality of the film is measured in terms of lines per minute (LPM) of the object that can be resolved in the imagery. The acceptable value of LPM for an aerial camera is about 50 to 60.

The scale of the image produced by the camera is given by the ratio of the principal distance of the camera (f) to the flying height (H), and is expressed as

$$S = \frac{f}{H} \qquad [6.7]$$

The principal distance of the camera, or the lens focal length is the distance between the film plane and the objective lens plane. The scale on a high altitude aerial photograph is nearly uniform over different parts of the image. However, the scale on a photograph taken

by a ground-based system varies widely depending upon variation in the distances of various features appearing on the image. The scale of an aerial photograph may very from 1:60,000 in case of high altitude photography to about 1:600 in case of low altitude photography.

The interplay of aperture setting, and the shutter speed influences the extent of distortion and appropriate exposure of the film for imaging. The total angular exposure is known as the Instantaneous Field Of View (IFOV). IFOV is proportional to the diameter of lens opening, and should be small to limit geometric distortions. At the same time, the shutter speed should be adjusted accordingly to provide appropriate exposure of the film. The relationship can be mathematically represented by the following expression

$$E = \frac{sd^2t}{4f^2} \qquad [6.8]$$

where

E = film exposure, J mm^{-2}

S = scene brightness, J mm^{-2} sec^{-1}

d = diameter of lens opening, mm

t = exposure time, sec

f = lens focal length

There are various metric and non-metric cameras that are used in ground-based photogrammetry. The single metric cameras include Hasselblad MK70, Rolleiflex 60006, Zeiss (Jena) UMK10/1318 FF, Kelsh K-470, and Wild P31 and P32. There are stereo-metric cameras, such as Zeiss DK40 and Jena IMK10/1318, Kelsh K-460 and K-490, and Pentax ST-120V, that consist of two cameras, usually mounted on a horizontal base bar. Usually, it is possible to change the relative position and orientation of the cameras.

Non-metric cameras are being increasingly used for photogrammetric purposes. There are several advantages in using the non-metric camera [59]:

- They are easily available.
- Their focus range is flexible.
- Some are motor-driven, allowing imaging at quick succession.
- Imaging can be done in hand held position.
- They are economical compared to metric cameras.

However there are some disadvantages too.

- Their lenses are of high resolution but they produce high distortion.
- Interior orientation is unstable.
- There are no fiducial marks on the image plane.
- There are no level bubbles for fixing exterior orientation before exposure.

6.3.2 Non-Photographic Camera

Unlike the aerial photographic camera, non-topographic cameras do not record images very directly onto a photographic film, but record image data using light sensitive detectors that generate electrical signals. The signals are then stored on magnetic tape or computer disk. These images can be directly fed into digital computers.

6.3.2.1 Beam Videocon (RBV)

RBV does not contain an image film. Instead, the image sensed by the RBV can be used to provide static or dynamic display on a cathode ray tube. The geometric distortion parameters can be corrected in the same manner as for a photographic camera by imaging an array of tick marks. Landsat uses the RBV with a 50 × 50 mm target surface and resolution of about 100 LPM. The advantage of the RBV over the

photogrammetric system is that the signals can be transmitted and need not be captured on film. Thus, it is suitable for satellite remote sensing and for ground-based systems.

6.3.2.2 Solid State Array Cameras

These cameras use one- or two-dimensional detector arrays of Charge Coupled Devices (CCDs) for image acquisition. The CCD is a solid state sensor that consists of microelectronic silicon chips. The sensor detects light and produces an electrical charge, the magnitude of which is proportional to the intensity of the light and exposure time. CCDs can record a wider range of light intensities than is possible with a photographic film or an RBV. A one-dimensional or linear array can produce a two-dimensional image by using a scanning system known as push broom scanning. However, a two-dimensional array can produce the image without a scanning device. Each detector in the array senses one pixel of the image field. The array size typically ranges from 256 × 256 to 2048 × 2048 pixels or more. This type of sensor is widely used in digital cameras, used for digital photogrammetric data acquisition.

6.4 Data Analysis

Analysis of remote sensing data involves two aspects: (1) interpretation of the image content and (2) presentation of the information in the form of an end product such as a map, or tabular data. Interpretation of the image data depends on several factors: (1) spectral sensitivity of the sensor, (2) presence or absence of atmospheric windows in the spectral ranges, (3) source, magnitude, and spectral composition of the energy, (4) geometric quality of the sensor and (5) availability of reference data. The data may be interpreted visually or by digital techniques. Some important aspects of remote sensing data are described in the following subsections.

6.4.1.1 Energy Interaction With Remote Object

The interaction of the radiant energy with the remote object provides clues to the identification of the object. Of the total energy ($E_I(\lambda)$) incident on the remote object, a part of it is reflected ($E_R(\lambda)$), a part is absorbed ($E_A(\lambda)$), and a part is transmitted ($E_T(\lambda)$), as illustrated in Figure 6.8. The relationship between these components can be expressed as

$$E_I(\lambda) = E_R(\lambda) + E_A(\lambda) + E_T(\lambda) \qquad [6.9]$$

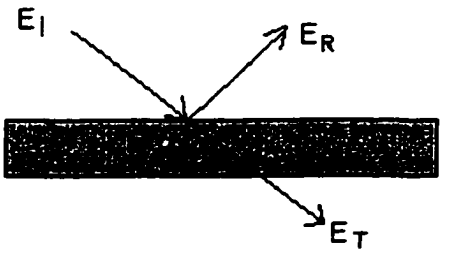

Figure 6.8 Energy interactions with object

For a given incident radiation, the ratio of the three components $E_R(\lambda)$, $E_A(\lambda)$, and $E_T(\lambda)$ will be different objects. Moreover, these components will be different for energy of different wavelengths. Therefore, the variations in interaction of energies at different wavelengths can provide reliable clues to identity of remote objects.

The sensor detects the reflected energy. The object reflecting energy may have a smooth surface that acts as a specular reflector or a rough surface that acts like a diffused reflector. The specular reflectors affect a mirror-like reflection while the diffuse reflector scatters the energy in all directions. Figure 6.9 illustrates the different types of reflectors. The roughness or smoothness of a surface is determined by magnitude of the surface irregularity in comparison with the

wavelength. For example, a rocky terrain may appear rough in long wavelength region and rough in the short wavelength region.

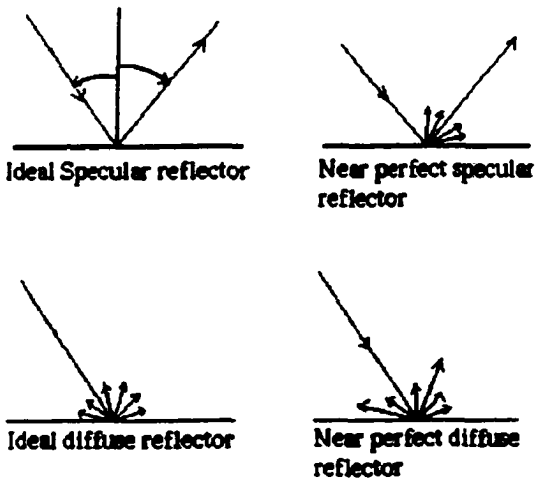

Figure 6.9 Types of reflectors

In remote sensing, the diffused reflectors are preferred to the specular reflectors because they convey more information about the surface. The ratio of reflected energy to the incident energy is termed the spectral reflectance and given in the expression

$$R_\lambda = \frac{E_R(\lambda)}{E_I(\lambda)} \qquad [6.10]$$

The value of the spectral reflectance for any feature over a range of electromagnetic spectrum produces the spectral reflectance curve for that object. The spectral reflectance curve is useful in interpretation of features. Figure 6.10 shows how maple and pine trees can be interpreted from the spectral reflectance curve.

The spectral reflectance curve provides clues for assessment of the type and condition of a feature type. Similaly, other materials such as concrete and steel on roadside features may be assessed from the analysis of digital images of these features. Therefore such images when analyzed and used for providing a VR model can provide enhanced information for management of the inventory of such resources. The next subsection presents a discussion on analysis of images using digital image processing techniques.

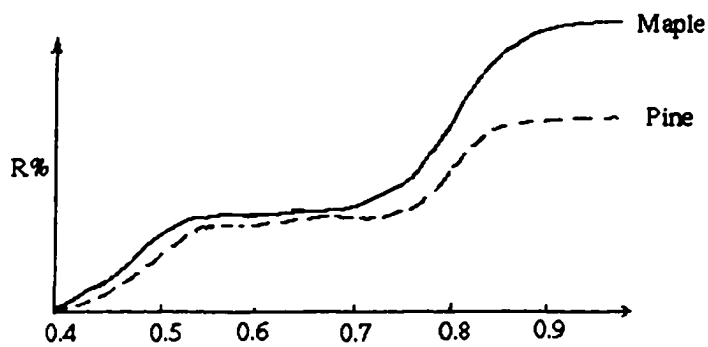

Figure 6.10 Spectral reflectance curve

6.5 Digital Image Processing

Availability of relevant hardware and software at affordable cost has made digital image processing techniques much more cost effective than visual analysis techniques. Basically, digital image processing techniques use the computer to read each pixel in an image and do some computation to create a new image that provides the information required by the user. The computation made at each pixel can be infinitely large in number. These operations may be put into the three generalized categories, which are briefly described below.

6.5.1 Image Rectification and Restoration

Image rectification involves initial processing of raw image data to correct for geometric distortion, to perform radiometric calibration and to eliminate noise. This operation is intended to improve the image data to provide a more faithful representation of the original scene. Geometric correction processes remove spatial distortions in the image. Radiometric corrections are applied to correct radiometric values of pixels arising from changed environmental conditions such as sun elevation in case of multi temporal data. Noise removal procedures restore the image to a more correct representation of the scene by

eliminating errors arising out of limitations of the various stages of the remote sensing process.

6.5.2 Image Enhancements

Image enhancement procedures improve the data to make it more amenable to visual interpretation. This is achieved by creating a new image that will yield more information that can be visually interpreted. The image enhancement techniques are either point operation or local operation. The contrast manipulation procedures enhance the image by gray-level thresholding, or level slicing, or contrast stretching or a combination of them. Spatial feature manipulation procedures use local operations such as spatial filtering, edge enhancement and Fourier analysis. Multi-image manipulation procedures use multiple bands of the images that use such techniques as multi-spectral band ratioing and differencing, principal components, canonical components, vegetation components and intensity-hue-saturation (IHS) color space transformation.

6.5.3 Image Classification

The image classification procedures categorize all pixels in an image into a number of classes or themes. Generally, a multi-band

image is used for digital image classification. It involves a quantitative assessment of each pixel to test whether it belongs to a specific class described by characteristics such as image texture, pixel proximity, feature size, shape, directionality, repetition and context. This approach is known as the spatial pattern recognition procedure, and it attempts to simulate the visual interpretation process. The classification procedures can be further categorized into supervised and unsupervised. In a supervised classification procedure, the user specifies a quantitative description of the classes to be identified. In an unsupervised classification, the pixels are grouped into clusters based on the inherent numerical and statistical patterns of the radiometric values. Primarily, three kinds of algorithms are used to classify an image: (1) minimum distance classifier, which assigns a pixel to a class that, is closest to the pixel in a multi-band space, (2) the parallelpiped classifier, which classifies a pixel as belonging to a specific category if the radiometric values of the pixel falls within the parellpipe of that category, and (3) Gaussian maximums likelihood classifier, that classify pixels based on the probability in a multi-dimensional space of the radiometric values.

6.6 Application of Remote Sensing in VR

In the context of the present research, remote sensing plays an important role in terms of acquiring the visual content of features for visualization in a VR environment. The images are acquired through a ground-based system where a digital camera is used as the sensor. The raw image may be suitable for texture modeling in mapping a generic VR scene. However, it may be desirable to enhance the image to make it more amenable to visual inspection of the features when visualized in a VR setting. In this research, the images captured by the video-logging system and an auxiliary digital camera contains high degree of perspective distortions. These images needed to be corrected so that a visually pleasing and accurate representation of the real scene were created for visualization in the CAVE. The next chapter describes modeling of the roadway scene that includes creating scene geometry and image processing required for realistic visualization of the scene.

CHAPTER 7 MODELING VR SCENE

Initially, constructions of virtual worlds were confined to environments with synthetically generated contents. However, with recent advances in computer graphics hardware, three-dimensional modeling and software tools, and three dimensional display capabilities, real world scenes can be modeled for visualization in a VR environment. This research models a VR scene of a roadside environment. The following subsections discuss the current approaches of modeling a VR scene and describe the stages of modeling it.

7.1 Modeling Approaches

The modeling steps involve various stages such as object detection, feature extraction, texture mapping and display. Modeling a VR scene can be categorized into two groups: (1) model based approach [60,61 ,62] and (2) image based approach [63,64 ,65]. Digital photogrammetric techniques are useful in both these approaches.

7.1.1 Model Based Approach

Important considerations in the reconstruction of virtual world with real world content include accuracy of the geometry and sense of realism in its display. The model-based approach consists of three distinct steps: (1) data collection, (2) camera calibration, and (3) reconstruction of the three-dimensional model. The first two steps are discussed at length in chapter 4 and chapter 3, respectively.

Digital photogrammetric techniques have been studied for their role in creating virtual worlds [66,67 ,68]. Often a Computer Aided Drafting (CAD) system is used to generate the model [69]. Scenes are also built by generating a point cloud of voxels [70,71] or a polyhedral object [72,73]. Laser ranging data are found to be useful for modeling a scene [74]. Some systems are built to accommodate interactive user input while building the scene geometry [75,76 ,77 ,78 ,79]. The digital images used for photogrammetric positioning of features are often used to render the scene [80,81]. Model based renderings provide greater versatility for user interactions and also provide a more realistic scene.

7.1.2 Image Based Approach

The Image based approach integrates and displays of appropriate images based on the viewer's position without construction of a

geometric model [82]. It usually involves synthesis of panoramic images [14], or display of spatially indexed images [83].

Image based rendering approach is efficient in terms of real time rendering of scenes A hybrid approach is developed to selectively replace some of the geometry with texture maps to affect a more efficient rendering of the scene [84].

7.2 VR Model of a Roadway Environment

The present research implements the VR environment of the roadside features in two stages: (1) a scene with simulated highway features, and (2) a scene with real world content. The simulated environment was implemented while the methodology for data acquisition by As Built Survey was being developed. Later on, when the geometric and texture data for the real world scene was acquired using the methodology developed by this research, the second stage was implemented to model the real world scene.

It is possible to create the scene geometry in two different ways: (1) by using available commercial software such as the Multigen Creator, Performer, etc., or (2) writing program codes using OpenGL routines, i.e., the brute force approach. The first approach lets the developer create the model quickly. However, there is a limited scope to

provide capabilities for interactive editing of the component features inside the VR environment. The second approach, on the other hand, involves more work at the outset, but it is easy to code the interaction into the model.

7.2.1 Modeling the Simulated Scene

The simulated scene was created as part of a project work for the course CprE-575X on *Introduction To Virtual Reality*. Dr. Carolina Cruz-Neira offered this course in the spring of 2000 at Iowa State University. The implementation of the simulated scene included the following aspects:

1. Construction of a model scene that contains a roadway and roadside feature geometry, and attribute data.
2. Providing scope for user interaction in the form of limited editing of the roadside feature objects and navigation in the virtual environment.
3. Providing simple geographic analysis functionalities.

These aspects have been discussed below in detail. The main file of implementation code for is included in Appendix E.

7.2.1.1 Modeling

The road scene model consists of a collection of generic features such as road pavements, median pavement markings, shoulders and traffic signposts. This model was supposed to demonstrate added capabilities of interactive editing as a required feature. Therefore, it was implemented by directly writing program codes. Roadway geometry of a 300 ft long two-way, two-lane highway segment with median, pavement markings and shoulders is modeled as shown in figure 7.1.

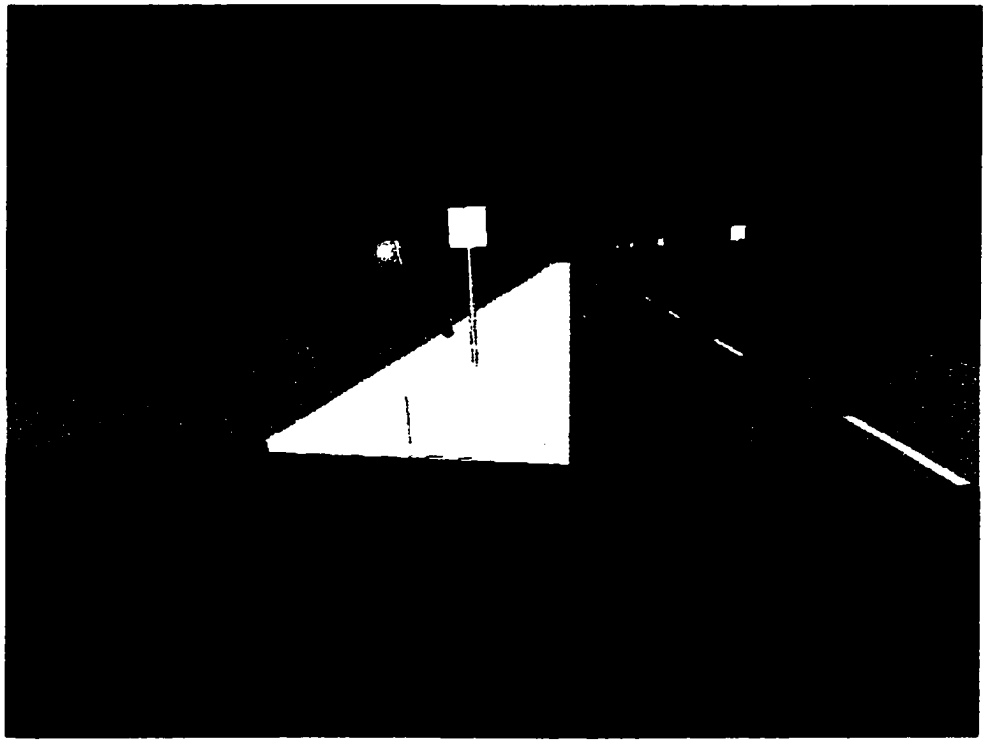

Figure 7.1 The roadway scene in a simulation window

A generic roadside feature in the form of a traffic signpost is also modeled. The attribute of the feature data is implemented as a part of the scene model.

7.2.1.2 Interaction

Interaction is provided in the form of navigation in the virtual environment and capabilities for limited editing of the roadside feature data. The user interacts with the virtual scene using a wand with three buttons. The wand buttons are programmed to operate in different modes to enable the user to interact with the virtual environment in three ways: (1) navigation inside the scene, (2) edit the scene, and (c) conduct a few simple geographic analysis. Figure 7.2 shows the multilevel menu of the wand interactions. The user can manipulate the wand button to get into the navigation mode and navigate inside the scene by moving forward or backward and turning sideways. Similarly, the user can get into the editing mode, and select/unselect features by touching the feature object with the wand and clicking a button. A selected feature may be picked up from the current location and moved to a different location as seen in figure 7.3. While the user is editing, the current location of the feature objects is displayed.

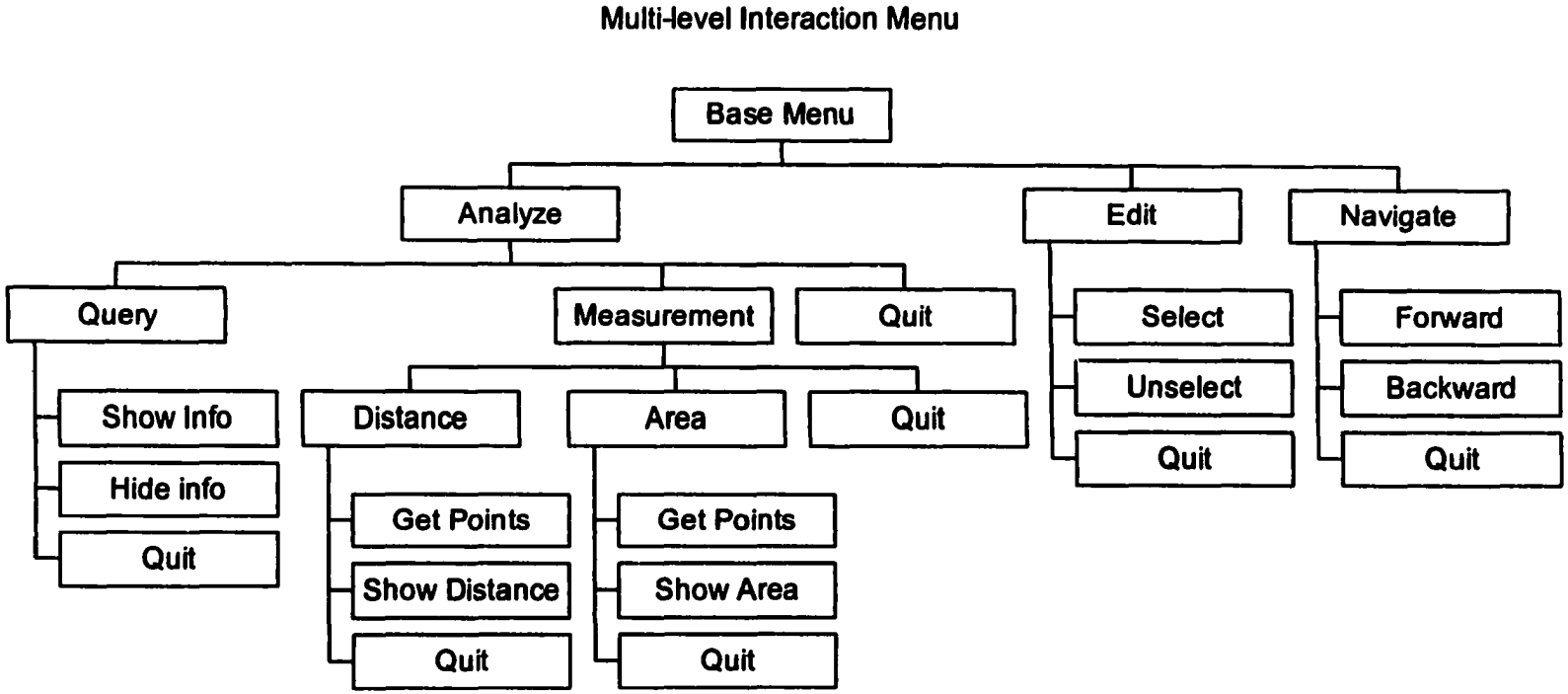

Figure 7.2 Wand interaction menu

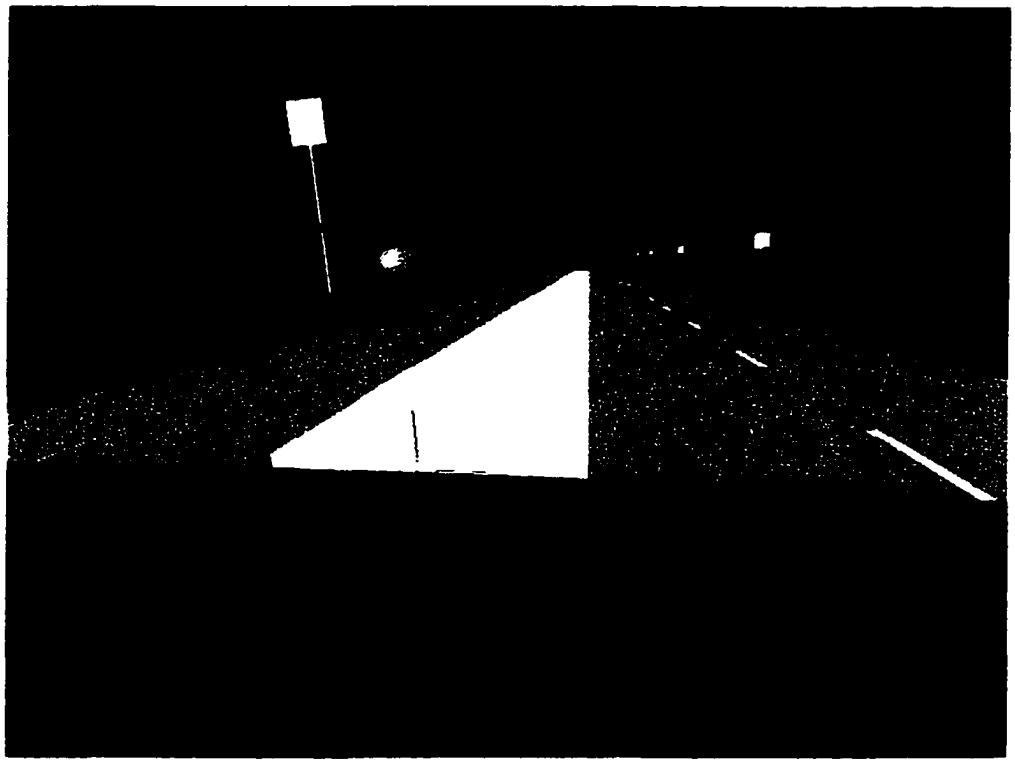

Figure 7.3 Editing the roadside feature

All the while, the mode of the wand buttons and corresponding available options are displayed in front of the user to make the interaction process user-friendly.

7.2.1.3 Geographic Analysis

Two kinds of geographic analysis capabilities are provided: querying the attribute information of a feature of interest and measuring distance and area.

To query a feature of interest, the user touches an object with the wand and clicks a button. The information is displayed in text format (Figure 7.4). To measure distance, the user places the wand at each of the points along the connected line segments and clicks the left button. A yellow line is drawn connecting those points until the end is signaled by click of the middle button (Figure 7.5). The yellow line disappears and the final length is displayed.

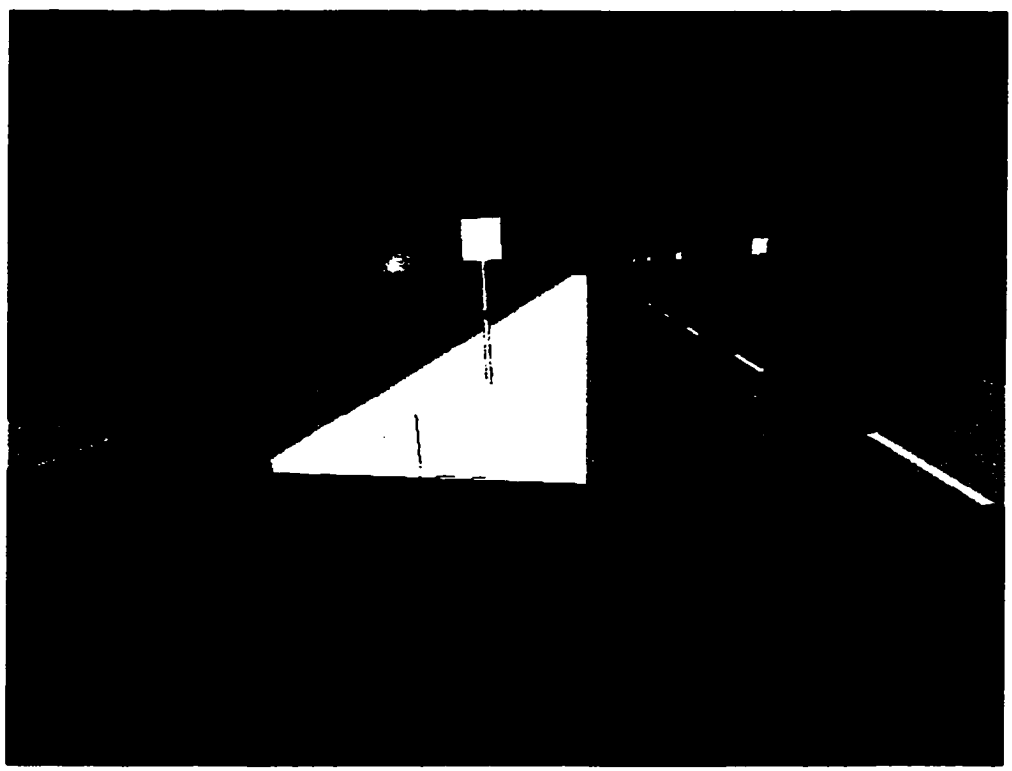

Figure 7.4 Querying the roadside feature

In case the of area measurement, a yellow outline of the polygon is drawn at each click of the left button and the area is progressively displayed (Figure 7.6). Since geographic data generally have significant resonance with geometrical parameters on a horizontal plan, the area and distances so displayed are the parameter values as projected on to a horizontal plane.

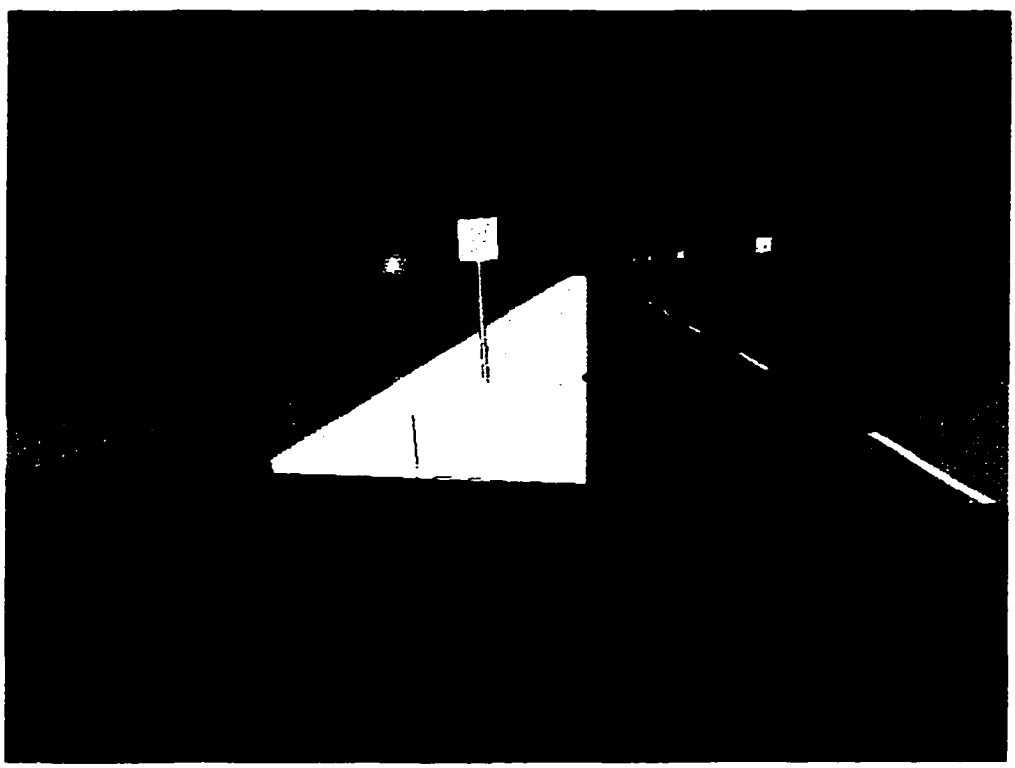

Figure 7.5 Measurement of distance inside VR environment

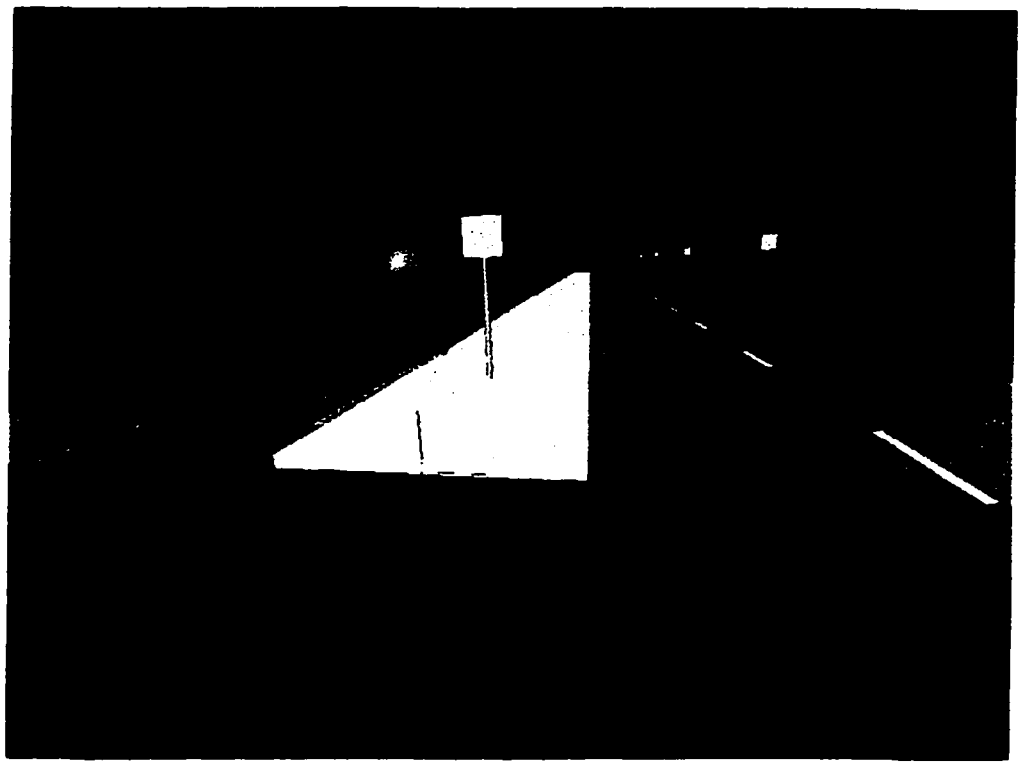

Figure 7.6 Measurement of area inside VR environment

7.2.2 Modeling the Real World Scene

A section of the Grand Avenue in the city of Ames, IA was selected for VR modeling for implementing a real world model. This section of the roadway contains a railroad bridge and a light post. The roadway passes below the railroad. The road section includes a four-lane undivided pavement and sidewalks, which are on a vertical curve. Modeling of the real world road section involved the following steps:

1. photogrammetric positioning of the road-section and roadside features including points on the bridge
2. modeling the bridge using CAD drawing.
3. modeling the combined geometry of the road section and the bridge
4. extraction of texture images from video-logging images
5. acquisition of additional images of the railway tracks, underside of the bridge and sidewalks using an auxiliary digital camera. These features were not captured by the video-logging system, but are required for a complete representation of the scene. Images on the underside of the bridge include samples of current condition of structural elements of the bridge, which can be of specific area of interest for inventory management.
6. mapping textures to the scene geometry after processing the texture images to remove excessive perspective.
7. implementing and displaying the scene model inside the CAVE environment.

The aspects are described in the following subsections.

7.2.2.1 Positioning of Features

The calibration procedure of the digital camera used for image acquisition is described in chapter 4. The procedure developed for photogrammetric feature positioning using the video-logging images is described in chapter 5. The spatial locations of the salient points of the road sections were determined in terms of X, Y, and Z coordinate values, which are then used to generate surfaces of the objects to be modeled. A sample of these points is plotted using AutoCAD as shown in the Figure 7.7. It shows an outline of the road section and one façade of the bridge and an electric pole.

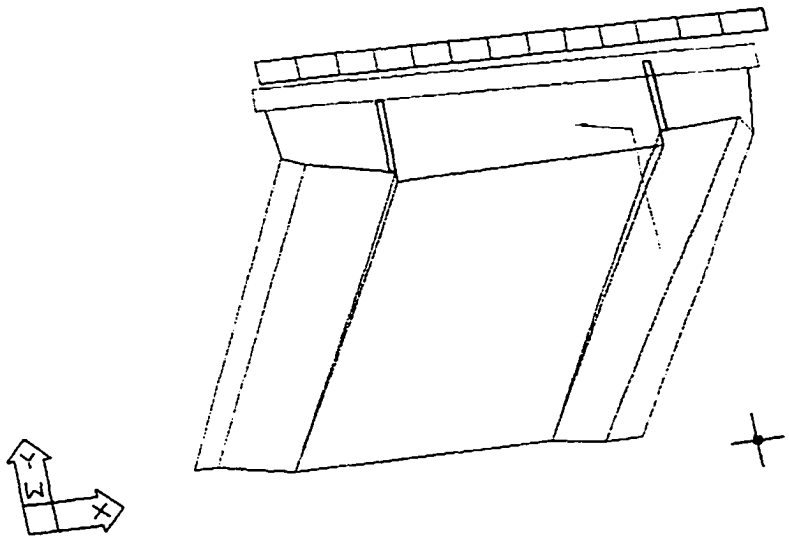

Figure 7.7 Photogrammetric feature positioning

A detailed modeling of the bridge requires determination of many points, which by photogrammetric techniques may consume a lot of time. New technology like laser scanning can be used to get the As Built geometry of the bridge. Laser scanning technology as provided by the Cyrax System [85] and other vendors have its own advantages and limitations, the use of which was beyond the scope of this research.

As an alternative, drawings of structural design of the *bridge* were used for modeling the VR scene. However, the structural drawings do not provide As Built information. The structural details were originally available in the form of design drawings, and were used to create a digital model in the form of an AutoCAD drawing. Appendix F describes the procedure for creating the AutoCAD drawing from the paper drawing. The AutoCAD drawing was taken as the basis for modeling the bridge and was imported into the *flt* file format so that it can be used directly by modeling software. Figure 7.8 shows the AutoCAD drawing of the bridge.

The conversion did not produce a perfect model. Some of the graphic elements were altered requiring a lot of cleanup before textures can be applied to the model. For example, some plan surfaces were imported as only line features instead of a surface. Such surfaces needed to be rebuilt so that texture mapping can be applied to the

geometry. Further, the structural drawing was originally prepared in units of inches. However, the feature coordinates were determined by digital photogrammetric techniques in units of meters. Therefore, this drawing was scaled to fit it with the scene model built using feature points. Please see Appendix G for more information.

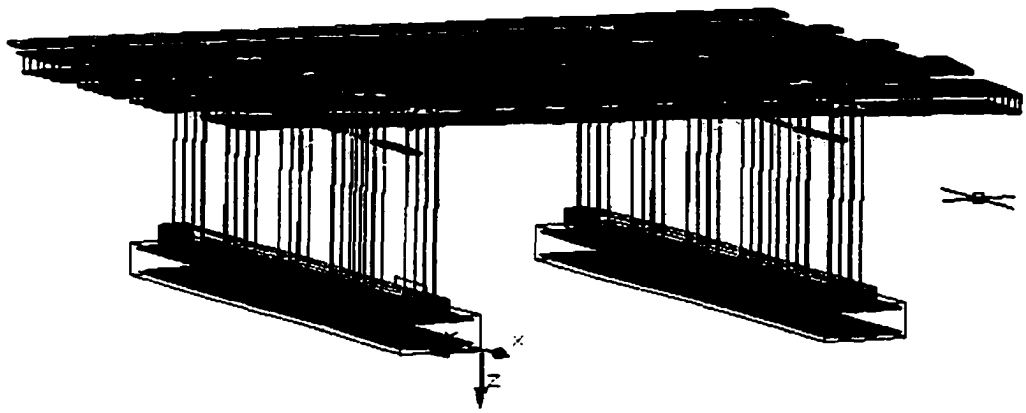

Figure 7.8 AutoCAD drawing of the bridge

Then photogrammetric positioning of the other road elements such as side slopes, sidewalks, and road pavements were used to complete the geometry of the scene. Figure 7.9 shows the scene model where the road features and the bridge are put together. The textured pavements and the bridge components can be seen on the image. The next subsection describes the aspects of texture mapping using images

captured at the site of the scene. Appendix G describes various aspects of creating the final roadway model to be displayed in CAVE.

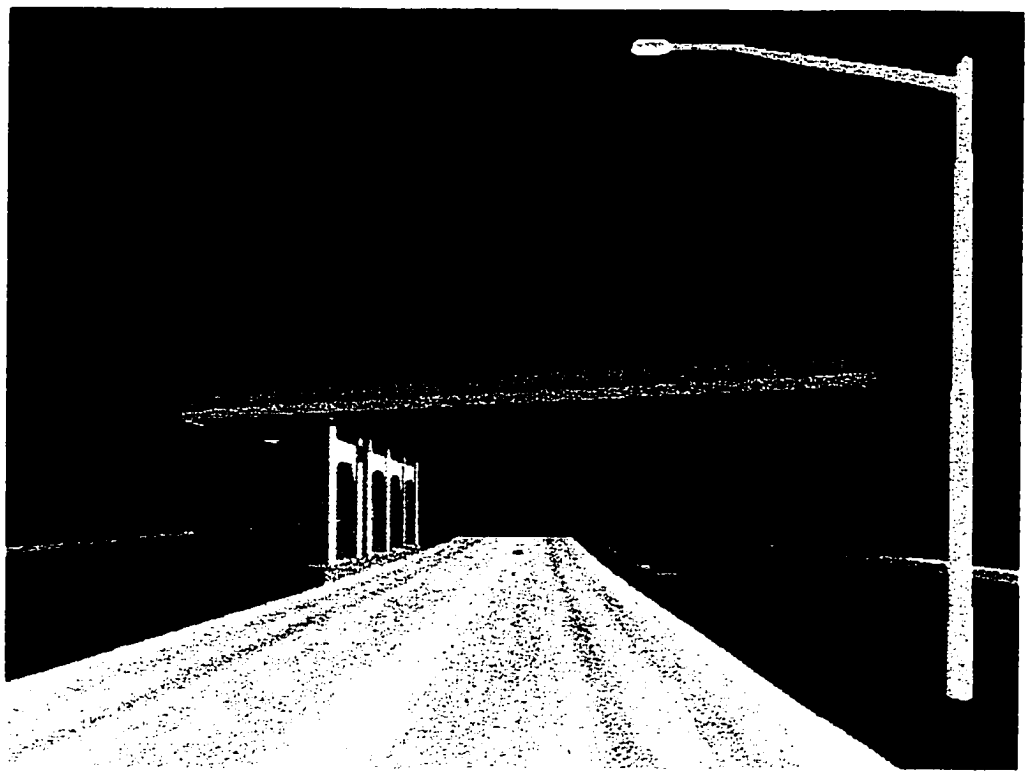

Figure 7.9 VR scene of the roadway

7.2.2.2 Texture

The images captured by the video-logging system can provide most of the textures required for rendering the roadway scene. In this research, the pavement textures are easily available from the video logging images. An auxiliary digital camera can be used to capture

additional images. A typical highway scene may require only few additional images or none at all. However, due to the particular site of a railroad underpass, a good number of such additional images of the roof of the underpass and railway tracks on top were collected to render the scene realistically.

The underside of the bridge presents elements that need the attention of the inventory manager. Concrete covers at the top of the different columns are striped to various extents (Figures 7.10). The figure shows that exposed reinforcement steel in the beams and columns exist at some locations.

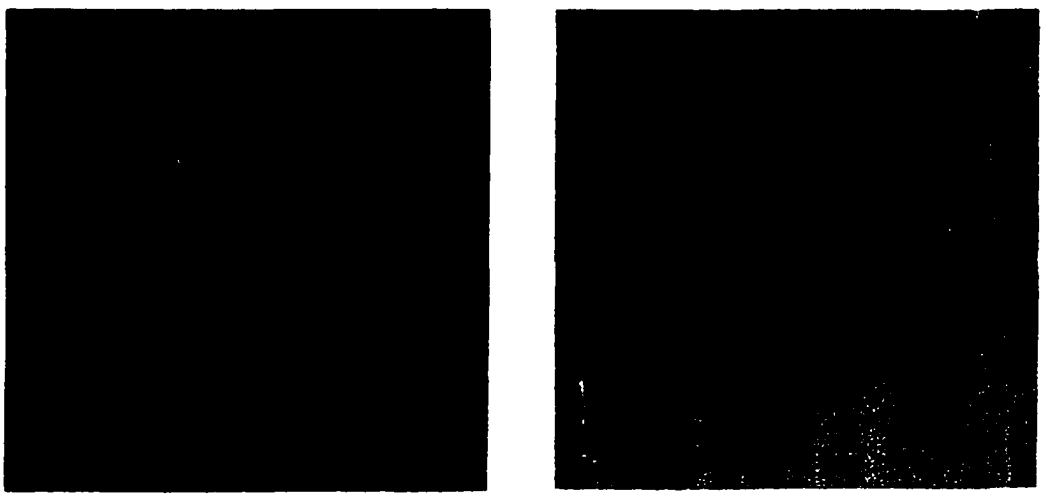

(a) Bad Concrete (b) Exposed Reinforcement

Figure 7.10 Damaged concrete and exposed steel

Further, the steel beams are seen to be rusting (Figure 7.11). Digital images were captured and texture mapped to the scene to represent the current condition of these structural features as shown in Figure 7.12.

Some images captured for texture mapping contained high degree of perspective distortions; parallel feature appears to converge. Texture mapping techniques fail to deliver good results when excessive distortions are present in the images as seen in figure 7.13. The perspective distortions present in the images were removed using image-processing software, Adobe Photoshop [86], which is described in the following paragraph.

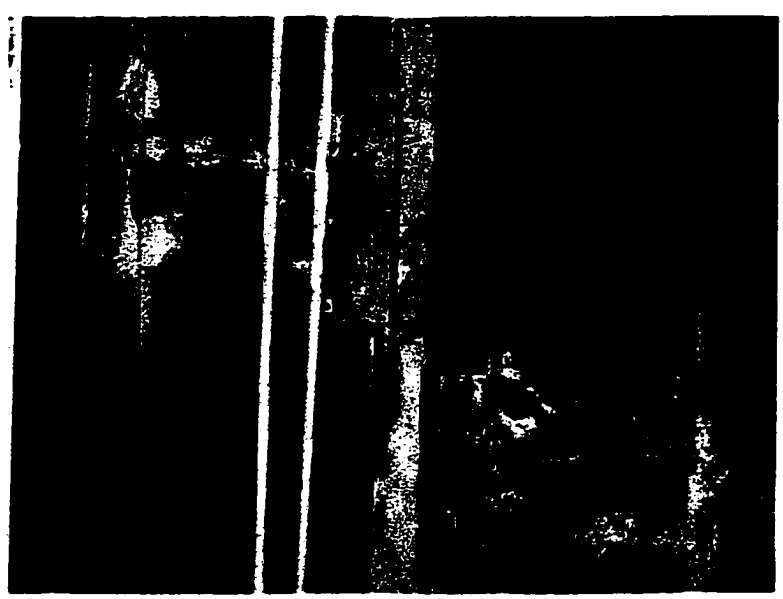

Figure 7.11 Rusting steel elements

Figure 7.12 Underside of the bridge

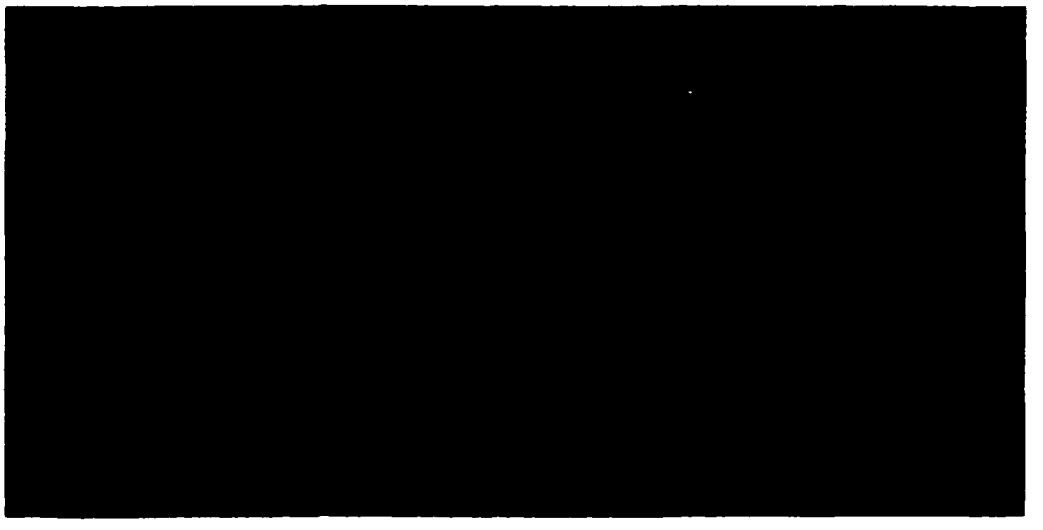

Figure 7.13 Crooked texture mapping of tracks

The Adobe Photoshop software presents a simple menu item to distort an image. After selecting an image to be edited on the display pane, the "Distortion" action can be accessed under the "Edit" menu item on the main menu bar. The user is then provided with four handles, which can be dragged using the mouse to correct the image. The image of the railway track in figure 7.14(a) below shows the original image collected at site, which contains perspective distortions that need to be corrected. The user can select the "Distort" action in Adobe Photoshop, and draw the two handles on top of image away from each other to produce the other image. Figure 7.14(b) shows the same image after rectification in Adobe Photoshop. The result is the scene with the railway track textures properly mapped as seen in figure 7.15.

(a) Original image (b) Corrected image

Figure 7.14 Rectifying texture images

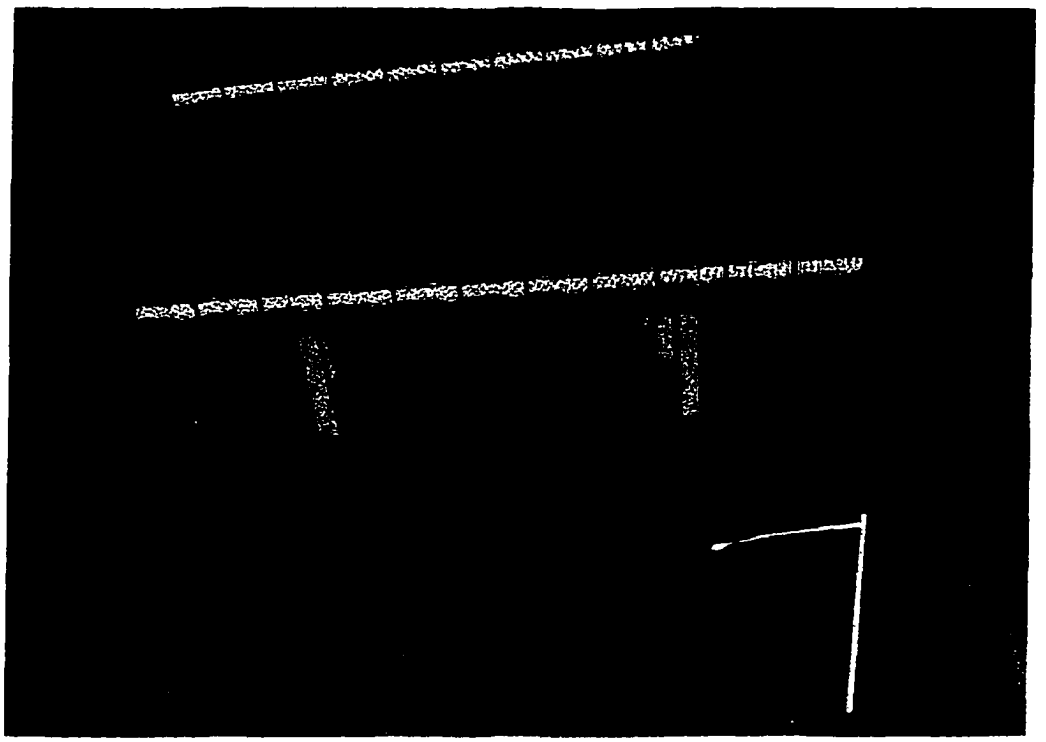

Figure 7.15 Correct texture mapping of the railway track

The texture for the pavements was extracted from the video logging images. Similar to the case of railway tracks, large distortions were present in these images due to ground based sensor system of the video log van as can be seen in Figure 7.16(a). Textures for the left lanes and right lanes were separately extracted and were rectified to get textures as shown in Figures 7.16(b) and 7.16(c) respectively. Figure 7.17 shows the scene with a view of the textured pavements under the bridge.

(a) Original image

(b) Left texture

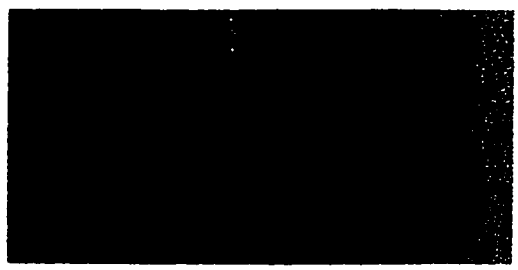

(c) Right texture

Figure 7.16 Texture mapping for road pavements

In addition to the pavements and the railway tracks, textures were captured for sidewalk and the concrete wall. These texture images did not contain any appreciable amount of distortions. Figure 7.18 shows the scene with a view of the sidewalk under the bridge.

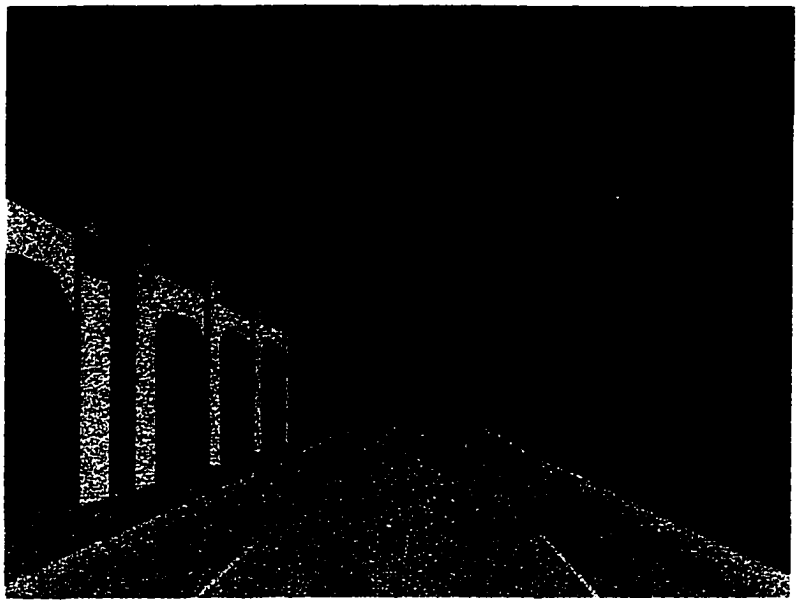

Figure 7.17 The scene with a view of the pavements

Figure 7.18 The scene with a view of the sidewalk

7.2.3 Software Tools for Modeling

The real world scene of the roadway as shown above was modeled using the *Multigen Creator* software package available on the Silicon Graphics Inc. (SGI) platform [87]. This software eliminates the necessity of writing complex codes to model the scene and saves much time in modification and rendering of the scene. A conversion software *Polytrans* available on the SGI platform was used to import the AutoCAD model of the bridge into the *flt* format that Multigen Creator can read directly. However, the import process was not perfect and was followed by clean up work in Multigen Creator. Software. More information about the process of creating the geometric model and texturing can be found in Appendix G.

7.3 About VRJuggler

The Multigen model was ported to the CAVE hardware and software through VRJuggler, which is an open source development tool for VR application [88,89]. VRJuggler is the result of active research by a team headed by Dr. Carolina Cruz-Neira at the Virtual Reality Application Center of the Iowa State University, Ames. VRJuggler hides

most of the hardware implementation issues from the developer, and thus reduces the complexity of building a VR application.

VRJuggler provides an object oriented development environment that allows user to develop applications independent of underlying technologies of the available VR system. At present, it supports a wide array of VR hardware on a variety of architectures that includes tracking systems, input devices such as glove and wand, different display system such as projection based system CAVE, and also Head Mounted Devices (HMD), desktop VR and Powerwall, making it very flexible.

VRJuggler is designed for optimal performance by giving applications direct access to graphics Application Programmer Interfaces (API) such as OpenGL and IRIS Performer. It supports multiple-processor machines as well as applications distributed across multiple machines and includes support for performance monitoring of applications and graphic subsystems.

It allows for easily adding new devices and reconfiguration or replacement of existing devices even while an application is running. Any VRJuggler application itself can be controlled or reconfigured at runtime by a Java-based graphical interface.

VRJuggler is available on different platforms including IRIX, GNU-Linux, BSD, Solaris, HP and Windows NT/2000.

CHAPTER 8 RESULTS AND CONCLUSIONS

This research has developed a methodology for efficient management of spatial feature inventory through visualization and analysis of spatial data in a VR environment. This chapter summarizes this research. Management of the roadside feature database inventory is used as a case study for this research. The video logging system is used for As Built Survey of the roadside features. The survey provides digital images and GPS positioning of images, which were used for feature positioning and texture mapping. The methodology developed includes a procedure for calibrating the digital camera described in chapter 4, and a procedure for positioning of feature points using sequential images described in chapter 5. The results presented in these two chapters are evaluated here. The Modeling of the VR scene is described in chapter 7 and the results are discussed here. And finally, recommendations for future work are provided.

8.1 Camera Calibration

The camera calibration site developed for this research permits repeated image acquisition. Calibration ensures correct orientation parameters being used for feature determination, as parameters on the video logging system are likely to be unstable.

The targets mounted on the building façade are easily accessible for the video-log van. The targets are established with an accuracy of 1.4 mm (X), 1.5 mm (Y) and 0.5 mm (Z) (See section 4.2.6.1). The calibration procedure using CALIB yielded interior and exterior orientation parameters of the camera. These parameters produced a positional accuracy of better than 3 cm in XY position and 10 cm in Z position of the targets (See table 4). The greater uncertainness of the Z-position, which is along the direction of the camera axis, is a manifestation of possible error in intersecting camera lens center from by the two Total Station machines used for triangulating the camera locations for calibration.

The CALIB accuracies were compared favorably with the results for commercial software SoftPlotter™ and actually yielded better accuracy as can be seen from Table 4.4. This validates the camera calibration procedure developed as part of this research

8.2 Feature Positioning

An analytical photogrammetric approach was adopted for feature positioning and the CALIB software was used. The number and interval between the images in a sequentially overlapping stereo-pair are important in cost-effectiveness and accuracy of the results. More images in computation may produce a more robust solution, but would require more image measurements. A smaller interval would increase cost for a given length of road section to be surveyed while a larger interval would degrade the positional accuracy of the features. The research yielded that two images can be used optimally with an interval of 75-100 feet between the images.

The software needs the exterior orientation of the camera and initial approximations of the feature locations. The exterior orientation of the camera is obtained from the calibration, and used with reference to a local coordinate system defined by the two camera positions as explained in section 5.2.3. The initial approximation of feature locations was then estimated with reference to the local coordinate system. The step-by-step procedure for estimating the initial feature locations is easy to follow and works very well.

The feature positions computed in the local coordinate system needs to be transformed to either State Plane Coordinates System

(SPCS) or the Universal Transverse Mercator System (UTM) for the numbers to be useful in a larger context. The Graphical User Interface (GUI) developed by using Visual Basic programming provides an easy and flexible way to transform the computed position (See figure 5.8). It is a simple GUI that contains six text fields for data input, two text fields do display results, and three buttons for user action. The user needs to only input the camera locations in the desired coordinates system to compute the transformation parameters. The feature position in X and Z coordinates as computed using CALIB, that are in local coordinate system (See figure 5.1) and need to be transformed, are input in the designated text fields. The Once all the necessary data are input, the "Transform" button becomes active. Then the user can click on this button to obtain the transformed coordinates. The "Clear" button lets the user to clear all fields to transform another feature location. The "Exit" button lets user to exit from the GUI.

8.3 Modeling the VR Scene

As described in chapter 7, the modeling was implemented in two stages to demonstrate the different approaches for modeling the VR scene. A simulated highway scene was implemented with the brute

force approach, while modeling software was used to model the real world scene using feature positions produced in this research.

The first approach demonstrates an implementation of the scene by writing C++ codes to include a multi-level wand menu for interaction with the scene that enables the user to interact with the scene. The interactions include editing the features inside the CAVE display, navigating inside the scene, and performing limited geographic analysis. The sample geographic data associated with the features were included as part of the program codes. Figure 8.1 shows a user navigating through and interacting the roadway scene inside CAVE.

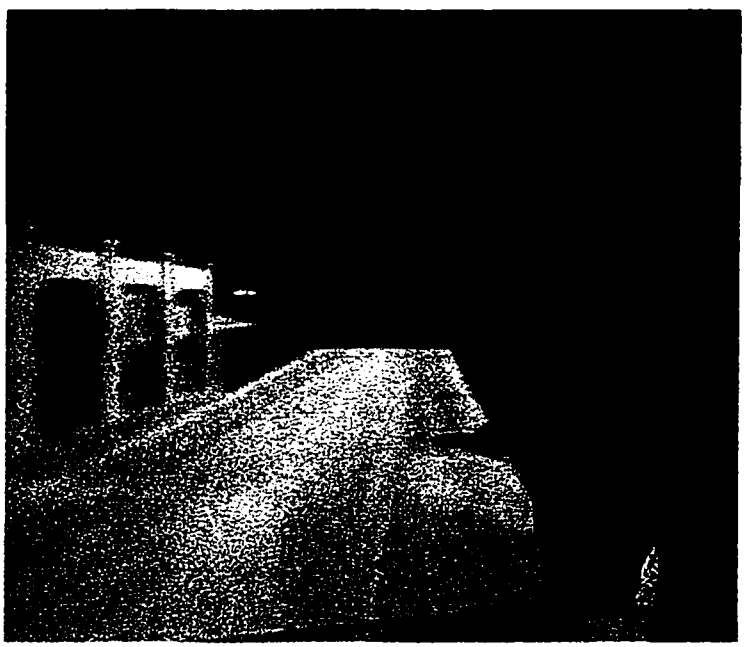

Figure 8.1 User in roadway model inside CAVE

The second approach demonstrates creation of a VR scene for a real roadway environment using feature positions determined in this research. The scene looks realistic with textures from the real site mapped on to the geometry of the scene. Figure 8.2 shows some digital images collected at site. Remote sensing and digital image processing techniques were used for texturing the roadway features in this scene.

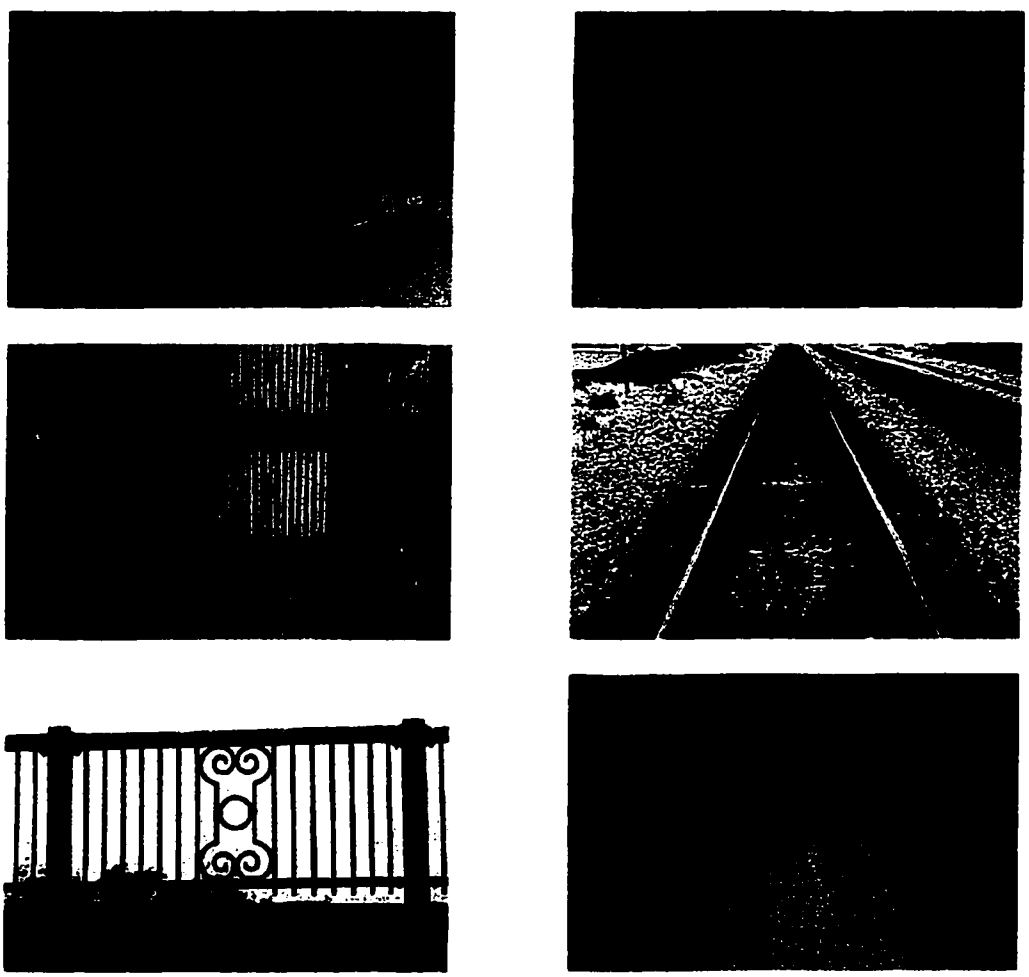

Figure 8.2 Original image sources for texture

The data analysis for inventory management in a VR environment, developed in this research involves distance and area measurements as simple query of the database. Our understanding of such interactions as overlay analysis, complex database query, and modeling of what if scenarios in virtual environment is still incomplete. This research has developed some of the analytical tools for spatial database inventory management using interactive virtual display.

This research has demonstrated the utility of structural drawings of roadway elements such as a bridge for modeling the scene geometry. Avoiding digitizing paper drawings if these drawings are already available in digital format can spare a lot of resources. However, this approach will not provide As Built information about the structure, and thus use of photogrammetric techniques is indispensable. This research has demonstrated how the two approaches can be optimally combined to get required information.

8.4 Recommendations

The versatility of the CALIB software can be seen from its use in both camera calibration and feature determination. However, at present, it runs on the command line and uses pre-existing data files. It is recommended that an integrated GUI be developed to increase

ease of data entry, data editing, program execution, and result evaluation.

At present, the coordinate transformation program TransCalib developed in this research is implemented to transform only N, E coordinates of the computed feature positions. This program can be extended to include elevation information too.

This research shows that digital photogrammetric methods can be combined with structural drawing in an optimal way to model scene geometry of complex road features like a bridge. However, new techniques such as laser scanning should be investigated as possible methods of As Built Survey to acquire geometry and dimensions of these complex features and supplement the combined data collection procedure used in this research.

For the roadway environment, it would be desirable to have enhanced editing capabilities to add new feature objects or delete existing ones while interacting with the virtual reality scene. This will enable the user to experience modeling the 'what if' scenario, and at the same time, enabling the user to choose textures for features will help to build a realistic scene during the runtime.

Separation of scene geometry from attribute database for the feature objects is another important consideration. This will ensure

efficient rendering of the scene by speeding up the complex database operations in a distributed computational environment.

APPENDIX A – VIRTUAL REALITY SYSTEMS

This appendix contains a list of sites that utilizes a CAVE-like projection based virtual reality system. The sites are listed under the categories of categorized of US Academic Institutions, Government Research Laboratories and Corporate Institutions as well as International Institutions.

Academic Institutions, USA

Boston University, Boston, MA

Indiana University, Bloomington, IN

Iowa State University, Ames, IA

Mississippi State University, Miss. State, MS

Penn State University, University Park, PA

UCLA (University of California)

University of Houston, Houston, TX

University of Illinois Chicago (EVL), Chicago, IL

University of Illinois (NCSA), Champaign, IL

University of Michigan, Ann Arbor, MI

Virginia Tech, Blacksburg, VA

Wright State University, Dayton, Ohio

US Government Research Laboratories

American Museum of Natural History, Hayden Planetarium, New York

Argonne National Laboratory, Argonne, IL

Defense Advanced Research Projects Agency (DARPA)

NASA/University of Houston

NASA, Hampton VA

Naval Research Lab, D.C.

National Institute for Occupational Safety and Health (NIOSH)

Morgantown, WV

US Industries

Atlantic Richfield Company, Plano, TX

Concurrent Tech Corp.

EDS, Detroit Virtual Reality Center

Exxon, Houston, Texas

FMC

General Motors

HRL Laboratories, Malibu CA

Landmark Graphics, Houston, TX

Lockheed Martin

NBC

SGI/Cray

SGI/Mountain View

Shell, Houston, TX

Texaco, Houston, TX

United Defense, Minneapolis, MN

International Sites

Australia – RMIT, Perth

Austria - Ars Electronica Center, Linz

Canada –Integrated Manufacturing Technologies Institute, Ontario

Canada - Research Institute for Multimedia Systems, Alberta

Germany - BMW AG

Germany - Damier-BenzAG, Stuttgart

Germany - General Motors/ Adam Opel AG, Stuttgart

Germany - German National Research Center for Information Technology, Schloss Birlinghoven

Germany - Fraunhofer Institute for Industrial Engineering (IAO),
Nobelstrasse

Germany - VVR FhG IDG, Darmstadt

Germany - Volkswagon AG

Greece - Foundation of the Hellenic World, Athens

Japan - Nissho Electronics Corporation, Tokyo

Japan - National Institute for Fusion Science

Japan - NTT/ICC (Inter Communication Center)

Japan - Sega

Japan - Tohwa University, Fukuoka

Japan - Tokyo Inst. Tech., Tokyo

Japan - University of Tokyo, Tokyo

Netherlands – SARA, Amsterdam

Netherlands - University Delft Niederland

Norway - Norsk Hydro ASA Exploration & Production, Sandslivn

Norway - Telenor Expo

Saudi Arabia - SAAD Trading

Singapore - NUS

Spain - gedas / UPC Technical University of Catalonia

Spain – SEAT, Barcelona

Sweden – Helsingborg,

Sweden – PDC Royal Institute of Technology Stockholm

Sweden - Swedish Inst. for Computer Science, Kista

Switzerland - SGI

Taiwan - Industrial Technology Research Institute – Hsinchu

APPENDIX B - IADOT VIDEOLOGGING SYSTEM SPECIFICATIONS

System Component Make	Model/Version
Image System	Mandli RDVX2000
Camera	Mandli RDVX2020
Camera Lens	Mandli RDVX2030
Camera Upgrade	Mandli RDVX ____
Central Processing Unit	Dell Precision 410/MMP
Image Processorf	Mandli RDVX3000
I/O Channel Processor	Mandli RDVX6000
Peripheral Processing Unit	Mandli RDVX4000
Norton Utilities	07-00-01992
Virus Scan	07-00-02307

APPENDIX C – FEATURE POSITIONING USING SOFTPLOTTER™.

SoftPlotter™ is a digital photogrammetric software. The basic workflow for the photogrammetric computations has been organized into individual modules such as the Block Tool, Stereo Tool, DEM Tool, Surface Tool, KDMS Tool and Mosaic Tool. Of all these modules, the two very relevant to the task at hand are the Block Tool and the Stereo Tool. Block Tool encompasses the whole gamut of block triangulation while the Stereo Tool enables computation of stereo viewing and measurements.

Block Tool

Clicking the appropriate icon on the main application interface can access the block tool. The operations in the block tool may be categorized into three basic parts: [1] input of data and [2] point measurements on digital images, and [3] computation. Data input are required for the calibrated camera interior orientation parameters of

the calibrated camera, initial estimates for the exterior orientation parameters of the camera, and the ground control point data. These are carried out by accessing various menu items as described below.

Project Definition

The definition of the project interface requires the user to specify many of the default parameters for the different stages in the block tool. This includes the projection parameters, sigma values for initial estimates of the exterior orientation parameters of the camera, collection interval of the Digital Elevation Model (DEM), etc. When the user specifies, a new project directory is created with subdirectories to save data in an organized manner. For example, the subdirectory named "raw" is created to contain all the digital images to be used for the project. Similarly, subdirectories named block, stereo, dem, tin, etc. are created to save data relevant to each of these tools. After a new project directory is created, the user needs to copy the digital images into the raw subdirectory.

Edit Camera Interface

This interface can be accessed through the menu item Edit-Camera. This interface provides the user a way to input camera calibration parameters. The parameters for some of the standard

camera are already available and the user can select the relevant camera from a list of available cameras. If the required camera is not already available, the user can add its parameters and save the information under its name so that in future it will be available on the list. The parameters to be input includes the principal point coordinates, focal length, the lens distortion parameters and coordinates of the fiducial points.

Edit Frame Interface

Edit Frame can be accessed through the menu item, Edit-Frame. This interface allows the user to specify the frames in the project. For each frame, the user specifies the corresponding digital image file, initial estimates for frame location and orientation angles and the corresponding standard errors. The software can use the digital image in many formats including TIFF and IMG.

Edit Ground Control Interface

To input the data of the control point data into the project, the user needs to access the menu item Edit->Ground Control, which permits the user to input these data into the project. The data can either be typed directly or imported from a text file or other software output formats such as Albany, Vexel, etc. The user may specify any

arbitrary record format for the import data file. Each record may contain such information as the point ID, point description, type of the control points, the X, Y and Z coordinates, and standard errors of these coordinate values. The type of the control point may be specified as Full Control (C), Horizontal Control (H), Vertical Control (V), or as a Tie Point (T). It is possible to save the user specified format for future use. When there are a large number of points to be input, the import option becomes very useful.

Interior Orientation Panel

At this stage, each of the images specified for the different frames must be interiorly oriented. The user may access the interface to do so by selecting the menu item, Activities->Interior Orientation. The process first involves a display of the relevant image in an image panel, selection of a record of a fiducial point on a tabular list and measurement of the corresponding image position using the cursor. The user may zoom onto the fiducial mark or manipulate the contrast and brightness of the image for finding the best results of the measurements. Once all the four, six or eight fiducial points are measured, the measurements may be saved and the procedure repeated for the next image. All the images must be measured in this

way before they can be used for the subsequent step of triangulation. For a few selected cameras, it is possible to choose the option of Automatic Interior Orientation (AIO) at this time. This step enables the software to collect the necessary data for transformation of measured image coordinates into photo coordinates as required for subsequent photogrammetric computations.

Ground Point Measurement

In this step, the user displays the images and measures the image coordinates of any ground points. The user basically measures the ground control points and then adds as many minimum tie points as required by the block triangulation procedure and any extra points of interest. A maximum of six images may be displayed concurrently. This helps to display all the images on which a single point may be appear. The user may zoom onto each of the displayed images or manipulate contrast and brightness independently to get a better measure of the position of the control point. The auto correlation technique finds the conjugate points on overlapping images. The points of different control types are displayed with colored identification codes for easy identification. The user measures each point one by one, re-measures unsatisfactory measurements, and finally saves accepted

values. The user can add as many tie points as wanted at this stage to the list of measured points.

Triangulation Interface

This interface allows the user the means to accomplish the block triangulation procedure. The user can specify the number of repetitions and the limit of convergence for the iterative adjustment procedure before initiating calculations. The computations are usually completed within a few seconds. At this time, the user can view results for acceptability. The user may accept the results and update the block data in the project, or if unacceptable, modify inputs using any of the interfaces described previously and re-run the computations. Upon satisfactory completion, the user may save the block data and exit.

Stereo Tool

If the relevant data has stereo overlaps, it is possible to generate a stereo display on the computer screen to view the terrain in three dimensions, which enables the user to extract three-dimensional position information on any point of interest. The stereo tool essentially computes stereo-rectification of the images with stereo overlap. It is necessary to successfully complete the triangulation procedures in the

block tool before the stereo tool can be used. The user can create a new stereo block by choosing appropriate images and proceed to stereo-rectification. Once the computation is complete, the overlapping images may be displayed on the computer screen alternately with a fast refreshing rate of 60 Hz. When the user puts on the special pair of glasses that alternates the viewer's left and right eyes to corresponding left and right images being displayed, the user experiences the three dimensional view. The stereo block so generated may be saved to view again without going through the processing stage again. While viewing the scene in the three-dimensional view, the user may measure any points of interest by manipulating the mouse with the appropriate keys on the keyboard.

In the present project, photos 137 and 139 constituted a pair of stereo images in the real sense of being simulated for the left and right eyes. This block is saved as the Stereo Block. In this case, a stereo view was available for viewing and measurement. The overlapping photographs 160 and 125 were positioned longitudinally in respect to the direction of the camera axis. This resulted in a large difference in the photo scale between the two images. Therefore, it was not feasible to actually view a three dimensional scene. This block of images was saved as the Longitudinal Block.

APPENDIX D - LISTING OF VISUAL BASIC PROGRAM CODE

This appendix contains a listing of the visual basic source file for the program for coordinate transformation from local coordinates to world coordinates.

```
'Clear All Fields Global variables
Const PI = 3.14159

'Clear All Fields Functions

Private Sub cmdClear_Click()      'Clear All Fields
txtN0.Text = ""
txtE0.Text = ""
txtNz.Text = ""
txtEz.Text = ""
txtNt.Text = ""
txtEt.Text = ""
txtCalibX.Text = ""
txtCalibZ.Text = ""
cmdTransform.Enabled = False
End Sub

Private Sub cmdExit_Click()
'Exit program
   End
End Sub

Private Sub cmdTransform_Click()
    'Transform Coordinates
    'Declare variables
```

```
    Dim N0      As Double       'Northing at origin
    Dim Nz      As Double       'Northing at z-axis point
    Dim Nt      As Double       'Northing of objet point after
'transformation
    Dim E0      As Double       'Easting at origin
    Dim Ez      As Double       'Easting at z-axis point
    Dim Et      As Double       'Easting of objet point after
'transformation
    Dim CalibX  As Double       'x-coordinate of object point
'from CALIB result
    Dim CalibZ  As Double       'z-coordinate of object point
'from CALIB result

    Dim dN      As Double       'Relative northing
    Dim dE      As Double       'Relative easting
    Dim dL      As Double       'Distance between camera
'positions
    Dim Az      As Double       'Azimuth of Local Z-axis

    Dim fN      As Double       'Sign factor for northing
    Dim fE      As Double       'Sign factor for easting
    Dim fX      As Double       'Sign factor for calib x-
'coordinate
    Dim fZ      As Double       'Sign factor for calib z-
'coordinate

    'Get user input
    N0 = Val(txtN0.Text)
    Nz = Val(txtNz.Text)
    E0 = Val(txtE0.Text)
    Ez = Val(txtEz.Text)
    CalibX = Val(txtCalibX.Text)
    CalibZ = Val(txtCalibZ.Text)

    'Find azimuth of Z-axis of calib system
    dN = N0 - Nz
    dE = E0 - Ez
    dL = Sqr(dN * dN + dE * dE)

    If dE = 0 Then              'The local z-axis is along N-S
'direction
        If dN = 0 Then          'The two camera positions are
'identical
            MsgBox "Invalid Image Positions", _
                    vbExclamation, _
                   "Data Entry Error"
            Exit Sub
```

```
        Else                        'Transform object point
'coordinates
            fN = dN / Abs(dN)
            Nt = Nz + fN * CalibZ
            Et = Ez - fN * CalibX
        End If
    ElseIf dN = 0 Then              'The local z-axis is along E-W
'direction
        fE = dE / Abs(dE)
        Nt = Nz + fE * CalibX
        Et = Ez + fE * CalibZ
    Else                            'The local z-axis is oblique
        If CalibZ = 0 Then          'The object point is on the
'local x-axis
            If CalibX = 0 Then      'The object point is same as
'the local origin
                Nt = Nz
                Et = Ez
            Else                    'Transform object point
'coordinates
                fX = CalibX / Abs(CalibX)
                Az = computeAzimuth(dN, dE)
                Az = Az - fX * PI / 2
                Nt = Nz + Abs(CalibX) * Cos(Az)
                Et = Ez + Abs(CalibX) * Sin(Az)
            End If
        Else                        'The object point is offset
'from the local x-axis
            fE = dE / Abs(dE)
            fZ = CalibZ / Abs(CalibZ)
            angle = Atn(CalibX / Abs(CalibZ))
            A = computeAzimuth(dN, dE)
            Az = A + fE * (PI / 2 - fZ * (PI / 2 + fE * angle))
            Nt = Nz + Abs(CalibZ) * Cos(Az)
            Et = Ez + Abs(CalibZ) * Sin(Az)
        End If
    End If

    'Display results
    txtNt.Text = FormatNumber(Nt, 3, vbTrue, vbFalse, vbFalse)
    txtEt.Text = FormatNumber(Et, 3, vbTrue, vbFalse, vbFalse)

End Sub

'Clear All Fields Routines for validating user entries
Private Sub txtCalibX_Validate(Cancel As Boolean)
    Cancel = showWarning(txtCalibX)
```

```
    If enableTransform = True Then cmdTransform.SetFocus
    End Sub

Private Sub txtCalibZ_Validate(Cancel As Boolean)
    Cancel = showWarning(txtCalibZ)
    If enableTransform = True Then cmdTransform.SetFocus
    End Sub
Private Sub txtE0_Validate(Cancel As Boolean)
    Cancel = showWarning(txtE0)
    enableTransform
    If enableTransform = True Then cmdTransform.SetFocus
    End Sub

Private Sub txtEt_Validate(Cancel As Boolean)
    Cancel = showWarning(txtEt)
End Sub

Private Sub txtEz_Validate(Cancel As Boolean)
    Cancel = showWarning(txtEz)
    If enableTransform = True Then cmdTransform.SetFocus
    End Sub

Private Sub txtN0_Validate(Cancel As Boolean)
    Cancel = showWarning(txtN0)
    If enableTransform = True Then cmdTransform.SetFocus
    End Sub

Private Sub txtNt_Validate(Cancel As Boolean)
    Cancel = showWarning(txtNt)
End Sub

Private Sub txtNz_Validate(Cancel As Boolean)
        Cancel = showWarning(txtNz)
    If enableTransform = True Then cmdTransform.SetFocus
End Sub

Public Function showWarning(txtBox As TextBox)
    If IsNumeric(txtBox.Text) = False And txtBox.Text <> ""
Then
        MsgBox "Numeric data expected", vbExclamation, "Data
Entry Error"
        showWarning = True
        txtBox.Text = ""
    Else: showWarning = False
    End If
End Function
```

```
'Clear All Fields Enable the Transform button
Public Function enableTransform()
    If txtCalibX.Text <> "" And IsNumeric(txtCalibX.Text) =
True And _
       txtCalibZ.Text <> "" And IsNumeric(txtCalibZ.Text) =
True And _
       txtN0.Text <> "" And IsNumeric(txtN0.Text) = True And _
       txtE0.Text <> "" And IsNumeric(txtE0.Text) = True And _
       txtNz.Text <> "" And IsNumeric(txtNz.Text) = True And _
       txtEz.Text <> "" And IsNumeric(txtEz.Text) = True _
       Then
        cmdTransform.Enabled = True
    Else: cmdTransform.Enabled = False
    End If
End Function

'Clear All Fields Compute the azimuth of local z-axis
Public Function computeAzimuth(N As Double, E As Double)
    Dim A As Double
    If N = 0 Then
        A = PI / 2
        If E < 0 Then
           A = 3 * PI / 2
        End If
    Else
        A = Atn(E / N)    'angle
        If N < 0 Then
            A = A + PI
        ElseIf dE < 0 Then
            A = 2 * PI + A
        End If
    End If
    computeAzimuth = A
End Function
```

APPENDIX E – LISTING OF SIMULATED VR SCENE CODE

```
/*************************************************************************
*
 *
 * File:     roadApp.cpp
 * Author:   Dwipen Bhagawati
 * Date:     March 24, 2000
 *
 * Note:     Adopted from practice excercise 2
 *

*************************************************************************
/

#include <math.h>
#include <GL/gl.h>
#include <GL/glu.h>
#include <GL/glc.h>
#include <roadApp.h>
#include <Math/vjQuat.h>
#include <iostream.h>
#include <string.h>
#include<strstream.h>

#include "navigation.h"
#include "RoadScene.h"

void draw_cube();

void roadApp::initGlState()
{
    GLfloat light0_ambient[] = { 0.1f,  0.1f,  0.1f,  1.0f};
    GLfloat light0_diffuse[] = { 0.8f,  0.8f,  0.8f,  1.0f};
    GLfloat light0_specular[] = { 1.0f,  1.0f,  1.0f,  1.0f};
    GLfloat light0_position[] = {0.0f, 0.75f, 0.75f, 0.0f};

    glLightfv(GL_LIGHT0, GL_AMBIENT,  light0_ambient);
```

```
    glLightfv(GL_LIGHT0, GL_DIFFUSE,  light0_diffuse);
    glLightfv(GL_LIGHT0, GL_SPECULAR,  light0_specular);
    glLightfv(GL_LIGHT0, GL_POSITION,  light0_position);

    GLfloat mat_ambient[] = { 0.0f, 0.0f,  0.0f,  1.0f };
    GLfloat mat_diffuse[] = { 0.7f,  0.7f,  0.7f,  1.0f };
    GLfloat mat_specular[] = { 1.0f,  1.0f,  1.0f,  1.0f };
    GLfloat mat_shininess[] = { 30.0f };
    GLfloat no_emm[] = { 0.0f,  0.0f,  0.0f,  1.0f };

    glMaterialfv( GL_FRONT, GL_AMBIENT, mat_ambient );
    glMaterialfv( GL_FRONT,  GL_DIFFUSE, mat_diffuse );
    glMaterialfv( GL_FRONT, GL_SPECULAR, mat_specular );
    glMaterialfv( GL_FRONT,  GL_SHININESS, mat_shininess );
    glMaterialfv( GL_FRONT,  GL_EMISSION, no_emm);

    glEnable(GL_COLOR_MATERIAL);
    glEnable(GL_DEPTH_TEST);
    glEnable(GL_NORMALIZE);
    glEnable(GL_LIGHTING);
    glEnable(GL_LIGHT0);
    glShadeModel(GL_SMOOTH);
    glEnable(GL_CULL_FACE);
}

void roadApp::myDraw()
{
    // Testing ....
  //if(mButton0->getData() == vjDigital::TOGGLE_ON)
  //  cout << "-- Toggle ON --" << endl;
  //if(mButton0->getData() == vjDigital::TOGGLE_OFF)
  //  cout << "-- Toggle OFF --" << endl;

  glClearColor(0.0, 0.0, 0.0, 0.0);
  glClear(GL_COLOR_BUFFER_BIT | GL_DEPTH_BUFFER_BIT);

  this->initGlState();
  this->renderLightsAndMaterials();

  glPushMatrix();

  glMatrixMode(GL_MODELVIEW);
  glMultMatrixf(mNavMatrix.getFloatPtr());

  // draw road ...
  glPushMatrix();
  scene->drawRoad();
  glPopMatrix();

  // draw feature
  /*
  for(int i = 0; i < fDataVec.size(); i++){
```

```
    glPushMatrix();
    glTranslatef(fDataVec[i]->pos[0],
         fDataVec[i]->pos[1],
         fDataVec[i]->pos[2]);
    glRotatef(-fDataVec[i]->asp, 0.0, 1.0, 0.0);
    feature->drawFeature(F_SPEED_LIMIT, fDataVec[i]->sel);
    glPopMatrix();
  }// end for
    */

  // Display texts ...
  glPushMatrix();
  glcContext ( glcGenContext () );
  glcFont ( glcNewFontFromFamily ( 1, "palatino" ) );
  glcFontFace ( 1, "bold" );
  glcScale ( 16.f, 16.f );

  // show distance line or area polygon ...
  if(wandButtonState == BUTTON_AREA){
    glColor3f(1.0, 1.0, 0.0);
    glPushMatrix();
    // draw the outline of the traced line or area
    glBegin(GL_LINE_LOOP);
    for(int i = 0; i < pointVec.size(); i++){
      glVertex3f(pointVec[i][0], pointVec[i][1], pointVec[i][2]);
    }// end for
    glEnd();
    glPopMatrix();

    char buf[100];
    ostrstream os(buf, 100);
    os<<"AREA = "<<area;
    glRasterPos2f ( -10.f, 6.5f );
    glcRenderString (os.str());
  }// end if

  else if(wandButtonState == BUTTON_DISTANCE){
    glColor3f(1.0, 1.0, 0.0);
    glPushMatrix();
    glBegin(GL_LINE_STRIP);
    for(int i = 0; i < pointVec.size(); i++){
      glVertex3f(pointVec[i][0], pointVec[i][1], pointVec[i][2]);
    }// end for
    glEnd();
    glPopMatrix();

    char buf[100];
    ostrstream os(buf, 100);
    os<<"DISTANCE = "<<distance;
    glRasterPos2f ( -10.f, 6.5f );
    glcRenderString (os.str());
  }// end else
```

```
// show feature info if ...
glColor3f ( 1.0, 0.0, 0.0 );
if(selFeatureIndex >= 0 && (wandButtonState == BUTTON_QUERY ||
                    wandButtonState == BUTTON_EDIT)){
  // here code to show the feature information ...
  // show location ...
  char buf[100];
  ostrstream os(buf, 100);
  os<<"Position : "<<fDataVec[selFeatureIndex]->pos[0]<<"   "
    <<fDataVec[selFeatureIndex]->pos[1]<<"   "
    <<fDataVec[selFeatureIndex]->pos[2];
  glRasterPos2f ( -10.f, 9.f );
  glcRenderString (os.str());

  if(wandButtonState == BUTTON_QUERY){
    glRasterPos2f ( -10.f, 7.5f );
    glcRenderString (fDataVec[selFeatureIndex]->name);
  }// end if
}// end if


//  display menu status ...
glColor3f ( 0.f, 1.f, 0.f );
glRasterPos2f ( -10.f, 11.f );
glcRenderString ("Left   Middle   Right");

switch(wandButtonState){
case BUTTON_BASE :
  glColor3f ( 1.f, 0.f, 0.f );
  glRasterPos2f ( -10.f,  12.f );
  glcRenderString ("BASE Menu");

  glColor3f ( 1.f, 0.f, 1.f );
  glRasterPos2f ( -10.f,  10.f );
  glcRenderString ("Analyze   Edit   Navigate");
  break;

case BUTTON_ANALYZE :
  glColor3f ( 1.f, 0.f, 0.f );
  glRasterPos2f ( -10.f,  12.f );
  glcRenderString ("ANALYZE Menu");

  glColor3f ( 1.f, 0.f, 1.f );
  glRasterPos2f ( -10.f,  10.f );
  glcRenderString ("Query   Measure   Quit");
  break;

case BUTTON_EDIT :
  glColor3f ( 1.f, 0.f, 0.f );
  glRasterPos2f ( -10.f,  12.f );
```

```
    glcRenderString ("EDIT Menu");

    glColor3f ( 1.f, 0.f, 1.f );
    glRasterPos2f ( -10.f,  10.f );
    glcRenderString ("Select   Unselect   Quit");
    break;

  case BUTTON_NAVIGATE :
    glColor3f ( 1.f, 0.f, 0.f );
    glRasterPos2f ( -10.f,  12.f );
    glcRenderString ("NAVIGATE Menu");

    glColor3f ( 1.f, 0.f, 1.f );
    glRasterPos2f ( -10.f,  10.f );
    glcRenderString ("Accelerate   Decelerate   Quit");
    break;

  case BUTTON_QUERY:
    glColor3f ( 1.f, 0.f, 0.f );
    glRasterPos2f ( -10.f,  12.f );
    glcRenderString ("ANALYZE-QUERY Menu");

    glColor3f ( 1.f, 0.f, 1.f );
    glRasterPos2f ( -10.f,  10.f );
    glcRenderString ("Show-Info   Hide-Info   Quit");
    break;

  case BUTTON_MEASURE:
    glColor3f ( 1.f, 0.f, 0.f );
    glRasterPos2f ( -10.f,  12.f );
    glcRenderString ("ANALYZE-MEASURE Menu");

    glColor3f ( 1.f, 0.f, 1.f );
    glRasterPos2f ( -10.f,  10.f );
    glcRenderString ("Distance   Area   Quit");
    break;

  case BUTTON_DISTANCE:
    glColor3f ( 1.f, 0.f, 0.f );
    glRasterPos2f ( -10.f,  12.f );
    glcRenderString ("ANALYZE-MEASURE-DISTANCE Menu");

    glColor3f ( 1.f, 0.f, 1.f );
    glRasterPos2f ( -10.f,  10.f );
    glcRenderString ("Get-points   Show   Quit");
    break;

  case BUTTON_AREA:
    glColor3f ( 1.f, 0.f, 0.f );
    glRasterPos2f ( -10.f,  12.f );
    glcRenderString ("ANALYZE-MEASURE-AREA Menu");
```

```
    glColor3f ( 1.f, 0.f, 1.f );
    glRasterPos2f ( -10.f,  10.f );
    glcRenderString ("Get-points   Show   Quit");
    break;
  }// end switch
  glPopMatrix();
  glPopMatrix();
}// end my draw


//: Function called after tracker update but before start of drawing
//  In the glove application, this function does the logic for
picking the
//  objects.
void roadApp::preFrame()
{
    //: we need to keep track of the wand, and the user.

    UserInfo    userInfo;
    TrackedInfo wandInfo;
    TrackedInfo headInfo;


    vjVec3 wandPos;
    vjMatrix invNav, wand_matrix;
    invNav.invert(mNavMatrix);

    // Do not remove the following couple of pieces of codes ...
    // They make sure that inav is accessible ...
    //cerr<<"navMatrix:"<<endl;
    for(int i = 0; i < 4; i++){
      for(int j = 0; j < 4; j++)
        //cerr<<mNavMatrix.getFloatPtr()[4*i+j]<<" ";
      mNavMatrix.getFloatPtr()[4*i+j] *= 1.0;
      //cerr<<endl;
      }

    //cerr<<"invNav :"<<endl;
    for(i = 0; i < 4; i++){
      for(int j = 0; j < 4; j++)
        //cerr<<invNav.getFloatPtr()[4*i+j]<<" ";
      invNav.getFloatPtr()[4*i+j] += 0.0;
      //cerr<<endl;
      }

    wand_matrix = *(mWand->getData());
    wand_matrix.postMult(invNav);
    wand_matrix.getTrans(wandPos[0], wandPos[1], wandPos[2]);
    wandPos.xformVec( invNav, wandPos );

    ////////////////////////
    // NAVIGATION         //
```

```
//////////////////////////////////////////////////////
static float userVelocity = 0;

int button0_state = mButton0->getData();
int button1_state = mButton1->getData();
int button2_state = mButton2->getData();

// Implement button selection menu
switch(wandButtonState){


case BUTTON_BASE :
  if(button0_state == vjDigital::TOGGLE_ON )
  wandButtonState = BUTTON_ANALYZE;
  else if(button1_state == vjDigital::TOGGLE_ON)
  wandButtonState = BUTTON_EDIT;
  else if(button2_state == vjDigital::TOGGLE_ON)
  wandButtonState = BUTTON_NAVIGATE;
  break;


case BUTTON_ANALYZE:
  if(button0_state == vjDigital::TOGGLE_ON)
  wandButtonState = BUTTON_QUERY;
  else if(button1_state == vjDigital::TOGGLE_ON)
  wandButtonState = BUTTON_MEASURE;
  else if(button2_state == vjDigital::TOGGLE_ON)
  wandButtonState = BUTTON_BASE;
  break;


case BUTTON_EDIT:

  if(button0_state == vjDigital::TOGGLE_ON){
  // select a feature and move ...
  selFeatureIndex = _selectFeature(wandPos);
  }// end if

  else if(button1_state == vjDigital::TOGGLE_ON){
  // unselect a feature ...
  if(selFeatureIndex >= 0){
      fDataVec[selFeatureIndex]->sel = false;
    fDataVec[selFeatureIndex]->pos = wandPos - wandOffset;
    selFeatureIndex = -1;
  }// end if
  }// end else if

  else if(button2_state == vjDigital::TOGGLE_ON){
  // move up to the base mode ...
  wandButtonState = BUTTON_BASE;
  }// end else if
```

```
    if(selFeatureIndex >= 0){ // reset feature position ...
    fDataVec[selFeatureIndex]->pos = wandPos - wandOffset;
    }// end if

    break;

  case BUTTON_QUERY:

    if(button0_state == vjDigital::TOGGLE_ON){
    // select a feature and move ...
    selFeatureIndex = _selectFeature(wandPos);
    }// end if

    else if(button1_state == vjDigital::TOGGLE_ON){
    // unselect a feature ...
    if(selFeatureIndex >= 0){
        fDataVec[selFeatureIndex]->sel = false;
      selFeatureIndex = -1;
    }// end if
    }// end else if

    else if(button2_state == vjDigital::TOGGLE_ON){
    // move up to the base mode ...
    if(selFeatureIndex >= 0){
        fDataVec[selFeatureIndex]->sel = false;
      selFeatureIndex = -1;
    }// end if

    wandButtonState = BUTTON_ANALYZE;
    }// end else if

    break;


  case BUTTON_NAVIGATE:

    if(selFeatureIndex >= 0){
      fDataVec[selFeatureIndex]->pos = wandPos-wandOffset;
    }

    if(button0_state){// accelerate ...
    userVelocity += 0.01f;
    }// end if

    else if(button1_state){// decelerate ...
    userVelocity -= 0.01f;
    }// end else if

    else if(button2_state == vjDigital::TOGGLE_ON){
    wandButtonState = BUTTON_BASE;
    }// end else if
    break;
```

```
case BUTTON_MEASURE:

  distance = area = area1 = area2 = 0.0;
  if(button0_state == vjDigital::TOGGLE_ON){
  // go to distance measuring mode ...
  wandButtonState = BUTTON_DISTANCE;
  }// end if

  else if(button1_state == vjDigital::TOGGLE_ON){
  // go to area measuring mode ...
  wandButtonState = BUTTON_AREA;
  }// end else if

  else if(button2_state == vjDigital::TOGGLE_ON){
  // move up one mode ...
  distance = area = area1 = area2 = 0.0;
  wandButtonState = BUTTON_ANALYZE;
  }// end else if

  break;


case BUTTON_DISTANCE: case BUTTON_AREA:
  /* get points and compute distance/area and display them */

  if(button0_state == vjDigital::TOGGLE_ON){

  if(pointVec.size() == 0){
    distance = area = area1 = area2 = 0.0;
    pointVec.insert(pointVec.begin(), wandPos);
  }// end if
  else if(pointVec.size() > 0) {
    pointVec.push_back(wandPos);
    int index = pointVec.size();
    distance = area = area1 = area2 = 0.0;
    for(int i = 1; i < index; i++){

      distance += sqrt(pow((pointVec[i][0]-pointVec[i-1][0]),
2.0) +
                       pow((pointVec[i][2]-pointVec[i-1][2]), 2.0));

      area1 += pointVec[i-1][0]*pointVec[i][2];
      area2 += pointVec[i][0]*pointVec[i-1][2];
    }// end for

    area1 += pointVec[index-1][0]*pointVec[0][2];
    area2 += pointVec[0][0]*pointVec[index-1][2];
    area = (area1-area2)/2.0;
    area = ((area < 0 ) ? -area : area);
  }// end else if
```

```
      }// end if

      else if(button1_state == vjDigital::TOGGLE_ON){
      pointVec.clear();
      }// end else if

      else if(button2_state == vjDigital::TOGGLE_ON){
      pointVec.clear();
      wandButtonState = BUTTON_MEASURE;
      }// end else if

      break;
    }// end switch

    userInfo.setVelocity( userVelocity );
    userInfo.setAngularVelocity( 0.01f );
    wandInfo.updateWithMatrix( *(mWand->getData()));
    userInfo.update( wandInfo, vjVec3(0.0f, 0.0f, 0.0f) );
    userInfo.getSceneTransform( mNavMatrix );
}// end preFrame()


int roadApp::_selectFeature(const vjVec3 & point){
  bool found = false;
  for(int i = 0; i < fDataVec.size() && !found; i++)
    found = fDataVec[i]->selectFeature(point);
  if(found){
    wandOffset = point - fDataVec[i-1]->pos;
    return i-1;
  }// end if
  else{
    wandOffset = vjVec3(0.0, 0.0, 0.0);
    return -1;
  }
}
```

APPENDIX F - AUTOCAD DRAWING FOR VR MODELING

This appendix gives an outline of procedure followed for creating a structural drawing of the bridge in a digital format using the Computer Aided Drafting (CAD) software AutoCAD™ by AutoDesk [90]. The source drawing detailing the structural elements of the railway bridge was obtained from the IADOT in a hardcopy format. These drawings included complicated details in plan view, front view, and cross-sectional views. The dimensions of each of the individual columns and beams and spacing between them were determined by reading these drawings.

Elements of the Bridge

It was found that the bridge alignment was not perpendicular to the road alignment. Farther, the width of the bridge actually increased from west to east. Thus, the foundation of columns on either side of the road supporting the superstructure was placed at an offset from each

other along the road direction. This also resulted in non-uniform spacing between the columns that supported the beams that in turn supported the deck. In addition, the beams on both sides of the road and resting on top of the columns were discontinuous between the second and the third columns. The deck beams spanning across the road were also discontinuous between these two pairs of column. All these details added up to the complexity of reproducing the drawing in the digital format (See figure 7.8). However the dimensions of the individual elements were a constant. For example, all columns were of same cross-sectional dimension and length. So all the pertinent structural details of the bridge were identified to create the drawing in the digital format.

The AutoCAD GUI

This section will briefly describe the steps involved in creating the digital drawing. An AutoCAD GUI looks like as in figure F.1. The elements of the GUI includes a menu bar for accessing commands through menu items, various tool bars for drawing, modification, object properties and such to select an action tool quickly, a command area for typing in commands, and a status area that shows the current

cursor position and time. Either choosing a menu item, or a tool or typing in a command at command prompt can affect same action. The toolbars provide an intuitive way for accessing various functions.

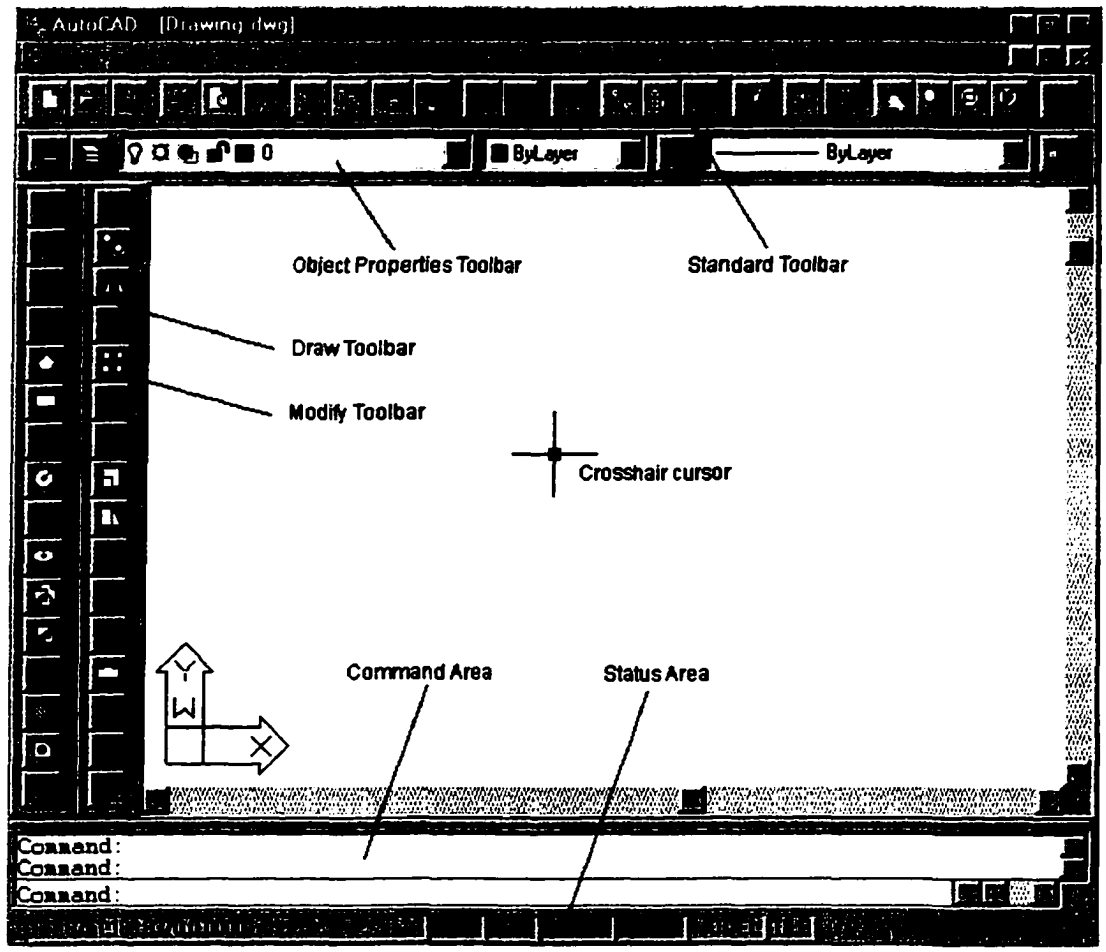

Figure F.1 Elements of AutoCAD GUI

Various too bars can be made to appear by choosing appropriate toolbars from the menu bar as shown in figure F.2. Elementary

drawing tools are provided on the drawing tool bar and include tools for drawing straight line, curved lines, circle, rectangle and more. Alternately, the same drawings can be affected by using commands such as line to draw a line and proceed to type in the start coordinate and the end coordinate of the line.

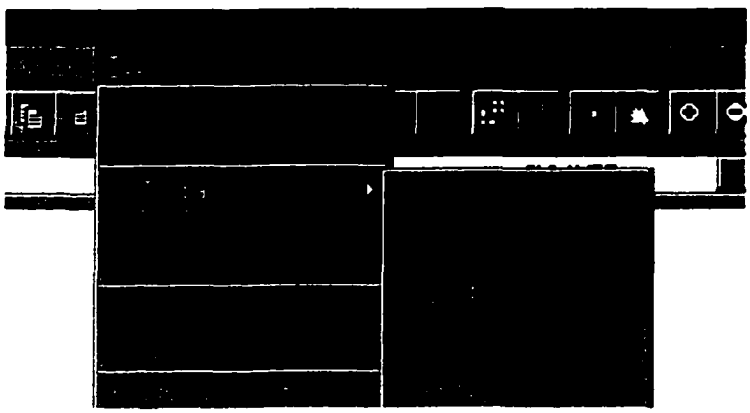

Figure F.2 Accessing toolbars

Organizing the Drawing

Organizing various components of the drawing lets the user work with it easily and smoothly. The first step in that direction is to set limits and units. Choosing the limits provides a border for the drawing are that can be easily viewed using the ZOOM functionality. In the present case, since the source drawing was available in units of inches,

therefore, the AutoCAD drawing was created in units of inches to avoid an extra step of converting units. A local coordinate system was adopted with the center at one corner of the column foundations on the west.

The other element of organizing the drawing is to combine elements belonging distinctive parts into separate groups for ease of manipulating them. For example, the drawing can be considered to be a combination of different entities such as columns, beams, foundations, stirrups, deck and more. A very convenient way to handle them separately is to put them in different layers of the drawing. The figure F.3 shows the options available with the layer concept.

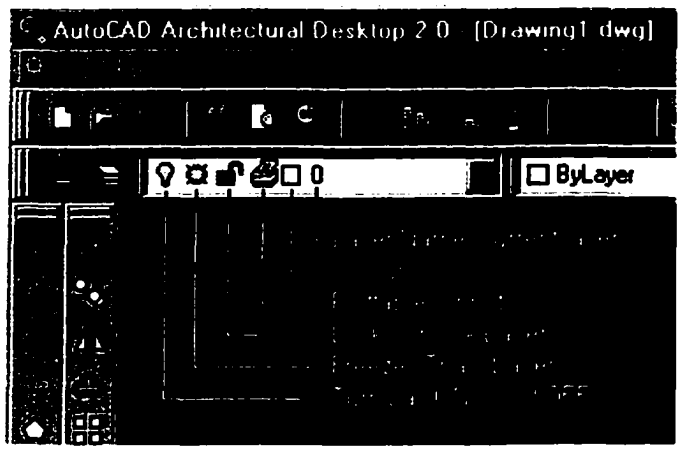

Figure F.3 Layers in AutoCAD

With this idea, separate layers were created for the beams, columns, stirrups and more. Individual layers may be displayed in different colors and line types, be locked or unlocked, frozen or thawed, and turned on or off individually. At one time the user works on that one layer only which is set as the current layer. In a complicated drawing as in the present case, turning off the other layers helps to look the drawing free of clutters.

Drawing the Bridge Model

The task at hand is to model the bridge, which is a three dimensional structure. The solids drawing tool bar (See figure F.4) available in AutoCAD became useful in such a situation. The solids toolbar includes such tools as 'sphere', 'wedge', 'torus', 'cone' extrude' and more. The 'extrude' tool is useful in creating a solid object by extruding a plan surface. For example, circle can be extruded to create a cylinder. This tool was used for such bridge elements as an H-beam, which has a complex but uniform cross-section along its length.

Figure F.4 Solids toolbar

In addition to the solids tool bar, AutoACAD also has three commands for 'Constructive Solid Geometry' (CSG): union, subtract, and intersect. Union joins objects together and discards any resulting internal surfaces. Subtract uses one solid to cut away a part of another solid, while intersection retains the common part of the two objects intersecting. The CSG tools can be accessed from the modify tool bar as shown in figure F.5.

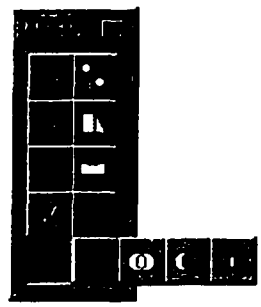

Figure F.5 Modify toolbar

The tools available on the snapping toolbar as shown in figure F.6 are also very useful. These tools include snapping to end of a line, intersections of lines, center of circle, nearest point and more and are useful when joining existing entities in the drawing. The zoom toolbar is useful in looking at details in a small part of the drawing or the looking at the complete drawing as a whole. Figure F.7 shows how the zoom tool bar can be accessed. Further, the tiled 3D Viewpoint tool was

used to look at the object in 3D. This tool presents options for the user to look at the object with the desired viewer orientation (Figure F.8).

Figure F.6 Object snap toolbar

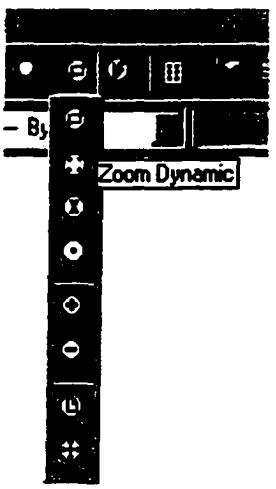

Figure F.7 Zoom options

Portability

An AutoCAD drawing can be saved as 'Drawing Interchange File Format (DXF) that can be read by many other graphics software. Therefore, the model of the bridge created using AutoCAD was saved

into an DXF format. In this case, the modeling was completed in Multigen Creator™ that cannot read DXF format directly. Therefore a conversion utility called 'Polytran' available on the Silicon Graphics Inc. (SGI) platform of the Virtual Reality Application Center (VRAC) at the Iowa State University was used to convert the DXF file into flt format, which is native to Multigen Creator™.

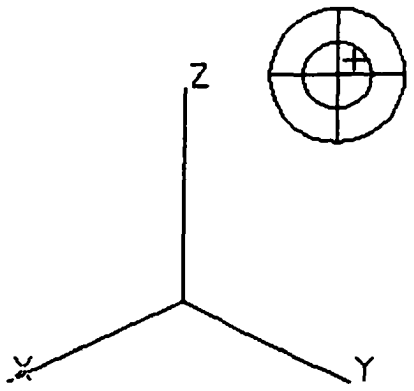

Figure F.8 Dynamic 3D viewing

APPENDIX G – MULTIGEN CREATOR™ FOR VR MODELING

This section briefly describes how Multigen Creator™ was used to create the Roadway scene using photogrammetric positioning and digital drawing file obtained from AutoCAD drawing. Multigen Creator™ is a product of the Multigen-Paradigm Inc. It is a tool for modeling 3D contents and contains interactive modeling toolsets for various tasks of building geometry, rendering and animation. The hierarchical view lets the user drag-and-drop facility to modify the model structure. The rendering process is controlled through Level Of Detail (LOD), culling, priority, logical switching, Degree Of Freedom (DOF) and other non-visual nodes for real-time rendering.

Multigen lets user create various entities such as line, plan, object and groups. These entities are actually nodes in a hierarchical structure that lets user manage database to achieve optimal performance at runtime, which may be an important issue in a large graphical database.

The native output from Multigen Creator™ are optimized OpenFlight (flt) files. These files can be ported to CAVE through VRJuggler, the VR open development platform at VRAC. In this research, Multigen Creator™ a 3D bridge model created in AutoCAD™ was integrated with photogrammetric positional and dimension data of other roadside features such as pavements, sidewalks, light posts etc. The following sections describe the process of integrating the two models to produce a single roadway scene model.

Cleaning Up Bridge Model

The 3D bridge model created in AutoCAD™ was imported from DXF format to the flt format using 'Polytran', a conversion utility available ob the SGI platform at VRAC in ISU. However the conversion process did not preserve the integrity of the bridge model. Some of the plan features were split into lines. But textures cannot be mapped to lines. Therefore an intensive cleaning operation had to done to restore the data integrity of the bridge model. The 'Isolate" feature in Multigen lets the user isolate a group of features at any level of the hierarchical data structure to be isolated so that the user can work without much of distracting details of surrounding features. This is similar to the layer concept in AutoCAD drawing but more versatile. In this case,

groups of entities that should belong to single objects were grouped logically in the database structure by simple drag-and-drop feature of Multigen Creator™ and restored to its original form. Different construction tools such as point, line, polygon, extrude, split-line, split-polygon were used. These tools are available through three methods: tools in detachable tool-chests, menu item on the standard menu bar, and hotkeys. With prolonged use of the software, the user gains proficiency in using the hitherto unfamiliar hotkeys, which are quick ways to access various editing actions.

Modeling Photogrammetric Feature Positioning

The digital photogrammetric methods adopted in this research yielded roadside feature positions in a real world coordinate system as well as feature dimensions, in units of meters. For example, positions of light posts and height of the light posts were determined. For ease of working, the position information was reduced to a local coordinate system with origin at the same position as in the bridge modeland the units were left unchanged. Using the various construction tools as mentioned above, the surfaces for the pavements, sidewalks, side slopes were developed and roadside objects such as light posts were

constructed. Finally, textures extracted from the video logging images. These textures were used to render the pavements and side slopes

Integration of Two Models

The bridge model and the roadway model were thus ready. But these were in relatively different scales as the bridge model was constructed in units of inches and the roadway model was constructed in units of meters. Since the roadway model included points on the bridge façade, it was possible to identify a few common points between the two models. These common points were use to scale the bridge model to match the size of the road model to create an integrated model in units of meters. The scale tool, the translation tool and the rotation tool available in the modify tool-chest of Multigen Creator™ were all used to match the two model and fine tune them to obtain a seamlessly integrated model for the roadway environment.

REFERENCES

1. Vince, J., *VR Systems*, Addison Wesley, Reading, Massachusetts, 1995

2. Aukstakalnis, S., and Blatner, D., Silicon Mirage: *The Art and Science of VR*, PeachPit Press, 1992

3. LaPrade, G. L., *In Manual of Photogrammetry*, American Society of Photogrammetry and Remote Sensing, 1980

4. Yao, W., *Autocorrelation techniques for soft photogrammetry*, Ph.D. Thesis, Iowa State University, 1997

5. Lillesand, T. M., and Kiefer, R.W., *Remote Sensing and Image Interpretation*, 4e, John Wiley and Sons Inc., NY, 1999

6. Sheppard, S.R.J., *Visualization Software Brings GIS Applications To Life*, GeoWorld, March 1999

7. Neves, N., Goncalves, P., Muchaxo, J., Jordao, L., Silva, J., and Videra, N., *Virtual GIS Room: Interfacing Information in Virtual Environments*, Environmental Systems Analysis Group, New

University of Lisbon, available at,

http://www.dcea.fct.unl.pt/gasa/papers/neves_jn/, June 1999

8. *ArcView 3D Analyst* available at,

http://www.esri.com/software/arcview/extensions/3dext.html, June, 1999

9. *Erdas Imagine Virtual GIS*, available at,

http://www.erdas.com/products/imagine_virtualgis.html, November, 1999

10. *K2VI*, available at www.k2vi.com/k2vi/k2vi.htm, September 2001

11. *GMS lab at UIUC* available at http://www.gis.uiuc.edu/, October 1999

12. Koller, D., Lindstrom P., Ribarsky W., Hodges, L. F., Faust, N., Turner, G., *Virtual GIS: A Real-time 3D Geographic Information System*, In Proceedings of Visualization 1995 GVU Technical Report 95-14, 1995

13. Polis, M. F., Gifford, S., J., and McKewon, D. M., Jr., *Automating the construction of large-scale virtual world*, Computer, 28:57-65, 1995

14. Hirose, M., Watanabe, S., and Endo, T., *Generation of Wide-Range Virtual Spaces Using Photographic Images*, 1998 IEEE Annual VR International Symposium, pp 234-241, 1998

15. Jeyapalan, K., Jaselskis, E., J., Smith, S., Stephan, B., Bernhard, C., and Bhagawati, D., *Automated Data Acquisition of Roadside Features*, Research Report to The WSDOT and FHWA, Research Contract No. GCA1217, 1998

16. Stuart, R., *Design of Virtual Environments*, McGraw-Hill Text, 1996

17. *Virtual workbench*, Georgia Institute of Technology Web page available at http://www.cc.gatech.edu/gvu/datavis/research/workbench.html, September 2001

18. Cruz-Neira, C., Sandin, D.J., DeFanti, T.A., *Surround-Screen Projection-Based Virtual Reality: The Design and Implementation of the CAVE.* ACM Computer Graphics, Vol. 27, Number 2, pp 135-142, July 1993

19. Cruz-Neira, C. *"Projection-based Virtual Reality: The CAVE and its Applications to Computational Science."* PhD Thesis, University of Illinois at Chicago, 1995

20. *About VRAC C2*: How It Works, available at, http://www.vrac.iastate.edu/about/selab/index.html, November 2001

21. *About VRAC C6*: How It Works, available at, http://www.vrac.iastate.edu/about/facilities/c6/index.html, November 2001

22. Jeyapalan, K., Yao, W., Bhagawati. D., *Soft Photogrammetry for Highway Engineering*, Research Report, IOWA DOT, 1998

23. Jeyapalan, K., Bhagawati, D *As Built Surveys For GIS Applications*, In Proc., ASPRS conference, Washington DC, May 22-26, 2000

24. *Van Collects Data Continuously at 30 mph*, Design-News, v.50[51] Sep 25, pp 28, 1995

25. *Software and Laser Survey Speed Roadway Redesign*, Civil-Engineering- (American Society of Civil Engineers). v. 65 pp 92, September 1995

26. *Signage Gunned Down in the Streets*, Civil-Engineering- (American Society of Civil Engineers). v. 65, pp 24+, June 1995

27. Pottle, D., *New Mobile Mapping System Speeds Data Acquisition*, Geomatic Info Magazine: GIM, v. 9, pp 51-53, September 1995

28. El-Sheimy, N., K. P. Schwarz, M. Gravel, *Mobile 3-D Positioning using GPS/INS/Video cameras*, Proceedings 1995 Mobile Mapping Symposium, May 24-26, pp 236-249, 1995

29. Li, R., M. A. Chapman, L. Qian, Y. Xin, and K.P. Schwarz, *Rapid GIS Database Generation Using GPS/INS controlled CCD Images,* ISPRS GIS/SIG, June 6-10, Ottawa, Canada, 1994

30. Novak K., *Mobile Mapping Technology for GIS data Collection,* Photogrammetric Engineering and remote Sensing, vol 61, No. 5, pp 493-501, May 1995

31. He, G., and K Novak, *Automatic Analysis of Highway Features From Digital Stereo Images,* International Archives of Photogrammetry and Remote Sensing, vol 29, part B3, pp 119-124, 1992

32. Dann, M. A., *Development of Local GIS for Williamson County Using Mobile Mapping technology,* Proceedings 1995 Mobile Mapping Symposium, May 24-26, pp 193-197, 1995

33. Blaho, G., and C. Toth, *Field Experiences with A Fully Digital Mobile Stereo Image Acquisition System,* Proceedings 1995 Mobile Mapping Symposium, May 24-26, pp 97-104, 1995

34. McCall, B., and J. Whited, *Video Imagery Systems for Highway Applications,* Report No. FHWA-DP-90-085-004, May 1990

35. Lanckton, A. H., *Photogrammetric Laser System,* Proceedings 1995 Mobile Mapping Symposium, May 24-26, pp 35-44, 1995

36. Scherzinger, B. M., *The Position and Orientation System (POS) for Land, Marine and Airborne Mapping,* , Proceedings 1995 Mobile Mapping Symposium, May 24-26, pp 75-84, 1995

37. Baraniak, D. W., *GPSVision™ ---A state of the Art Mobile Mapping System,* Proceedings 1995 Mobile Mapping Symposium, May 24-26, pp 256, 1995

38. El-Hakim, S.F., Brenner, C., and Roth, G., A Multi-Sensor *Approach To Creating Accurate Virtual Environments,* ISPRS Journal of Photogrammetry and Remote Sensing, vol 53, pp 379-391, 1998

39. Livingston, R. G., Berndsen, C. E., Ondrejka, R., Spriggs, M., Kosofsky, L. J., Steenburgh, D. V., Norton, C., and Brown, D., *Aerial Camera,* In Manual of Photogrammetry, American Society of Photogrammetry,Falls Church, VA, 4e, 1980.

40. Fryer, J. G., *Camera Calibration in Non-Topographic Photogrammetry,* In Non-Topographic Photogrammetry, American Society of Photogrammetry and Remote Sensing, Falls Church, VA, 2e, 1989

41. Wolf, P.R., *Elements of Photogrammetry,* McGraw-Hill Book Company, 2e, 1983

42. Jeyapalan, K., *Lecture Notes,* CE 517 Remote Sensing and Digital Photogrammetry, Fall 1997.

43. Wester-Ebbinghaus, W., *Trends in Non-Topographic Photogrammetric Systems,* In Non-Topographic Photogrammetry, American Society of Photogrammetry and Remote Sensing, Church Falls, VA, 2e, 1989.

44. Wei, G., Q., Song, D. M., *Implicit and Explicit Camera Calibration: Theory and Experiments.* IEEE transactions on Pattern Analysis and Machine Intelligence, vol. 16 pp 469-80, May 1994

45. Huttori, S., Myint, Y., *Automatic Estimation of Initial Approximations of Parameters for Bundle Adjustment,* Photogrammetric Engineering and Remote Sensing, vol. 61, pp. 909-15, July 1995

46. Obercampf, D., DeMenthon, D., M., Davis, L., S., *Iterative Pose Estimation Using Coplanar Feature Points,* Computer Vision and Image Understanding, v. 63, pp 495-511, May 1996

47. Banihashemi, A., *A Fourier approach to camera orientation,* In IEEE Transactions on Pattern Analysis and Machine Intelligence, volume 15, number 11, pp 1197- 1202, 1993

48. Wei, G., Q., Arbter, K., Hirzinger, G., *Active Self-Calibration of Robotic Eyes and Hand-Eye Relationships With Model*

Identification, IEEE Transactions on Robotics and Automation, vol 14, pp 158-66, February 1998

49. Jeyapalan, K., *Use of GPS for Photogrammetry,* Iowa DOT Project HR 342, January 1993

50. Karara, H., M., *Non-Topographic Photogrammetry,* In Manual of Photogrammetry, American Society for Photogrammetry, Falls Church, VA, 1980.

51. Faig, W., *Non-metric and Semi-metric Cameras : Data Reduction,* In Non-Topographic Photogrammetry, American Society for Photogrammetry and Remote Sensing, 2e, 1989.

52. Abdel-Aziz, Y. I., and Karara, H. M., *Direct Linear Transformation from Comparator Coordinates into Object-Space Coordinates,* ASP Symposium on Close-Range Photogrammetry, 1971

53. Abdel-Aziz, Y. I., and Karara, H. M., *Photogrammetric Potentials of Non-Metric Cameras,* Civil Engineering Studies, Photogrammetry Series No. 36, UI, 1974

54. Abdel-Aziz, Y. I., *Expected Accuracies and Convergent Photos,* PE, November, 1974

55. Peak Performance Technologies Inc. Motion Measurement Systems, *Peak-5 User's Reference Manual Version 5.0.7,* March 1993.

56. Bradley, J., *XV,* Version 2.21, Bradley@cis.upenn.edu., 1992

57. Jeyapalan, K., *Remote Sensing*, Chapter in Urban Planning And Development Application In GIS, ASCE, 2000

58. Jeyapalan, K., *Photogrammetry*, Chapter in Encyclopedia of Earth System Science, Academic Press, 1991

59. Atkinson, K. B., *Instrumentation for Non-Topographic Photogrammetry*, In Non-Toopographic Photogrammetry, American Society of Photogrammetry and Remote Sensing, Falls Church, VA, 2e, 1989

60. Koch, Reinhard, *Model-Based 3-D Scene Analysis from Stereoscopic Image Sequences*, ISPRS Journal of Photogrammetry and Remote Sensing, vol 49, no 5 pp 23-30, 1994

61. Förstner, W., Gülch, E., *Automatic Orientation And Recognition In Highly Structured Scenes*, ISPRS Journal of Photogrammetry and Remote Sensing, vol 54, no 1, pp 23-34, 1999

62. Henri Veldhuis, George Vosselman, *The Edhoc Reconstruction Of Straight And Curved Pipes Using Digital Line Photogrammetry*, ISPRS Journal of Photogrammetry and Remote Sensing, vol 53 no 1 pp 6-16, 1998

63. Chen S. E., Williams, L. *View Interpolation For Image Synthesis*, Proc. SIGGRAPH, pp 279-288, 1993

64. Szeliski, R., *Image Mosaics For Virtual Environments*, IEEE Comput. Graph. Appl. Vol 16 no 2, pp 22-30, 1996

65. Kang, S.B., *A Survey Of Image Based Rendering Techniques,* Technical report CRL 97/4, Cambridge Research Lab, Digital Equipment Corp., 1997

66. Banerjee, P., *Virtual Reality-Aided Facility Layout Design*, Seminar handout, Department of Industrial and Manufacturing Engineering, ISU, February 25, 1999

67. *3D Construction Company*, available at http://www.3dconstruction.com/ June 1999

68. *ShapeQuest Inc.* available at http://www.shapequest.com, September 2001

69. Huang, Y., Trinder, J.C., *Object Recognition Based On Boundary Description*, Photogrammetric Engineering and remote Sensing, vol 65, no 8, pp 915-921, 1999

70. Gibson, D. P., Campbell, N. W., Thomas. B. T., *Iterative Generation of 3-D Models from a Set of 2-D Images*, In Eurographics UK, pp 135-145, 1998

71. Gruen, A., Wang, X. *CC-Modeler: A Topology Generator For 3-D City Models*, ISPRS Journal of Photogrammetry and Remote Sensing, vol 53, no 5, pp 286-295, 1998

72. Faugeras, O., Robert, l., Laveau, S., *3D Reconstruction Of Urban Scenes From Image Sequences*, Computer Vision and Image Understanding, vol 69 no 3, pp 292-303, 1998

73. Frank, A., Heuvel, van den., *3D Reconstruction From A Single Image Using Geometric Constraints*, ISPRS Journal of Photogrammetry and Remote Sensing, vol 53, no 6, pp 354-368, 1998

74. Sequeira, V., Ng, K., Wolfart, E., Goncalves, J.G.M., Hogg, D., *Automated Reconstruction Of 3D Models From Real Environments*, ISPRS Journal of Photogrammetry and Remote Sensing, vol 54, no 1, pp 1-22, 1999

75. Poulin, P., Ouimet, M, Marie-Claude, F., *Interactively Modeling With Photogrammetry*, In: Eurographics, Eurographics rendering workshop, Vienna, Austria, June 1998, Edited by George Drettakis and Nelson Max, pp 93-104, 1998

76. Leymarie, F. et al., Realise: *Reconstruction Of Reality From Image Sequences*, In: International Conference On Image Processing, pp. 651-654 http://www/inria.fr/roborvis/projects/Realise, 1996

77. Debevec, P.E., Taylor, C.J, Malik, J., *Modeling And Rendering Architecture From Photograph: A Hybrid Geometry And Image Based Approach*, Proc. SIGGRAPH 1996, pp 11-20, 1996

78. Weik, S., Grau, O., *Recovering 3D Geometry Using A Generic Constraint Description*, In: ISPRS96 - 18thCongress of the International Society for Photogrammetry and Remote Sensing, 1996

79. *PhotoModeler*, available at http://www.photomodeler.com, September 2001

80. Hanke, K., Mostafa, A.E., *The 'Digital Projector' Ray tracing As A Tool For Digital Close-Range Photogrammetry*, ISPRS Journal of Photogrammetry and Remote Sensing, vol 54, no 6 pp 35-40, 1999

81. Dorffner, L., Forkert, G., *Generation And Visualization Of 3D Photo-Models Using Hybrid Block Adjustment With Assumptions On The Object Shapes*, ISPRS Journal of Photogrammetry and Remote Sensing, vol 53, no 6, pp 369-378, 1998

82. Kang, S.B., *Geometrically Valid Pixel Reprojection Method For Novel View Synthesis*, ISPRS Journal of Photogrammetry and Remote Sensing, vol 53 no 6, pp 342-353, 1998

83. Chapman, D., Deacon, A., *Panoramic Imaging And Virtual Reality - Filling The Gap Between The Lines*, ISPRS Journal of Photogrammetry and Remote Sensing, vol 53, pp 311-319 1998

84. Aliaga, D., Lastra, A.A., *Architectural Walkthrough Using Portal Textures*, Proc. IEEE Visualization, pp 355-363, 1997

85. *Cyra Technology: Cyrax Scanning Case Studies*, available at, http://www.cyra.com/cases.html September 2001

86. *Adobe Photoshop*, available at, http://www.adobe.com/products/photoshop/main.html, September 2001

87. *Multigen Creator 2.3*, http://www.multigen.com/products/creator.htm, August 2001

88. Allen Bierbaum, Christopher Just, Patrick Hartling, Kevin Meinert, Albert Baker, and Carolina Cruz-Neira, *"VR Juggler: A Virtual Platform for Virtual Reality Application Development"*. Published at IEEE VR 2001, Yokohama, March 2001

89. *VRJuggler – The Virtual Reality Platform*, available at, http://www.vrjuggler.org/ September 2001

90. *AutoDesk - AutoCAD*, available at http://www3.autodesk.com/adsk/section/0, 616714-123112,00.html September 2001

ACKNOWLEDGEMENTS

The author would like to express sincere appreciation to all those who helped to make this thesis possible.

To Dr. Kandiah Jeyapalan for his role as the major professor and his present guidance throughout the study.

To Dr. John M. Pitt, Dr. Say Kee Ong, Dr. Thomas S. Colvin and Dr. U. Sunday Tim fir their continuous support and encouragement throughout this research.

To Kevin Kane for providing an opportunity to work at the ISU GIS Facility during major part of this research.

To Dr. Judy Vance and Dr. Carolina Cruz-Neira for providing opportunities and knowledge in the realms of virtual reality.

To Dr. Edward J. Jaselskis, along with Dr. Jeyapalan, for involving the author with the research project that turned out to be the founding ground for this research.

To the Iowa Department of Transportation for financial support for the research project that provided the video-logging data for this research.

To Patrick D. Brown and Steven D. Deines for reviewing the thesis.

To Eric C. Olson for helping with modeling the virtual scene and demonstration of the model at the C6 CAVE.

To Senthil K Panjetty-Kumarad and Ramesh.Aumbuliyur-Como for their help at various stages of this research.

And finally, to his family, for patiently putting up with the hardship that a graduate student has to go through, and for providing encouragement at all times.